Gelein M. de Koeijer

Energy Efficient Operation of Distillation Columns and a Reactor Applying Irreversible Thermodynamics

This thesis has been submitted to
Department of Chemistry
Norwegian University of Science and Technology

in partial fulfillment of the requirements for
the Norwegian academic degree
DOKTOR INGENIØR
May 2002

Institutt for kjemi
Norges teknisk-naturvitenskapelige universitet
N-7491 Trondheim
Norway

Doktoringeniøravhandling 2002:41
IFK 2002:58
ISBN 82-471-5436-6
ISSN 0809-103x

Acknowledgements

This thesis is dedicated to my father, Rinus de Koeijer. He passed away suddenly in November 1998. I miss him.

The first one I would like to thank is my thesis adviser, Signe Kjelstrup. Her sincere interest in thermodynamics and open mindedness were important factors for me to leave Holland and start a new life in Trondheim. The fact that she nearly always made time for a question or discussion was an invaluable support during the project. I am very grateful to Hedzer van der Kooi for introducing me into the world of second law thermodynamics. Next, Dick Bedeaux is thanked for his attempts to explain an engineer the theory of irreversible thermodynamics. A special thanks to Ricardo Rivero and all I met in amazing Mexico City for their hospitality. I would also like to thank the other co-authors and contributors in chronological order: Bernd Gross, Prof. K.F. Knoche, Torben Ravn Andersen, Agnar Målsnes, Kjell Rostad, Peter Salamon, Gino Siragusa, Markus Schaller, Karl Heinz Hoffmann, Audun Røsjorde, and Eivind Johannessen. Especially their critical comments and questions were absolutely necessary for getting things correct.

The pleasant and challenging atmosphere at the group of Physical Chemistry made work very enjoyable, especially during the coffee breaks. Moreover, Audun, Lars, Martin and Terje deserve a big thank-you for the computer support and the fantastic Linux computers. My research was not possible without them. Bjørn, Eivind, and Pieter are thanked for checking preliminary versions of my thesis.

The Research Council of Norway is thanked for a grant for my research project. And Instituto Mexicano del Petroleo is thanked for the travel expenses to Mexico. This money enabled me to experience Japan, USA, Mexico, and Turkey.

During my stays in Holland I could count on a warm welcome at my parents' home in Gouda, together with my mother Geraldien and my sister Aletta, thank you! As last I would like to thank the one who always comes first: Ann Cicilie for her love.

Abstract

In this thesis the entropy production rates of diabatic distillation columns and a SO_2 converter were minimised. This is the same as maximising the second law energy efficiency of the systems. The development of chemical industry can be made more sustainable by knowing this minimum. We found that the entropy production rate of distillation could be reduced up to 50 %. In order to achieve this reduction, heat exchangers were added on each tray. The characteristics of an optimum distillation column were presented. Furthermore, the entropy production rate of a SO_2 converter was reduced with 16.7 % by altering the heights of catalytic beds, transfer areas of heat exchangers, and temperature differences over heat exchangers. These reductions show that there is still a large improvement potential in chemical industry. By applying the improved operations the world oil production can be reduced in the order of magnitude of 1 %. A similar reduction in the emission of the greenhouse gas CO_2 can be expected.

For deriving the entropy production rate in a systematic manner the theory of irreversible thermodynamics was useful. A simpler and a more complicated equation for the entropy production rate of distillation were derived. The simpler equation used only one force-flux product. It was suitable for minimisation of the entropy production rate of columns with the assumption of equilibrium between the outlets on each tray. The more complicated equation was able to describe satisfactorily the entropy production rate of an experimental column that separated the non-ideal mixture water-ethanol. It was next used to derive an extended set of transport equations for distillation, that includes the interface and the Soret effect (or thermal diffusion). Finally, irreversible thermodynamics was used to describe the contribution to the entropy production rate of heat transfer in heat exchangers. This contribution had a significant impact on the results of the minimisations.

A method that can provide the chemical industry the thermodynamically optimum operation of distillation columns and reactors was constructed and exemplified. Once the system and its boundaries are determined, the objective function with its constraints and variables are set up. Several suitable minimisation procedures can be used. Finally, the design of the thermodynamically optimum system is obtained from the state of minimum entropy production rate.

Contents

1 Introduction

1.1 Motivation

1.1.1 Need for sustainable development

This thesis is motivated by the need to make development sustainable. The definition of sustainable development is *'development that meets the needs of the present, without compromising the ability of future generations to meet their own needs'*. This is the definition from the World Commission on Environment and Development (1987). In the report of the Club of Rome (Meadows and Randers 1972) it was predicted that society must undergo large changes to have sustainable development, see also Meadows et al. (1992). Most importantly, the ways we fulfil our energy demand have to change drastically, since non-renewable energy stocks (e.g. oil, gas, coal) are used for this purpose at the moment. The report also predicts that the shift to sustainable development might even lead to an energy crisis. The oil crises in 1973 and 1979-1980 showed that society is indeed vulnerable for fluctuations in the energy market. Currently, a potential danger of climate change increases the necessity of making development sustainable. One of the causes of the climate change is most probably the emission of the greenhouse gas CO_2 from the use of the non-renewable stocks. Therefore 108 governments agreed to reduce their CO_2 emissions with the Kyoto protocol (UNFCCC 1997). This protocol mentions *'Enhancement of energy efficiency in relevant sectors of the national economy'* and *'Promotion, research, development and increased use of new and renewable forms of energy'* as measures to reduce CO_2 emissions. These measures are also two main ones for reaching sustainable development. Renewable forms of energy are for example generated from the sun, wind, and biomass. Energy efficiency and developing renewable energy forms are linked. The use of the limited renewable energy forms must be done preferably as energy efficient as possible.

1.1.2 Distillation and reactors

According to Humphrey and Siebert (1992), chemical industry accounts for 27 % of the industrial energy use in the USA in 1991. The process of distillation uses 40 % of that. So, distillation accounts for 11 % of the industrial energy use in the USA. Another large energy demander in chemical industry are the reactors. Thus, increasing the energy efficiency of these processes can be a significant factor for increasing the overall energy efficiency of society

and sustainability level of development. Distillation columns and most of the reactors are based on well-known technology, and one might expect that they are fully developed. The oldest study found on improving the efficiency of distillation was by Miller (1935). But it is known that there is still a large potential for improvement, see Fonyo (1974a,b), Linnhoff and Smith (1979), Rivero (1993), Sauar (1998), Nummedal (2001). This potential for optimisation is the motivation to study distillation and reactors. The largest part of the thesis is about distillation, while one reactor system is also investigated.

1.1.3 Minimising the entropy production rate

Enhancement of the energy efficiency is done by minimising the entropy production rate. The second law of thermodynamics says that for all processes the entropy production rate is equal or larger than zero, i.e. $dS^{\text{irr}}/dt \geq 0$. The entropy production rate is a measure of the departure from reversibility. Since there are no completely reversible processes in reality, every real process produces entropy. The second law efficiency for work requiring processes, like distillation, is defined as (called *thermodynamic* efficiency by Smith and Van Ness (1987)):

$$\eta^{\text{II}} = \frac{\dot{W}^{\text{ideal}}}{\dot{W}^{\text{ideal}} - T^0 \left(dS^{\text{irr}}/dt\right)} \tag{1.1}$$

where $\dot{W}^{\text{ideal}}$ is the minimum required work of the process:

$$\dot{W}^{\text{ideal}} = \left(\sum \dot{\phi} \left(H - T^0 S\right)\right)^{\text{in}} - \left(\sum \dot{\phi} \left(H - T^0 S\right)\right)^{\text{out}} \tag{1.2}$$

$\dot{\phi}\left(H - T^0 S\right)$ is the theoretical work obtained when a flow $\dot{\phi}$ is brought from its present state to a defined reference state, i.e. exergy or available work (Kotas 1995). For a given process, the reference temperature ($T^0 = 298.15$ K) and the minimum required work are fixed. So, minimising the entropy production rate is the same as maximising the second law efficiency. This type of minimisation is known in the field of mechanical engineering, see Bejan (1996).

The minimisation of entropy production rate is a different optimisation than maximising the first law efficiency. The first law of thermodynamics says that energy is conserved. Its energy efficiency is defined for work requiring processes as (called *thermal* efficiency by Smith and Van Ness (1987)):

$$\eta^{\text{I}} = \frac{\text{minimum work required}}{\text{heat input}} = \frac{\dot{W}^{\text{ideal}}}{\sum Q^{\text{in}}} \tag{1.3}$$

Maximising the first law efficiency is only useful if the heat input, $\sum Q^{\text{in}}$, is the only important factor. Since maximising the second law efficiency takes all factors into account by the entropy production rate, it is therefore preferred. These optimisations are independent however. By maximising one, the change of the other one is not given beforehand. It depends on the choice of variables, constraints, and objective function for a given system.

1.1.4 Irreversible thermodynamics as a tool

Irreversible thermodynamics describe phenomena inside systems in terms of fluxes and driving forces, e.g. heat and mass transfer and reactions. Non-zero fluxes and forces mean that the system operates a certain distance from equilibrium. The necessity for irreversible thermodynamics is growing, as more accurate knowledge about phenomena inside systems is required for further improvement (Demirel and Sandler 2001, Wesselingh 1997). This is the motivation to use irreversible thermodynamics in this thesis. The theory of irreversible thermodynamics is described in Kjelstrup and Bedeaux (n.d.), Førland et al. (2001), Kuiken (1994), De Groot and Mazur (1985). Irreversible thermodynamics is also called non-equilibrium thermodynamics.

Irreversible thermodynamics is based on the local entropy production rate in $\mathrm{W/K\,m^3}$. By filling the energy balance, mass balance, charge conservation, second law of thermodynamics, into the Gibbs equation, the local entropy production rate σ is derived as the sum of the products of fluxes J_l'' and local driving forces X_l'' :

$$\sigma = \sum_l J_l'' X_l'' \tag{1.4}$$

In this derivation local equilibrium is assumed (Hafskjold and Ratkje 1995). The total entropy production rate of a process in W/K (dS^{irr}/dt) is obtained from the integration of the local entropy production rate over the volume:

$$\frac{dS^{\text{irr}}}{dt} = \int_{\mathbb{V}} \sigma d\mathbb{V} \tag{1.5}$$

The flux of phenomenon l can be written as a sum of products of phenomenological coefficients and forces:

$$J_l'' = \sum_m \ell_{lm} X_m'' \tag{1.6}$$

Alternatively, the force of phenomenon l can be written as a sum of products

of phenomenological coefficients and fluxes:

$$X_l'' = \sum_m r_{lm} J_m'' \tag{1.7}$$

The coefficients in Eq 1.6 are conductivities, while the ones in Eq. 1.7 are resistivities. These sums of products can be used to describe a manifold of entropy producing phenomena, including coupling. But the flux is not linear in the forces for all phenomena . Reactions are the best known exceptions.

Equations 1.6 and 1.7 provide a systematic manner of describing phenomena, which produce entropy. However, the full non-equilibrium model can become complex, or necessary information (e.g. the coefficients) can be lacking. An entropy balance of the system (see e.g. Bejan (1996), Smith and Van Ness (1987)) can then be used:

$$\frac{dS^{\text{irr}}}{dt} = \left(\sum \dot{\phi} S\right)^{\text{out}} - \left(\sum \dot{\phi} S\right)^{\text{in}} - \sum \frac{Q}{T} \tag{1.8}$$

The first two terms on the right hand side are the flows of entropy from the molar flows in and out of the system, while the last term is the contribution of heat flows in and out. The absolute entropies are calculated from equations of state. Since this balance requires less information than the flux-force equations, it is easier to apply.

This thesis can be seen as a continuation of the Master's thesis of De Koeijer (1997), and the Ph.D. theses of Sauar (1998) and Nummedal (2001). Sauar studied energy efficient process design by equipartition of forces with applications to distillation and chemical reaction. The theorem of equipartition of forces (EoF)[1] says that for a process at minimum entropy production rate the driving forces should be equal along the transport path, provided that the total production is the only constraint. Its derivation is based on irreversible thermodynamics and Euler-Lagrange minimisation. Nummedal (2001) minimised the entropy production rate for heat exchangers, ammonia reactor, and primary steam reformer. His results showed that the state of minimum entropy production rate can be different than the theorem of EoF suggested. The reasons were that the studied systems were more complicated and non-linear, and that the constraints did not comply with the ones leading to EoF. This thesis continues the work of Nummedal with an emphasis on distillation.

[1] In Sauar (1998) it is called the principle of equipartition of forces.

1.2 Purpose

The purpose of this thesis is to determine the most energy efficient operation of distillation columns and a reactor by applying irreversible thermodynamics. For this purpose the entropy production rate is minimised, which is the same as maximising the second law energy efficiency. The aim of the minimisation is to provide chemical industry the thermodynamically optimum operation. The development of chemical industry can be made more sustainable by knowing this minimum.

1.3 Optimisation of distillation

1.3.1 The model

Since the largest part of the thesis is about optimisation of distillation, an introduction is given here. A distillation column is often a steel slim column with sieve trays inside. Figure 1.1 shows a sketch of a column, and Figure 1.2 shows a sieve tray.

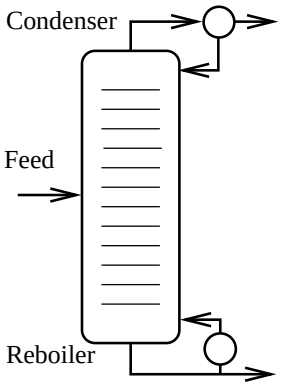

Figure 1.1. Sketch of an adiabatic distillation column

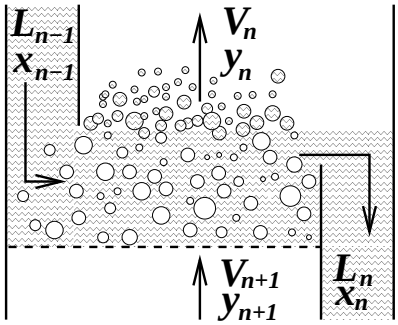

Figure 1.2. Sketch of sieve tray number n

A distillation column separates a feed mixture into two fractions with different boiling temperatures and compositions. On each tray a part of the separation is done. The two flows arriving at the tray, vapour flow V_{n+1} and liquid flow L_{n-1}, are not in equilibrium with each other. Due to mass and heat transfer across the liquid/vapour interface, these flows are brought closer to equilibrium, and leave as V_n and L_n. The top product (distillate) contains the fraction with the lower boiling point, while the bottom product contains the fraction with

the higher boiling point. The top section above the feed is also called the rectifying section, and the section below the feed the stripping section.

A model of distillation is an important tool for studying its behaviour, since experiments on industrial scale are expensive. King (1980) gives an overview. In the context of this thesis, these models can be divided into equilibrium and non-equilibrium types. The equilibrium model is the oldest and most convenient. It assumes that the flows leaving each tray are in equilibrium with each other. As the name already indicated, the non-equilibrium model assumes that the flows leaving the tray are not in equilibrium with each other, see also Taylor and Krishna (1993), Wesselingh (1997), Krishna and Wesselingh (1997). In this work it is pursued to use a fully non-equilibrium model. But at the start of the thesis, the model had to be simple, and we used a model with the equilibrium assumption. Irreversible thermodynamics is then applied to gain insight and experience. Later in the thesis, non-equilibrium models are studied.

All the results are obtained from steady state models. This means that all aspects that are related to time (control, fouling, start-up/shut-down) are not taken into account. These aspects should be taken into account in a later stage.

1.3.2 Adiabatic versus diabatic distillation

A conventional column has only two heat exchangers: the reboiler at the bottom and the condenser at the top, and it is called an adiabatic distillation column, see Fig. 1.1. A known measure for increasing the second law efficiency is to put in heat exchangers on each tray. The theoretical concept was published by Fonyo (1974a) and is shown in Fig. 1.3. He suggested to put side reboilers and condensers after each tray. The column has a vertically stretched diamond shape, because the diameter is taken linear with the vapour flow. Rivero (1993), Le Goff et al. (1996) studied this type of distillation in more depth, and did experiments on a rectifying column. They put the heat exchangers inside the column, and called it diabatic (= non-adiabatic) distillation. Figure 1.4 shows a sketch of the diabatic rectifying column.

In this thesis diabatic distillation is studied. The difference between adiabatic and diabatic columns can be shown with a McCabe-Thiele diagram, see King (1980). Figure 1.5 shows these. The operating lines in the adiabatic column are (nearly) straight, because the vapour and liquid flows are (nearly) constant

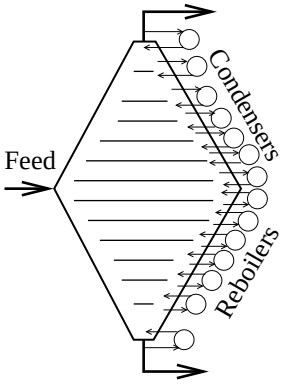

Figure 1.3. Reversible column from Fonyo (1974a)

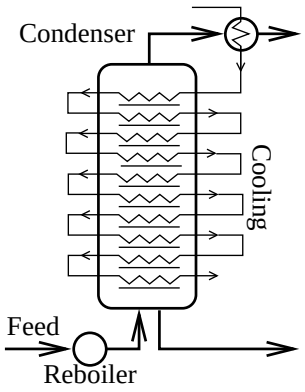

Figure 1.4. Experimental diabatic rectifying column from Rivero (1993)

from tray to tray in each section. The heat exchangers in the diabatic column enable the flows to differ from tray to tray. So, the operating lines can be curved, as shown in the figure. Transport phenomena produce less entropy if they operate closer to equilibrium. So, it is beneficial to put the operating lines as close to the equilibrium line as possible. This means that putting the operating lines roughly parallel to the equilibrium line would be beneficial for the diabatic column.

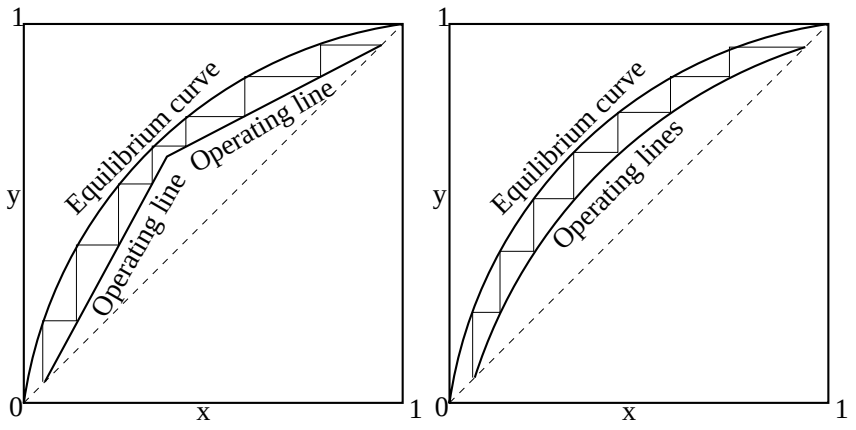

(a) Adiabatic (b) Diabatic

Figure 1.5. McCabe-Thiele diagram of adiabatic and diabatic column

By comparing the McCabe-Thiele diagrams of the adiabatic and diabatic columns, it can be seen that the operating lines of the diabatic column are overall closer than the ones of the adiabatic one (at constant number of trays, and in- and output compositions and flows). So, the ability of the diabatic column to operate closer to equilibrium is one reason why this type of column can be more energy efficient than the adiabatic column. Coupled to this ability, diabatic distillation enables cooling at a higher temperature, and heating at a lower temperature than the adiabatic column. In both cases the negative sum of duties dived by temperature ($-\sum Q/T$, see Eq. 1.8) becomes less. This can also be seen from the Carnot efficiency. These arguments are rough, but valid.

It is pursued in this thesis to determine how to operate this column at minimum entropy production rate with a given separation performance. The question is now to determine how much heat must be removed, or added in those extra heat exchangers. The exact solution is more complicated than Fig. 1.5 suggests. A sketch of the diabatic column at minimum entropy production is drawn in the conclusions as a follow-up of Figs. 1.3 and 1.4.

The benefits of reducing the entropy production rate in distillation may seem not as straightforward as the ones of reducing the energy demand. The reason is that entropy is a measure for the quality of energy. By reducing the entropy production rate, the quality of the inlets are decreased, and/or the quality of the outlets are increased. This can be explained more practically for the case of heating with steam: one needs steam at a lower temperature as input, or receives steam at a higher temperature as output. For cooling with water the same applies: one needs water at a lower temperature, or receives water at a higher temperature. Especially the higher outlet temperatures can make a significant difference. A cooling water outlet can turn from useless in adiabatic column to useful in a diabatic column, which was shown experimentally by Rivero (1993).

1.3.3 Other optimisations

The most common thermodynamic optimisation in distillation until now is not the one of the second law efficiency. But it is the minimisation of the energy demand, i.e. maximising the first law efficiency, see Eq. 1.3. Koehler et al. (1995) gave a review on this topic. The number of trays, location of feed tray and reflux ratio are examples of the main variables. These minimisations are mainly done for adiabatic columns, because these are most common in industry. An economically sound optimisation would be the maximisation of

the net present value of a project (Park and Sharp-Bette 1990). This property decides in the capitalistic system whether a project is going to be done or not. The differences in net present value between the adiabatic and diabatic distillation are still being discussed, but Tondeur and Kvaalen (1987), Kauchali et al. (2000) gave indications that diabatic distillation can be economically feasible. However, it must be said that this is not certain before a design of a diabatic column on industrial scale is worked out. Until then, the results of this thesis can best be seen as a direction in which chemical engineers can design their plants.

1.3.4 Other separation technologies

Beside distillation, there are many other types of separation, like membrane, crystallisation, absorption, and extraction processes. King (1980) discussed several of those. Furthermore, Humphrey and Siebert (1992) calculated that membrane separation has a theoretical first law efficiency of 100 %. But they also say that this separation process can be very expensive. The same publication states that distillation is reliable, has a simple flow-sheet, and has often the lowest capital cost. In the literature other operations with higher second law efficiency than adiabatic distillation columns are described. Adding the heat, that is released in the condenser, via a heat pump in the reboiler is known technology, see King (1980). Furthermore, Mah et al. (1977) evaluated a distillation column with different pressures in rectifying and stripping section; this makes it possible to add the heat, that is removed in the rectifying section, to the stripping section. They called it Secondary Reflux and Vapourisation (SRV) distillation. This type of distillation is used to develop Heat Integrated Distillation Columns (HIDiC), where the reboiler and condenser are removed from the SRV column. The most recent publication found on HIDiC is by Nakaiwa et al. (2001). A HIDiC is also called Internal Thermally Coupled Distillation Column (ITCDIC), see Liu and Qian (2000). Both SRV columns and HIDiC/ITCDIC have a higher energy efficiency than the adiabatic column. But they need compressors which lead to an additional entropy production rate. Furthermore, their direct heat integration between stripping and rectifying section might make it difficult to follow the heat in- and outputs from the state of minimum entropy production rate, which are proposed in this thesis. Finally, a Petlyuk (or thermally coupled) column is an interesting design for separating three components in one column, see again King (1980). It has a higher first law efficiency than two adiabatic columns, but Agrawal and Fidbowsky (1998) showed that this column does not always have higher second law efficiency than the two adiabatic columns.

1.4 Thesis outline

This thesis contains 6 chapters that have been or will be published. The work started in the spring of 1998. Two promising methods for minimising entropy production rate in distillation were already published: the theorems of Equipartition of Forces (EoF, Sauar et al. (1995)) and Equipartition of Entropy Production (EoEP, Tondeur and Kvaalen (1987))[2]. Their simplicity and the improvement potential of distillation were the main reasons to start. There were many open questions. The first one to answer was how to determine the location of two heat exchangers with the EoF theorem. A diabatic column with only two extra heat exchangers has industrial significance, and was easier to optimise than a fully diabatic one (De Koeijer et al. 1999, 2002a).

The thesis starts with the decision to find the global minimum of the entropy production rate of a fully diabatic column, i.e. heat exchangers on all trays. Chapter 2 and De Koeijer and Kjelstrup (2000) contain the development and application of a numerical and analytical method for minimising the entropy production rate of two different columns. Meanwhile, two other methods were published in Schaller et al. (2001), Andresen and Salamon (2000). This led to discussions, and it became clear that the methods needed to be compared. The comparison is given in Chapter 3 and De Koeijer et al. (2001).

The results in the first two chapters were theoretical and computational ones. In order to obtain more understanding, the systems also needed to be studied experimentally. Cooperation with R. Rivero provided the necessary experimental data on diabatic distillation. Experimental verification of the theories is presented in Chapter 4 and De Koeijer and Rivero (2002). The contribution of the heat exchanger was also studied. This led to the next project, presented in Chapter 5 and De Koeijer et al. (2002b). The objective function was extended with the entropy production rate due to heat transfer in the heat exchangers. This meant that the system finally contained the whole column.

An indication that coupling between heat and mass transfer is significant in distillation was also found in Chapter 4. This was further investigated, in combination with our aim to take away the assumption of equilibrium between the flows that leave the tray. In Chapter 6 and Kjelstrup and De Koeijer (2002), we derived an extended set of transport equations with overall coefficients, that quantified the influence of the Soret effect and interface. Finally, optimisation of reactors was also investigated, like Sauar (1998) did. The knowledge ob-

[2]Like EoF, EoEP was called a principle

tained from distillation was used for the minimisation of entropy production rate in a SO_2 converter in Chapter 7.

2 Minimising Entropy Production Rate in Binary Tray Distillation

Gelein de Koeijer and Signe Kjelstrup

Norwegian University of Science and Technology
Department of Chemistry, Physical Chemistry
N-7491 Trondheim
Norway

This paper was published in
International Journal of Applied Thermodynamics, Volume 3, Number 3, pages 105-110, 2000
and
Proceedings of ECOS 2000, ISBN 9036514665, Volume 3, pages 1451-1460, 2000, Enschede, The Netherlands.

Abstract

In this work we increase the second law efficiency in an ideal binary tray distillation column by allowing heat exchangers on all trays. We find by numerical optimisation the duties of the heat exchangers that gives the highest second law efficiency of the column. The entropy production rate was reduced by 30-50% compared to adiabatic operation for two different columns. The numerical optimum was in agreement with the result of an Euler-Lagrange minimisation in which the total entropy production rate was described by irreversible thermodynamics. The minimum was not characterised by equipartition of forces.

2.1 Introduction

Distillation is widely used in the process industry despite its low second law efficiency (5-20%). We have studied the addition of heat exchangers on the trays as a way to increase the efficiency in ideal binary tray distillation, that is diabatic distillation, see Rivero (1995) and Le Goff et al. (1996). In this work we allow heat exchangers on all trays. The aim of the work is to find the variation of the duties of these exchangers across the column (called duty profile) that gives the minimum entropy production rate. A numerical method will be compared with an analytical method based on irreversible thermodynamics. We optimise two different example columns that perform a given separation, i.e. the same amounts and mole fractions in the distillate and bottom. Another objective is to compare the solutions of the methods with the principle of equipartition of forces. This principle says that the force is constant on each tray in the case of minimum entropy production (Sauar 1998, Kjelstrup Ratkje et al. 1995). It is known that this solution is not true if the number of constraints on the minimisation is increased beyond that of constant production (amount of transferred mass), see Bedeaux et al. (1999). Sauar (1998) also found limitations to the principle of equipartition of forces.

2.2 The system

The binary tray distillation column has heat exchangers on all trays. We calculate the entropy production rate due to heat and mass transport through the liquid-gas interface on each tray, see Eq. 2.1 below. The entropy production rate due to the temperature difference between the in- and outlet of the cooling and heating media is not taken into account at this stage.

Table 2.1. Column parameters

	Alkane	Alcohol
Component 1	n-pentane	methanol
Component 2	n-heptane	isopropyl alcohol
Pressure (bar)	1.00	0.75
Feed (mol/s)	100	100
Distillate (mol/s)	26.531	48.913
Bottom (mol/s)	73.469	51.087
x_1^{F}	0.270	0.500
x_1^{D}	0.990	0.970
x_1^{B}	0.010	0.050
Trays	15	19
Feed tray	8	10

The column is defined by the pressure, feed flow (F), distillate flow (D), number of trays (N), feed tray location, mole fractions in the feed (x_i^{F}), and the mole fractions in the distillate (x_i^{D}), see Table 2.1. Mass balances then gives the bottom flow (B) and the mole fractions in the bottom (x_i^{B}). These parameters are also given in the table. The reboiler and condenser are the first and last tray, respectively. The feed tray is the one which gives minimum entropy production rate in the adiabatic column.

2.3 Theory

2.3.1 Three flows and their corresponding forces

Figure 2.1 illustrates the details of the processes on a tray. The flows and mole fractions below tray number n have subscript n; the flows and mole fractions above tray number n have subscript $n+1$[1].

The flow of component i on tray n, $J_{i,n}$, is the flux times the area of transfer. This area is assumed to be constant during the equilibration process on the trays. The entropy production rate for tray number n is then (De Koeijer et al. 1999)[2]:

$$\frac{dS_n^{\mathrm{irr}}}{dt} = J_{\mathrm{q},n}\Delta_n\left(\frac{1}{T}\right) - J_{1,n}\frac{1}{T_n}\Delta_n\mu_{1,T} - J_{2,n}\frac{1}{T_n}\Delta_n\mu_{2,T} \tag{2.1}$$

[1] In the rest of the thesis the other way of numbering will be used, where the flows that leave the tray have the same number.

[2] See De Koeijer et al. (2002a)

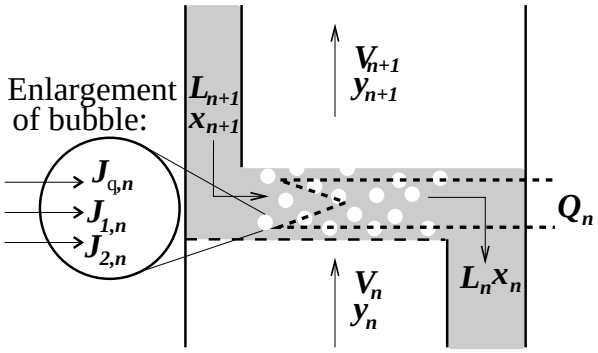

Figure 2.1. Schematic representation of a tray

The flows are the flows of measurable heat $(J_{\mathrm{q},n})$[3] and mass $(J_{i,n})$ from the liquid into the gas phase. The forces for mass transport$(-\Delta_n \mu_{i,T}/T_n)$ and heat transport$(\Delta_n\,(1/T))$ are obtained by integrating between the vapour in- and outlets of tray n (with the assumption of a constant averaged flow during the equilibration process). In terms of vapour mole fractions (y) we have for the force for mass transport:

$$X_{i,n} = -\frac{1}{T_n}\Delta_n \mu_{i,T} = -R \ln \frac{y_{i,n+1}}{y_{i,n}} \tag{2.2}$$

In the integration, it is assumed that the process ends when there is equilibrium on the tray. The assumptions behind Eq. 2.1, are not correct on a molecular level, but provide a good approximation for this work.

2.3.2 The entropy production rate in reduced form

The expression 2.1 is still complicated, and a simplified version is sought. Our experience so far in Kjelstrup Ratkje et al. (1995), De Koeijer et al. (1999) is that the thermal force and flow gives a small contribution to the entropy production (<8%). We shall therefore neglect the first term to the right in Eq. 2.1. The two remaining terms are related by the Gibbs-Duhem equation. We shall use:

$$-\overline{y}_n \Delta \mu^{\mathrm{V}}_{1,T} = \Delta \mu^{\mathrm{V}}_{2,T} \quad \text{where} \quad \overline{y}_n = \sqrt{\frac{y_{1,n} y_{1,n+1}}{y_{2,n} y_{2,n+1}}} \tag{2.3}$$

[3] De Groot and Mazur (1985) and Kjelstrup and Bedeaux (n.d.) use $J'_{\mathrm{q},n}$ for the same property

By integrating only over variations in the vapour phase, we have assumed that the entropy production rate in the system is in the vapour, and/or at the boundary between gas and liquid. The reduction of the entropy production rate to a one flow - one force expression is now possible:

$$\frac{dS_n^{\mathrm{irr}}}{dt} = (-J_{1,n} + \overline{y}_n J_{2,n})\frac{1}{T_n}\Delta\mu_{1,T} = J_n^{\mathrm{tot}} X_{1,n} \tag{2.4}$$

Better approximations for the flows and forces than these may be found when phenomenological coefficients become available (Bedeaux et al. 1999), and we do not longer need the assumption of equilibrium between liquid and vapour at the outlets on all trays. The entropy production rate on a tray can be calculated from Eq. 2.4, but also from the entropy balance on each tray:

$$\frac{dS_n^{\mathrm{irr}}}{dt} = V_{n+1}S_{n+1}^{\mathrm{V}} + L_n S_n^{\mathrm{L}} - V_n S_n^{\mathrm{V}} - L_{n+1}S_{n+1}^{\mathrm{L}} - \frac{Q_n}{T_n} \tag{2.5}$$

The entropies (S) are given by an equation of state, and Q_n is the heat added from the heat exchanger at tray n and temperature T_n. We shall use Eq. 2.5 to evaluate Eq. 2.4.

2.3.3 Euler-Lagrange minimisation

The minimum value of the entropy production rate in Eq. 2.4 is pursued, given the boundary conditions listed in Table 2.1. The minimisation problem can be formulated as Biegler et al. (1997):

$$\begin{aligned}
\min \quad & \sum_1^N \frac{dS_n^{\mathrm{irr}}}{dt} = \sum_1^N J_n^{\mathrm{tot}} X_{1,n} \\
\text{s.t.} \quad & Fx_1^F - Bx_1^B = Dx_1^D = \sum_1^N J_{1,n} = I_1 \\
& Fx_2^F - Bx_2^B = Dx_2^D = \sum_1^N J_{2,n} = I_2 \\
& R\ln\left(\frac{x_1^D}{x_1^B}\right) = \sum_1^N X_{1,n} = I_3 \\
& R\ln\left(\frac{x_2^D}{x_2^B}\right) = \sum_1^N X_{2,n} = I_4
\end{aligned} \tag{2.6}$$

The two constraints on the flows, with values I_1 and I_2, represent the productions (or transferred amounts of mass) of the two components. The last two constraints, I_3 and I_4, fix the energy levels of the output flows (the chemical potentials of the two components). The four constraints are independent of one another. By working out Eq. 2.6, we obtain:

$$2J_n^{\mathrm{tot}} = -\lambda_1 \ell_{1,n} - \lambda_2 \ell_{2,n} - \lambda_3 + \lambda_4 \overline{y}_n \qquad \text{where} \qquad \ell_{i,n} = \frac{J_{i,n}}{X_{1,n}} \tag{2.7}$$

The λ's are the Lagrange multipliers. The result does not depend on the variable chosen for the minimisation ($X_{1,n}$, $X_{2,n}$, $J_{1,n}$, $J_{2,n}$ or J_n^{tot}). The minimum entropy production rate should be characterised by Eq. 2.7. The equation means that we neither have a uniform distribution of forces, nor of entropy production.

2.4 Calculation procedure

The tray column simulation method described earlier by De Koeijer et al. (1999) gave mole fraction -, flow -, and temperature profiles. Entropies were obtained from the Peng-Robinson equation of state. The entropy production was calculated according to Eqs. 2.4 and 2.5. A minimisation algorithm was constructed, called a bouncing algorithm[4], containing a random and a deterministic part. The numbers given in the following are illustrative. To start, a duty profile was chosen that did not violate mass and/or energy balances. The randomisation part consisted of the generation of a new profile by a random stepwise increase or decrease of the duty on one random tray. The new duty profile was simulated accordingly. In the cases that the entropy production rate became higher or that the mass- and/or energy balances were violated, the new duty profile was rejected, and a new random step was made from the previous duty profile. In the case that the entropy production rate became smaller, the new duty profile was accepted as a new starting point. As the deterministic element the random step was multiplied by an exponentially decreasing factor f. In this way the entropy production rate decreased to a minimum. To bounce out of a possible local minimum, the entropy production rate was multiplied by a factor 1.5 and the procedure repeated 1000 times, starting with a high value for the factor f. In this way the entropy production can bounce out of a local minimum and hopefully end up bouncing around the global minimum. We cannot prove that this numerical procedure guarantees a global minimum.

[4]This algorithm is similar to the ones in Chapters 3 and 5, and is called the Monte Carlo algorithm

On the other hand, we were able to reproduce the results by repeating the procedure, with different starting points and algorithm parameters. Also the bouncing in and out of local minima could be observed.

2.5 Results and discussion

2.5.1 Consistency of data sets

The entropy production rate was calculated from Eq. 2.4 and plotted as a function of the entropy production rate from Eq. 2.5 for all trays in the adiabatic as well as the diabatic columns. Figure 2.2 gives the results for the pentane-heptane column and Figure 2.3 gives the same for the methanol-isopropylalcohol column. Each point in the figures represents one tray.

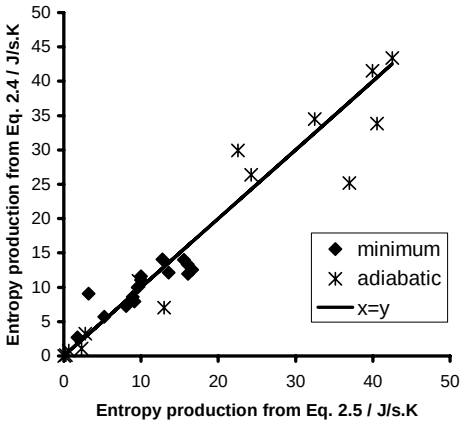

Figure 2.2. The entropy production rates by alkane separation of Eqs. 2.4 and 2.5

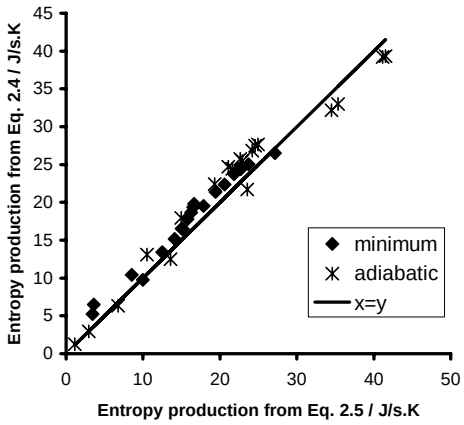

Figure 2.3. The entropy production rates by alcohol separation of Eqs. 2.4 and 2.5

We see that there is good consistency between results from the two equations for both columns with minimum entropy production rate, see the dark points in both figures. Only for the adiabatic column that separates alkanes, the consistency was less good. The consistency is overall remarkable, considering the number of assumptions that we have used. Model errors in the Peng-Robinson equation of state may also contribute to the deviations.

2.5.2 The duty and temperature profiles from the numerical minimisation procedure

The results of the numerical minimisation are given in Figure 2.5 for the alcohol column and in Figure 2.4 for the alkane column. The duty profile in the corresponding adiabatic columns are also given in the figures. The heat exchanger at tray number 1 is the reboiler and the heat exchanger at the tray number 15 (alkane column) or 19 (alcohol column) is the condenser. The total entropy production rate in the alkane column was reduced with 47% (from 295.3 to 156.4 J/s K) and in the alcohol column with 29% (from 425.1 to 300.8 J/s K) by applying the given duty profiles.

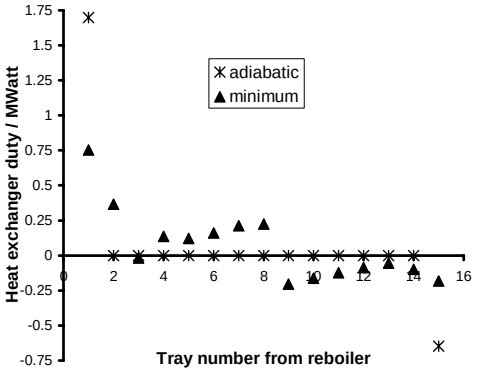

Figure 2.4. Duty profiles of the alkane separating columns

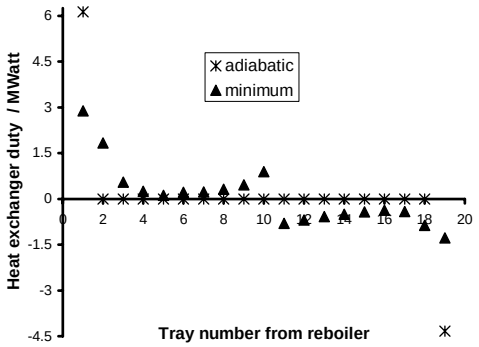

Figure 2.5. Duty profiles of the alcohol separating columns

The adiabatic columns have a large positive heat supply in the reboiler, and a large negative heat supply (i.e. a heat release) in the condenser. Otherwise the duties on the trays are zero, as required by the definition of an adiabatic column. The diabatic columns with minimum entropy production rate have the highest positive duties in the reboiler, next to the reboiler and below the feed tray. The highest negative duties are in the condenser, next to the condenser, and above the feed tray. The corresponding temperature profiles are given in Figure 2.6 and 2.7.

The first observation is that the profiles of the columns with minimum entropy production rate are straighter. Secondly, in both profiles the differences between adiabatic and minimum columns are smaller for alcohol separation than for alkane separation (compare Figures 2.4 and 2.6 with 2.5 and 2.7). This explains the different relative savings on entropy production rate in the

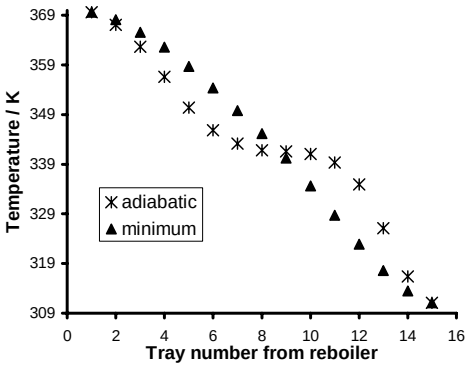

Figure 2.6. Temperature profiles of the alkane separating columns

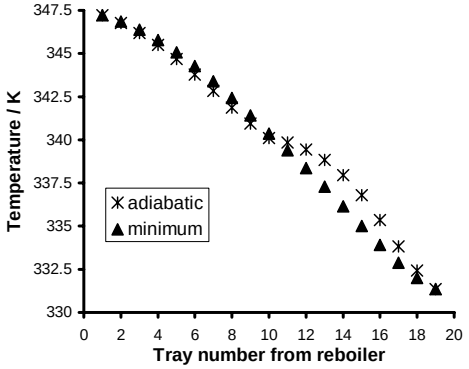

Figure 2.7. Temperature profiles of the alcohol separating columns

two columns. The absolute values of the duties and temperatures given here depend on parameters in Table 2.1.

2.5.3 Comparison of the Lagrange and numerical minimisation procedure

The results from Figures 2.4, 2.5, 2.6, and 2.7 were fitted to Eq. 2.7 using multi-variable linear regression. The resulting Lagrange multipliers and their standard errors are given in Tables 2.2 and 2.3.

Table 2.2. Lagrange multipliers of the minimum entropy producing alkane column

	referring to		unit
λ_1	$\ell_{1,n}$	-1.26±0.11	J/mol K
λ_2	$\ell_{2,n}$	3.08±0.24	J/mol K
λ_3	intercept	-5.64±0.73	mol/s
λ_4	$\overline{y}_n$	1.56±0.098	mol/s

Table 2.3. Lagrange multipliers of the minimum entropy producing alcohol column

	referring to		unit
λ_1	$\ell_{1,n}$	-0.734±0.063	J/mol K
λ_2	$\ell_{2,n}$	1.20±0.10	J/mol K
λ_3	intercept	-17.8±1.6	mol/s
λ_4	$\overline{y}_n$	7.06±0.53	mol/s

The tables show that Eq. 2.7 reproduces the results well. The regression coefficients for the fit were 0.995 for the alkane separating column and 0.989 for the alcohol separating column, and rather straight normal probability plots were observed. The data for the adiabatic columns did not show compliance with equation 2.7. It was observed that the compliance increased with decreasing entropy production rate. The signs of the Lagrange multipliers seem likely. The two components are transferred through the phase boundary in opposite directions. The Lagrange multipliers of the forces and flows, should therefore have opposite signs for the two components, which is indeed observed. We conclude that Eq. 2.7 is a good model for the minimum entropy production rate of these two binary distillation columns. Mathematical expressions for the Lagrange multipliers are now lacking. Such expressions will make the theory independent of the numerical minimisation. A more quantitative analysis of the entropy production rate is required before industry can use the results. We have neglected the contribution of the cooling/heating media in the heat exchangers to the entropy production of the total column. This is most probably a non-negligible contribution.

2.5.4 Comparison with isoforce operation

For a column with minimum entropy production, Sauar (1998) and Kjelstrup Ratkje et al. (1995) have derived the principle of equipartition of forces using only the first two constraints given above in Eq. 2.6. The operating path of the column was then given by an equal distribution of the forces (isoforce operation). The in- and output mole fractions were not restricted. The literature on this principle supported that this operation was possible (Sauar et al. 1997), but Sauar (1998) observed also limitations. Mass balances appeared to be violated in the upper part of a column. We conclude that in general binary diabatic distillation with fixed separation has not enough freedom to adjust to isoforce operation. To come closer to isoforce operation, the designer must be willing to remove the constraints on the forces and to restrict only the amounts of transported mass. A design measure to get the forces more equal on each tray might be to feed on each tray, in addition to the heat exchangers. This might solve the observed mass balance violations. The importance of this work lies more in the method than in the obtained results. Numerical minimisation methods, like the bouncing algorithm[5] used here, provide the minimum value of the entropy production rate, but no theoretical basis for it. Our work aims to give such a basis, by investigating the nature of minimum entropy produc-

[5] i.e. Monte Carlo algorithm

tion rate. Systematic efforts should be made to characterise column boundary conditions, that are compatible with minimum entropy production rate. Diabatic distillation is a well known method to reduce entropy production rate, see Rivero (1995). But isoforce operation represents a minimum in entropy production rate that need more degrees of freedom in design than offered by diabatic distillation. It is important to understand the minimum entropy production rate in a diabatic column. But it is also important to find boundary conditions that give isoforce operation, because this operation has yet a lower minimum entropy production rate.

2.6 Conclusion

A numerical method has been demonstrated that finds the state of minimum entropy production rate in distillation columns with heat exchangers on all trays. The method gives results that are consistent with a theoretical description, based on irreversible thermodynamics and the Euler-Lagrange method. For diabatic distillation with fixed separation it is required that also in- and output energy levels are constraints in the Euler-Lagrange variation. The calculation was simplified with sufficient accuracy, when the entropy production rate was described with only one force and one flow. Future work is now to include the contribution of the heat exchangers into the theoretical minimisation, and to a priori determine the values of the Lagrange multipliers.

Acknowledgement

The Research Council of Norway is thanked for a grant to Gelein de Koeijer.

3 Comparison of Entropy Production Rate Minimisation Methods for Binary Diabatic Tray Distillation

Gelein de Koeijer[1], Signe Kjelstrup[1], Peter Salamon[2], Gino Siragusa[2], Markus Schaller[3], Karl Heinz Hoffmann[3]

1. Norwegian University of Science and Technology
Department of Chemistry, Physical Chemistry
N-7491 Trondheim
Norway

2. San Diego State University
Department of Mathematical Sciences
CA 92182-7720 San Diego
USA

3. Chemnitz University of Technology
Institute of Physics
D-09107 Chemnitz
Germany

This paper was published in
Proceedings of ECOS 2001, ISBN 975-97568-2-2, volume II, pages 667-677, 2001, Istanbul, Turkey.

Paper II is not included due to copyright.

4 Entropy Production and Exergy Loss in Experimental Distillation Columns

Gelein de Koeijer* and Ricardo Rivero

Instituto Mexicano del Petroleo
Exergy group
07730 Mexico City
Mexico

* current address:
Norwegian University of Science and Technology
Department of Chemistry, Physical Chemistry
N-7491 Trondheim
Norway

This paper is sent in for publication

Abstract

Diabatic distillation, i.e. with heat exchangers on all trays, can increase the second law efficiency drastically compared to adiabatic distillation. The purpose of this research was to describe the entropy production rate in one adiabatic and one diabatic experimental water/ethanol rectifying column by applying the theory of irreversible thermodynamics. As a benchmark for the description, an exergy analysis of the two columns was used. This analysis showed that the diabatic column looses 39 % less exergy than the adiabatic column. Heat and mass transfer on the trays and in the heat exchangers determined the entropy production, and neither pressure nor mixing effects played a large role in these columns. The significance of this work is the experimental confirmation of the theory on diabatic distillation.

4.1 Introduction

Most of the distillation columns are adiabatic with a reboiler at the bottom, a condenser at the top, and adiabatic trays in between. If heat exchangers are added on each tray, the second law efficiency can be increased drastically, see Fonyo (1974a,b), Le Goff et al. (1996), Agrawal and Fidbowski (1996), Sauar et al. (1997). Distillation with heat exchangers on all trays is called diabatic distillation, and has been studied with several designs and different names. Mah et al. (1977) evaluates a diabatic distillation column with different pressures in rectifying and stripping section; this makes it possible to add the heat, that is removed in the rectifying section, to the stripping section. They call it Secondary Reflux and Vaporisation (SRV) distillation. Liu and Qian (2000) take out the reboiler and condenser from the SRV column, and call it Internal Thermally Coupled Distillation Columns (ITCDIC). Here, only a diabatic rectifying column is considered with condenser and reboiler, and with neither compressors nor valves.

Nearly all publications on these types of distillation have been based on theoretical simulations that use the assumption of equilibrium on all trays, except two: Rivero (1993) and Rivero et al. (1993), who have published experimental data on diabatic distillation of ethanol/water. Although the assumption of equilibrium on all trays is a convenient way of modelling, it is incorrect according to Wesselingh (1997) for real distillation. In general there is a need for non-equilibrium descriptions for correct modelling of distillation columns.

Irreversible thermodynamics is a general theory that describes non-equilibrium processes, see Førland et al. (2001), De Groot and Mazur (1985). It describes the entropy production rate systematically, including coupling, in terms of fluxes and driving forces. The use of irreversible thermodynamics is relatively new to the field of distillation, and is still under development. The pillar of irreversible thermodynamics is the entropy production rate. So, it is by origin suitable for processes where second law analysis and optimisation are important. Diabatic distillation is typically such a process. A model for non-equilibrium distillation based on semi-empirical chemical engineering is however established, see for example Taylor and Krishna (1993), Krishnamurthy and Taylor (1985a,b). But a well established model based on the entropy production rate from irreversible thermodynamic can provide a good alternative.

Irreversible thermodynamics has already been used for describing heat and mass transfer through the interface in simulated equilibrium columns, see Sauar (1998), De Koeijer et al. (1999)[1], De Koeijer and Kjelstrup (2000), but not yet for columns where the theory is made for: real non-equilibrium columns. Furthermore, the second large contributor to the irreversibilities in diabatic distillation, the heat transfer in the heat exchangers, is not taken into account. This contribution will be included in this work, so that all heat and mass transfer on the trays and in the heat exchangers are described. The purpose of this work is to investigate how the description performs by applying it to experimental results of water/ethanol rectifying columns. The data of one diabatic and one adiabatic non-equilibrium column as published by Rivero (1993) and Rivero et al. (1993) will be used. The second purpose is to analyse the experimentally measured irreversibilities with the theoretical descriptions from irreversible thermodynamics. Such analyses have been done by Taprap and Ishida (1996), Ray and Sengupta (1996) for simulated columns. Their results will be compared.

4.2 Experimental set-up

The experimental column was described in detail by Rivero (1993). Here follows a short summary. Two (run 1 and 9) of the 68 runs in Rivero (1993) are chosen: one adiabatic and one diabatic. This choice is based on the similarity of mole fractions and flows of the feed and products. The other runs were not suitable for comparison. A scheme of one tray can be found in Figure 4.1. A scheme of the columns can be found further on in Figure 4.2. The design

[1] See De Koeijer et al. (2002a)

parameters are given in Table 4.1.

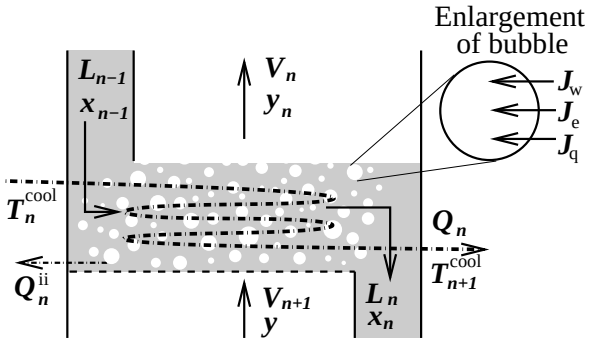

Figure 4.1. Scheme of a tray.

Table 4.1. Column parameters.

Number of trays	10
Diameter (m)	0.15
Distance between trays (m)	0.275
Total height (m)	2.90
Total plate area/active plate area (10^{-4} m^2)	176.7/154.6
Plate height (10^{-3} m)	2
Perforation diameter (10^{-3} m)	2
Number of perforations (-)	125
Heat exchanger coil area (10^{-4} m^2)	240
Heat exchanger coil diameter (10^{-3} m)	6.35
Downcomer height above tray (10^{-3} m)	20
Downcomer area (10^{-4} m^2)	11.05
Condenser heat exchange area (m^2)	1.00
Reboiler heat exchange area (m^2)	0.500
Oil flow into reboiler (kg/s)	0.160
Temperature of oil going into reboiler (K)	433.5
Temperature of water going into condenser (K)	287.1

4.3 Exergy analysis as a benchmark

For assessing the performance of the equations from irreversible thermodynamics (see Eqs. 4.5, 4.10, and 4.16 further on) a benchmark is needed. Rivero (1993) already performed an exergy analysis (Kotas 1995) of the experimen-

tal results. This will be used as the benchmark. Exergy loss and entropy production rate are related to each other by the Gouy-Stodola theorem:

$$\Delta \dot{E}x = T^0 \frac{dS^{\mathrm{irr}}}{dt} \tag{4.1}$$

By dividing the exergy loss by the temperature of the surroundings ($T^0 = 298\ K$), the corresponding entropy production rate of the exergy benchmark is obtained. The better an equation from irreversible thermodynamics describes this corresponding entropy production rate, the better that equation is.

The exergy loss in Rivero (1993) is divided into losses on the trays (Eq. 4.2), losses in the heat exchangers (Eq. 4.3), and outputs. The contributions due to heat and mass transfer on the trays, and due to heat transfer in the heat exchangers are pursued to be described with irreversible thermodynamics. The losses due to the outputs are the same as their corresponding exergy value. These outputs are not described by irreversible thermodynamics, because the main interest is the irreversibilities on the trays and in the heat exchangers. The exergy loss on tray n ($\Delta_n \dot{E}x$) is calculated with an exergy balance over the tray (see Figure 4.1 for the symbols and numbering):

$$\Delta_n \dot{E}x = V_{n+1} Ex^{\mathrm{V}}_{n+1} + L_{n-1} Ex^{\mathrm{L}}_{n-1} - V_n Ex^{\mathrm{V}}_n - L_n Ex^{\mathrm{L}}_n + Q_n \left(1 - \frac{T^0}{T_n}\right) \tag{4.2}$$

The exergy loss in the heat exchanger ($\Delta_n \dot{E}x^{\mathrm{HX}}$) is calculated with a balance over the heat exchanger:

$$\Delta_n \dot{E}x^{\mathrm{HX}} = \dot{m} \left(Ex^{\mathrm{cool}}_n - Ex^{\mathrm{cool}}_{n+1}\right) - Q_n \left(1 - \frac{T^0}{T_n}\right) \tag{4.3}$$

Imperfect insulation of the trays causes a small heat output (Q^{ii}_n) on each tray. This output is calculated with the energy balance. Its exergy loss is calculated by:

$$\Delta_n \dot{E}x^{\mathrm{ii}} = Q^{\mathrm{ii}}_n \left(1 - \frac{T^0}{T_n}\right) \tag{4.4}$$

Equations 4.2 and 4.3 form an accurate way for obtaining the exergy losses due to all phenomena taking place on the trays and in the heat exchangers (mass transfer, heat transfer, mixing, turbulence, pressure drop etc.). But in this analysis it lumps all phenomena together, and does not distinguish between these phenomena. Exergy analysis based on balances can distinguish however

between the contributions of heat transfer, mass transfer and pressure difference. But it can neither determine coupling, nor distinguish between the components of the phenomena, the forces and flows. Irreversible thermodynamics has these features per definition. In contrast to exergy analysis, irreversible thermodynamics does not need entropies and enthalpies for calculating the entropy production rate.

4.4 Irreversible thermodynamics

4.4.1 Heat and mass transfer through the interface

A common conclusion in previous analyses of irreversibilities in distillation (Taprap and Ishida 1996, Ray and Sengupta 1996) is that mass transfer is the largest contributor to the entropy production rate. They differ in what the other large contributors are. Ray and Sengupta (1996) calculated that the drag on the bubbles and work against the liquid during bubble growth are significant contributions. Taprap and Ishida (1996) does not mention this, but shows via Energy Utilisation Diagrams that the contribution of mixing is comparable to the one of mass transfer. In this work the focus will be only on the mass and heat transfer, and it will be shown that that is sufficient. So, pressure and mixing effects are not taken into account.

Figure 4.1 gives a scheme of tray n with the variables, including numbering. The enlargement of the bubble shows the three flows through the interface causing the entropy production rate. J_{w} and J_{e} are the number of moles of water and ethanol transferred per second from the liquid into the vapour, i.e. mass transfer rates through the phase boundary. J_{q} is the corresponding measurable (or Fourier type) heat flow through the interface, or alternatively heat transfer rate. In this section only the equations used in this work are given. Other descriptions and further details about the background and assumptions can be found in Sauar (1998), Kjelstrup Ratkje et al. (1995), De Koeijer et al. (1999)[2]. The entropy production rate on tray n due to heat and mass transfer through the interface are described by three flow-force products:

$$\frac{dS_n^{\mathrm{irr}}}{dt} = J_{\mathrm{q},n}X_{\mathrm{q},n} + J_{\mathrm{w},n}X_{\mathrm{w},n} + J_{\mathrm{e},n}X_{\mathrm{e},n} \tag{4.5}$$

In this equation the J's are the flows (or integrated fluxes or transfer rates) and the X's are the average driving forces between inlets and outlets of tray n. The averaging of the forces and the integration of the fluxes are discussed

[2]See De Koeijer et al. (2002a)

by De Koeijer et al. (1999) and Kjelstrup Ratkje et al. (1995). The average force for heat transfer on tray n is:

$$X_{\mathrm{q},n} = \Delta\left(\frac{1}{T}\right) = \frac{1}{2}\left(\frac{1}{T_{n+1}} - \frac{1}{T_{n-1}}\right) \tag{4.6}$$

Because water-ethanol is a non-ideal mixture, the driving force for mass transfer must include the activity coefficients (γ). The average force of component i on tray n is:

$$X_{i,n} = -\frac{1}{T}\Delta\mu_{i,T} = \frac{1}{2}R\ln\frac{x_{i,n-1}\gamma_i(x_{i,n-1})P_i^*(T_{n-1})x_{i,n}\gamma_i(x_{n,i})P_i^*(T_n)}{y_{i,n}y_{i,n+1}P^2} \tag{4.7}$$

The saturation pressures (P_i^*) are calculated with the integrated form of the Clausius-Clapeyron equation for a regular solution. The Margules parameters for the activity coefficient are $A_{12} = 1.6711$ and $A_{21} = 0.9006$. The pressure is assumed to be constant at 10^5 Pa. Alternative driving forces have been proposed by Zemp et al. (1997), Taprap and Ishida (1996), Gani and Bek-Pedersen (2000), which are all useful in their context. However, the difference in chemical potential is preferred in this work, because it is a direct result of the derivation of the entropy production rate (Førland et al. 2001). The flow of moles of component i through the interface is derived in the interface frame of reference from the mass balance over the vapour phase:

$$J_{i,n} = V_n y_{i,n} - V_{n+1}y_{i,n+1} \tag{4.8}$$

The measurable heat flow is derived from the energy balance over the vapour phase:

$$\begin{aligned} J_{\mathrm{q},n} =& V_n(T_n^{\mathrm{V}} - \overline{T}^{\mathrm{V}})\left[y_{\mathrm{w},n}C_{P,\mathrm{w}}^{\mathrm{V}} + y_{\mathrm{e},n}C_{P,\mathrm{e}}^{\mathrm{V}}\right] - \\ & V_{n+1}(T_{n+1}^{\mathrm{V}} - \overline{T}^{\mathrm{V}})\left[y_{\mathrm{w},n+1}C_{P,\mathrm{w}}^{\mathrm{V}} + y_{\mathrm{e},n+1}C_{P,\mathrm{e}}^{\mathrm{V}}\right] \end{aligned} \tag{4.9}$$

$\overline{T}^V$ is the arithmetic average temperature of the vapour, i.e the average temperature at which the components are transfered through the interface. For an equilibrium column, Eq. 4.5 can be simplified to one force-flow product. The thermal contribution is neglected, all entropy production is located in the vapour phase, and the Gibbs-Duhem equation is applied. This is done by De Koeijer and Kjelstrup (2000), and satisfactory results were obtained for two different columns. The description for the entropy production rate was:

$$\begin{aligned} \frac{dS_n^{\mathrm{irr}}}{dt} &= \left(J_{\mathrm{w},n} - \overline{y}_n J_{\mathrm{e},n}\right) X_{\mathrm{w},n}^{\mathrm{V}} \\ &= \left(J_{\mathrm{w},n} - \sqrt{\frac{y_{\mathrm{w},n}y_{\mathrm{w},n+1}}{y_{\mathrm{e},n}y_{\mathrm{e},n+1}}}J_{\mathrm{e},n}\right) R\ln\frac{y_{\mathrm{w},n}}{y_{\mathrm{w},n+1}} \end{aligned} \tag{4.10}$$

This equation contains only one force-flow product, which is in agreement with the one thermodynamic degree of freedom in a column with equilibrium on all trays. The performance of this one flow-force equation will be compared, together with three flow-force equation, with the exergy benchmark. The existence of these two equations claiming to describe the same, but with different assumptions, shows both an advantage and a disadvantage of the use of the theory of irreversible thermodynamics. The advantage is that one has insight about the phenomena that produce entropy due to all the beforehand posed assumptions. The disadvantage is that it demands (complex) knowledge of the transfer phenomena. In the case of diabatic distillation, there are good reasons for the extra effort accompanied by the use of irreversible thermodynamics. First, the desired higher second law efficiency makes entropy production rate a key issue. Secondly, a full phenomenological analysis can provide a good understanding, and hence a well founded design for this promising process.

4.4.2 Heat transfer in the heat exchangers

The local entropy production rate due to heat transfer (σ in J/K.s.m^3) can be described as a product of measurable heat flux (J/s.m^2) and thermal driving force (1/K.m):

$$\sigma = J''_{\mathrm{q}} \nabla \left(\frac{1}{T} \right) \tag{4.11}$$

By integrating the flux (J''_{q}) and averaging the driving force between the cooling water and the liquid in the column, one gets the entropy production rate in J/K.s in terms of flow ($J_{\mathrm{q},n}$) in J/s and average force in 1/K:

$$\frac{dS_n^{\mathrm{irr,HX}}}{dt} = J_{\mathrm{q},n} \Delta \left(\frac{1}{T} \right) = Q_n \left(\frac{1}{\overline{T}_n^{\mathrm{cool}}} - \frac{1}{T_n^{\mathrm{column}}} \right) = Q_n X_n^{\mathrm{HX}} \tag{4.12}$$

In this expression, the arithmetic average of the temperature of the cooling medium is used:

$$\overline{T}_n^{\mathrm{cool}} = \frac{T_n^{\mathrm{cool}} + T_{n+1}^{\mathrm{cool}}}{2} \tag{4.13}$$

The mass balance over the vapour phase shows that the sum of the mass flows are the same as the difference between the vapour flows. And it is this difference between the vapour flows that can be assumed to be largely caused by the duty of the heat exchanger. In terms of equations this becomes:

$$J_{\mathrm{w},n} + J_{\mathrm{e},n} = V_n - V_{n+1} \approx \frac{Q_n}{\Delta_{\mathrm{vap}} \overline{\overline{H}}} \tag{4.14}$$

Table 4.2. Measured results of the adiabatic and diabatic columns.

	Diabatic	Adiabatic
Feed (mol/s)	0.318	0.331
Distillate (mol/s)	0.028	0.030
Bottom (mol/s)	0.291	0.301
Feed temperature (K)	344.8	358.4
Distillate temperature (K)	291.6	349.3
Bottom temperature (K)	369.1	370.8
Feed mole fraction ethanol (-)	0.0675	0.0710
Distillate mole fraction ethanol (-)	0.6972	0.7073
Bottom mole fraction ethanol (-)	0.0073	0.0074
Top pressure (10^5 Pa)	0.994	1.011
Bottom pressure (10^5 Pa)	0.995	1.021
Water flow into condenser (and heat exchangers) (mol/s)	2.10	3.11
Measurement error in temperatures (K)	0.11	0.45
Measurement error in mole fractions (-)	0.012	0.008

The average heat of vapourisation ($\Delta_{\text{vap}}\overline{H}$) is in this column given by:

$$\Delta_{\text{vap}}\overline{H} = \frac{\sum_1^{10} Q_n}{V_1 - V_{11}} \tag{4.15}$$

These relationships are only true if a linear relation between duty of the heat exchanger and the increase of vapour flow can be assumed. By combining with Eq. 4.5, the total entropy production rate for tray n with a heat exchanger becomes:

$$\frac{dS_n^{\text{irr}}}{dt} = J_{\text{q},n}X_{\text{q},n} + J_{\text{w},n}X_{\text{w},n} + J_{\text{e},n}X_{\text{e},n} + \Delta_{\text{vap}}\overline{H}\,(J_{\text{w},n} + J_{\text{e},n})\,X_n^{\text{HX}} \tag{4.16}$$

This equation describes all heat and mass transfer on the tray and in the heat exchangers, but not mixing and pressure effects. It is also valid for the condenser and reboiler where there are no driving forces over the interface present, leaving only the last term.

4.5 Results and Discussion

4.5.1 Experimental Results

The measured flows, mole fractions, pressures and errors of the adiabatic and diabatic column are given in Table 4.2.

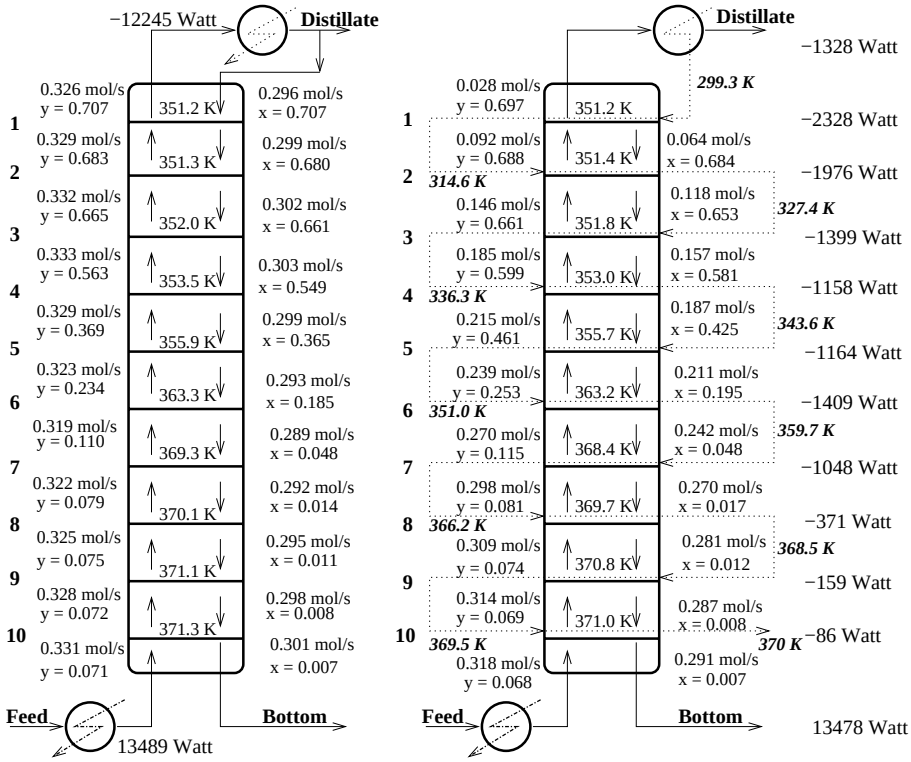

(a) Adiabatic column. (b) Diabatic column.

Figure 4.2. Results per tray of adiabatic and diabatic column.

The columns performed nearly the same separation. The results of the measurements on the trays of the adiabatic and diabatic column are given in Figure 4.2. The mole fractions x and y are related to ethanol. The flows in mol/s are at the left of the column the vapour flows, and on the right side the liquid flows. The temperatures in bold-italic are the temperatures of the cooling water, while the temperatures on the trays are temperatures of the liquid on the trays. The duties are the amount of heat added (positive sign) or removed (negative sign) on the nearest heat exchanger, reboiler or condenser. The dotted lines represent the flow of the cooling water. In the adiabatic column it flowed only through the condenser, while in the diabatic column it flowed first through the condenser, and then down through all the coils on the trays (see also Figure 4.1).

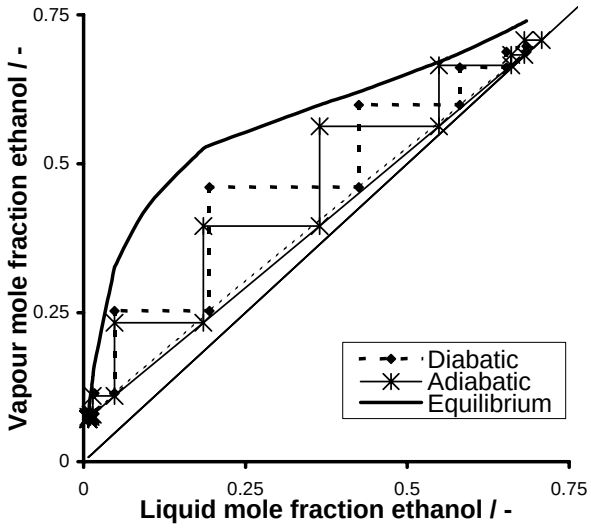

Figure 4.3. McCabe-Thiele diagram of adiabatic and diabatic column.

In order to asses how far both columns operated from the equilibrium, the McCabe-Thiele diagram in mole fractions is presented in Figure 4.3. Both columns operated rather far (up to 0.26 in mole fraction) from equilibrium in the middle part of the column. It is clear that a model using the assumption of equilibrium on the trays will be inaccurate for these columns. The diabatic column operated closer to the equilibrium line than the adiabatic one. Also a slightly bent operating line of the diabatic column can be observed, while the adiabatic operating line is near straight.

4.5.2 Exergy analysis

Figures 4.5 and 4.4 present the Grassmann diagrams (Kotas 1995) of the adiabatic and diabatic columns in terms of percents (adiabatic: 1%=42.7 J/s, diabatic: 1%=41.0 J/s).

These diagrams show the differences in locations and amounts of exergy losses. The arrows into the system are the exergy inputs, while the arrows pointing outward are the exergy products or losses. The arrows downward point out losses, and the arrows to the right out of the system are useful products. The cooling water input into the condenser is not depicted in both figures because this had a negligible exergy value. All the labels 'water' refer to the cooling water, and not to the water in the mixture. The arrows labelled 'heat loss' are

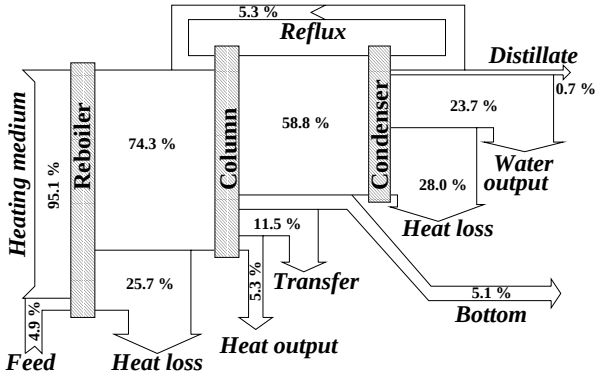

Figure 4.4. Grassmann diagram of adiabatic column.

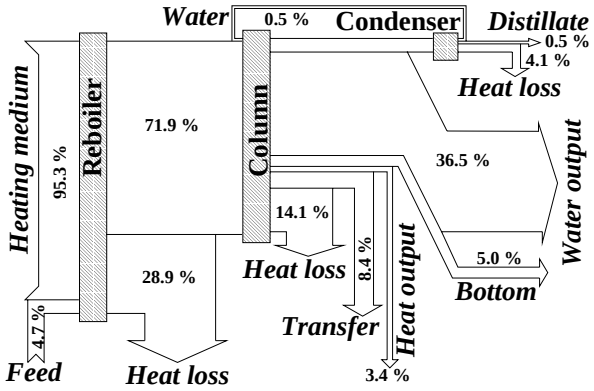

Figure 4.5. Grassmann diagram of diabatic column.

Carnot type losses. The arrow labelled 'transfer' are losses due to heat and mass transfer through the interface in the column. The heat outputs from the column to the environment due to imperfect insulation are also drawn. First of all, it becomes clear that the largest input for both distillation columns was the heating medium (oil), and not the feed. Also the largest output was neither the distillate nor the bottom product, but heat and output losses/products. The main improvement by adding heat exchangers, i.e. diabatisation, was on the temperature of the cooling water. In the adiabatic column the cooling water coming out was a useless output at 340 K, i.e. the water output arrow pointing down. However, in the diabatic column the water came out at 370 K and was not a useless output anymore, i.e. the water output arrow pointing to the right. This 30 K made the difference between useful and useless. It could

have been used for heating somewhere else in a plant. This means that also for a real non-equilibrium distillation process the diabatic way of operation had a higher second law efficiency than the adiabatic way. The exergy loss was overall reduced with 39%, and this can be called a major improvement. The output due to imperfect insulation was higher in the adiabatic column than in the diabatic columns. Probable causes could be a different surroundings temperature, better insulation due to use of heat exchangers, or model error of the absolute enthalpy model.

4.5.3 Heat and mass transfer through the interface

Figure 4.6 compares the results of the exergy benchmark in Eq. 4.2 with the results of the three force-flow description in Eq. 4.5 and the one force-flow description in Eq. 4.10 for the adiabatic and diabatic column.

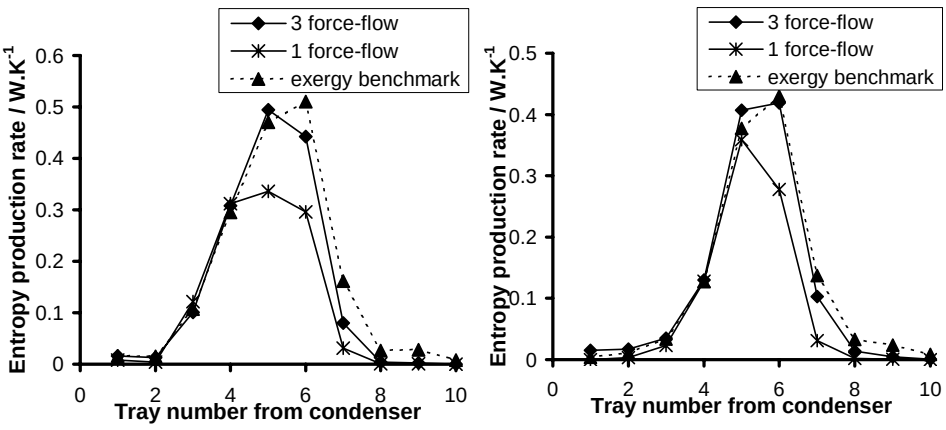

(a) Adiabatic column. (b) Diabatic column.

Figure 4.6. Results of Eqs. 4.5 and 4.10 compared with exergy benchmark.

The 3 flow-force description from irreversible thermodynamics follows the exergy benchmark well in the first 5 trays for both columns, afterwards the 3 flow-force points are lower than the exergy benchmark. But the qualitative match is such that it can be concluded that in these columns mass and heat transfer explains nearly all entropy production rate on a tray. The 3 flow-force descriptions explains 90 % in the adiabatic and 96 % in the diabatic column of the total entropy production. The other potential large contributions from

pressure drop and mixing (Taprap and Ishida 1996, Ray and Sengupta 1996), seem not to be significant in these columns. Because the pressure difference over the whole column was small, it is plausible that the pressure drop has no large effect, see Table 4.2. That these extra effects can be present, can be seen from the exergy benchmark having a higher value on tray number 5-8. So, Eqs. 4.5 did not describe all the phenomena that produce entropy. Concluding, the mass and heat transfer through the interface in Eq. 4.5 describes the main trends, and were the main contributors to the total entropy production rate in these columns.

In both figures the one flow-force description in Eq. 4.10 predicted less accurately the entropy production than the three flow-force Eq. 4.5. Also the trends were caught worse. From these observations it is concluded that the one flow-force equation was too simplified for these real non-equilibrium columns, despite the satisfactory results in De Koeijer and Kjelstrup (2000). The reason is that the assumptions behind Eq. 4.10 are not valid for these columns.

4.5.4 Heat transfer in the heat exchangers

Figure 4.7 shows the contribution of the heat exchangers for the diabatic column as calculated by Eqs. 4.12 and 4.14, compared to the exergy benchmark in Eq. 4.4.

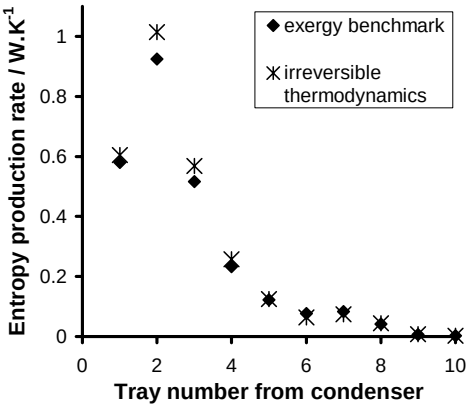

Figure 4.7. Entropy production due to heat transfer in heat exchangers compared with exergy benchmark.

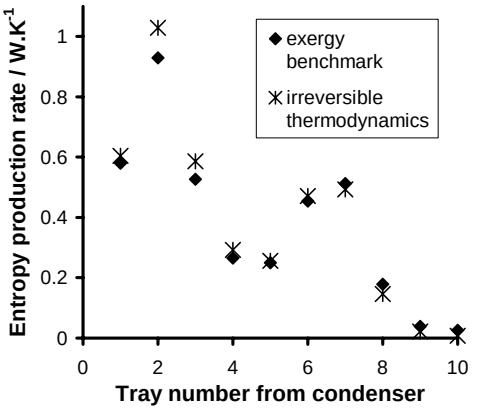

Figure 4.8. All irreversibilities in diabatic column compared to exergy benchmark.

The value for the average heat of vapourisation, $\Delta_{\text{vap}}\overline{H}$, was 38195 J/mol.

Both trends and values of the exergy benchmark were predicted remarkably well. So, nearly all entropy production rate was described by the one flow ($\Delta_{\text{vap}}\overline{H}\,(J_{\text{w},n} + J_{\text{e},n})$) and average force ($X_n^{\text{HX}}$). The effects of not described phenomena, like pressure drop, played an insignificant role in the heat exchangers of the diabatic column.

Figure 4.8 gives the sum of all contributions in Eq. 4.16 in the diabatic column compared to the exergy benchmark, i.e. the sum of the values in Figures 4.6 and 4.7. Also here no large differences could be observed between the results of the equations from irreversible thermodynamics and the exergy benchmark. It is concluded that Eq. 4.16 predicted well the entropy production due to heat and mass transfer through the interface and due to heat transfer in the heat exchangers in the diabatic column.

4.5.5 Analysis of the irreversibilities

Due to diabatisation, the entropy production rate on the trays and in the heat exchangers decreased from 9.31 to 7.75 J/K.s, calculated from the exergy benchmark and Guoy-Stodola theorem in Eq. 4.1. As previously argued, the description that uses irreversible thermodynamics can provide more insight than the overall exergy analysis. Since it was concluded that heat and mass transfer on the trays and in the heat exchangers could explain nearly all entropy production rate in the columns, these transfer phenomena will be analysed.

An interesting question is: what has changed due to the diabatisation? This question was answered by looking at the mass flows (Eq. 4.8) through the interface and their corresponding driving forces (Eq. 4.7) in the diabatic and adiabatic column in Figure 4.9.

The main differences were observed in the flows through the interface, especially of ethanol. By diabatisation a large part of the flow was taken away from the condenser (tray number 0) into the column. This means actually that the flow was moved from pure condensation (the condenser) to locations with mass and heat transfer (the trays). The sum of the absolute ethanol flows through the interface (from condenser to tray no. 10) was 0.437 mol/s in the adiabatic case, while this was only 0.200 mol/s in the diabatic column. This explains largely why the diabatic column had less entropy production rate due to heat and mass transfer than the adiabatic column.

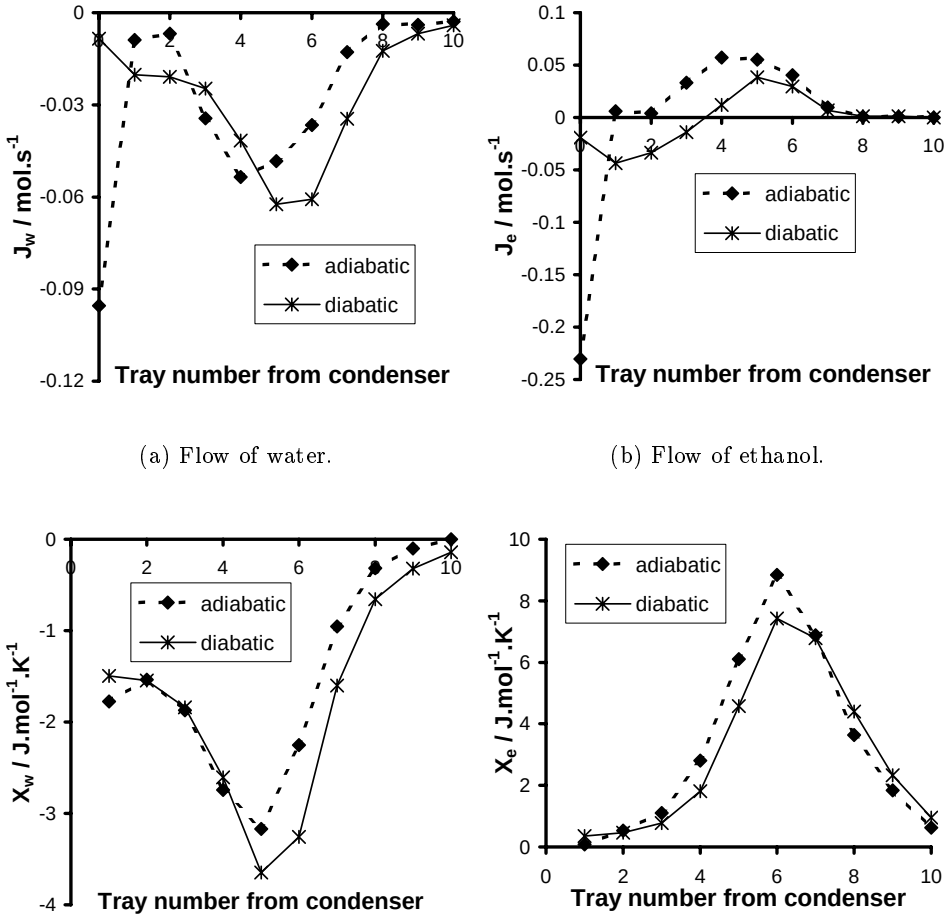

(a) Flow of water.

(b) Flow of ethanol.

(c) Force of water.

(d) Force of ethanol.

Figure 4.9. Driving forces and flows through interface in adiabatic and diabatic columns.

A similar but smaller redistribution was observed for the water flow through the interface. However, the sum of the absolute water flows through the interface from condenser to tray no. 10 was 0.307 mol/s in the adiabatic column and 0.297 mol/s in the diabatic column. There was only a small difference because the direction of the water flow was the same in the condenser and on the trays. The driving forces for water and ethanol transfer turned out to be

rather similar in the diabatic and adiabatic columns, despite the different mole fraction profiles in the McCabe-Thiele diagram in Figure 4.3. It is concluded that the diabatisation changed mainly the ethanol flow through the interface.

The contribution from the heat transfer in the heat exchangers (including condenser and reboiler) decreased from 7.67 J/s in the adiabatic column to 6.56 J/s in the diabatic column. This was caused by the redistribution of the heat removal to higher temperatures. Removing heat at a higher temperature is more favourable. This is explained by the Carnot efficiency, which can be derived from the theory of irreversible thermodynamics, see Førland et al. (2001). The sum of the absolute heat transfer in the heat exchangers (including condenser and reboiler) increased slightly from 25.7 10^3 J/s in the adiabatic column to 25.9 10^3 J/s in the diabatic column. This effect should increase the entropy production rate, but was by far not large enough to compensate for the redistribution of the heat removal to higher temperatures.

Figure 4.10 shows the three contributions to the entropy production rate due to heat and mass transfer through the interface (i.e. the three flow-force products in Eq. 4.5) on each tray of the diabatic column.

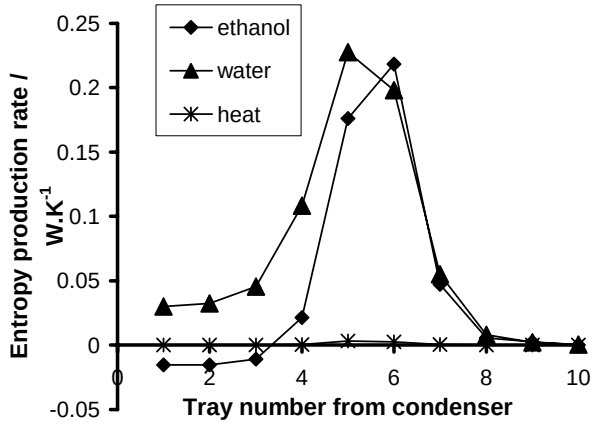

Figure 4.10. Three contributions of Eq. 4.5 to entropy production due to heat and mass transfer through interface in diabatic column.

First of all, mass transfer accounted nearly for all entropy production rate. The contribution of heat transfer through the interface seems to be negligible. But a surprising behaviour shows up: the contribution of the ethanol mass transfer was negative on the first three trays, because the ethanol force and flow had opposite sign. The sum of the three contributions was positive, as

the second law demands. This means that ethanol was transfered against its own gradient. It can be explained by looking at how forces and flows depend on each other in terms of resistances (Førland et al. 2001):

$$X_{\mathrm{e}} = r_{\mathrm{ee}} J_{\mathrm{e}} + r_{\mathrm{ew}} J_{\mathrm{w}} + r_{\mathrm{eq}} J_{\mathrm{q}} \tag{4.17}$$

The resistance r_{ee} is related to normal Fick's diffusion of ethanol, and the second law dictates that it is always positive. The coupling resistance for interdiffusion of ethanol and water is r_{ew}, and r_{eq} is the resistance for coupling between heat and ethanol transfer (or thermal diffusion or Soret effect). So, the only physical explanation for the negative entropy productions is that coupling in the form of thermal diffusion and interdiffusion was larger than the Fick´s diffusion. However, the negative numbers are rather small for drawing a solid conclusion. Although not likely, they could be blamed to inaccurate measurements and models. But confirmation of this observation is obtained from the data from De Koeijer and Kjelstrup (2000), where the entropy production rate is minimised for two diabatic columns. In both columns negative contributions can be clearly identified (not shown in publication).

It is said that the heat-mass coupling is negligible because the thermal gradients are not large and not sustained long enough, see Taylor and Krishna (1993). Equation 4.17 shows that a heat flow is enough for the heat-mass coupling to have an effect, and that thermal gradients are not necessary. The heat flow is in its turn generated by the driving forces for mass transfer by the reciprocal coupling effect. So, as long as there is mass flow, there is heat flow, and there is an effect due to heat-mass coupling. Hafskjold et al. (1993) says that it may be important, but the effect of mass-mass coupling (or interdiffusion) is most probably larger. Concluding, these negative contributions to the entropy production rates are a strong indication that coupling was an important factor in this diabatic rectifying column. This conclusion means that the contribution from heat transfer could not be neglected, even if it is a small contribution (0.6 % of the total entropy production rate). It is certainly a part of this coupling and might be significant. Because the established non-equilibrium distillation model in Taylor and Krishna (1993) do not take all coupling into account, this model might be in error for diabatic distillation. However, it is not yet possible to give a good quantitative estimate of this error because there are, except for Rivero (1993) and Rivero et al. (1993), no experimental data available on diabatic distillation.

4.6 Conclusions

The first conclusion is that the existing three flow-force description of entropy production rate due to heat and mass transfer through the interface was in agreement with the results of an exergy analysis. This is based on data from two experimental non-equilibrium rectifying columns, separating ethanol from water. This means that mass transfer through the surface determined largely the entropy production rate in these columns. The second conclusion is that the entropy production rate due to heat transfer in the heat exchanger was well described by one product of flow and average force. The third and most important conclusion is that diabatic distillation has proved to have also for a real non-equilibrium column significantly lower exergy loss (39% less) than adiabatic distillation. Furthermore, an analysis of the flows and forces showed that the diabatisation mainly redistributed the ethanol flow through the interface. Also a strong indication is given that coupling of heat and mass transfer was a non-negligible factor in diabatic distillation. All these conclusions are building stones for the further development and optimisation of diabatic distillation.

Acknowledgements

Instituto Mexicano del Petroleo is thanked for the travel expenses for Gelein de Koeijer. The Research Council of Norway is thanked for a grant to Gelein de Koeijer. Signe Kjelstrup is thanked for her valuable discussion.

5 The Role of Heat Exchangers in Optimum Diabatic Distillation Columns

Gelein de Koeijer, Audun Røsjorde and Signe Kjelstrup

Norwegian University of Science and Technology
Department of Chemistry, Physical Chemistry
N-7491 Trondheim
Norway

This paper is accepted for publication in:
Proceedings of ECOS 2002, Berlin 2002, Germany.

Abstract

We improved our model for minimisation of entropy production rate in diabatic tray distillation. The entropy production rate was the objective function, which had contributions from heat and mass transfer on the tray and from a heat exchanger on the same tray. Four distribution rules for heat transfer area were investigated. The heat exchangers had a significant effect on the entropy production rate, but their relative effect reduced with increasing thermal driving forces in the heat exchangers. In the limit of infinitely large forces, the results of an adiabatic column were obtained. The area distribution rule with constant average force in each heat exchanger had the lowest entropy production rate of the studied rules. Possible consequences for column design were discussed. Two minimisation algorithms were used with similar outcome; the *Matlab*® function *fmincon* being the fastest and most accurate.

5.1 Introduction

In the last 10 years there has been a discussion about minimising the entropy production rate in diabatic distillation, see Rivero (2001), De Koeijer et al. (2001), Schaller et al. (2001), De Koeijer and Kjelstrup (2000), Sauar et al. (1997), Rivero (1993). A diabatic distillation column has heat exchangers on all trays, and it is known for three decades that this type of distillation produces less entropy, see Fonyo (1974a,b). Distillation is a separation method that demands large inputs of energy, and even small improvements can save large amounts of energy. Like this work, nearly all publications are based on simulations. Rivero (1993) has given experimental results, however, which confirm that a diabatic column has significantly lower entropy production rate than a conventional adiabatic column (with one reboiler and one condenser).

Most of the focus until now has been on the entropy production rate of heat and mass transfer on the trays, i.e. on separation. The reason has been to start with a simple model. But diabatic distillation requires heat exchangers, and they also produce entropy. The contribution from the heat transfer in the heat exchangers has not been taken into account until now.

The purpose of this work is to study how the heat exchangers influence the state of minimum entropy production rate in diabatic distillation, independent of the operating conditions for the heat exchangers. We shall show that their role is

substantial, and will influence the solutions. There are now several methods available (De Koeijer and Kjelstrup 2000, Nummedal 2001) that enable us to deal with the more complicated minimisation problem. We shall use two of them, namely a Monte Carlo algorithm (De Koeijer et al. 2001) and an algorithm that uses the function *fmincon* in *Matlab*®, see The MathWorks Inc. (2001).

5.2 The system

The system was described by De Koeijer et al. (2001). It consists of a distillation column with heat exchangers on all trays, see Fig. 5.1.

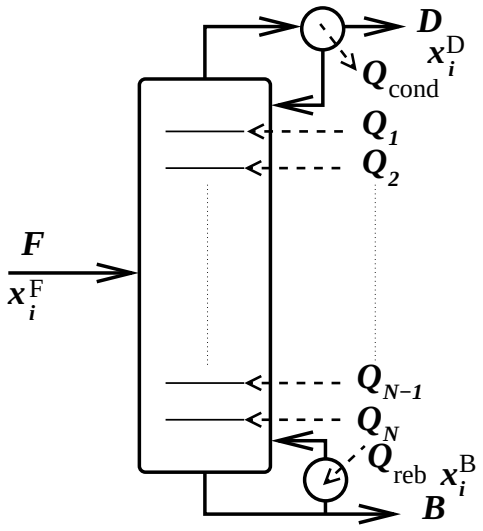

Figure 5.1. A sketch of the diabatic distillation column

The column has 20 trays, and splits an equimolar benzene/toluene flow (1 mol/s) into 0.95 benzene mole fraction in the distillate and 0.05 in the bottom. The feed and products are liquids at their boiling point. The pressure is constant (10^5 Pa). We assume equilibrium between the flows leaving each tray. The equilibrium conditions were calculated with the integrated Clausius-Clapeyron equations for a regular solution, with the Margules equation for the activity coefficients. The Margules parameters are -0.0356 and 0.0619 (Gmehling and Onken (1977), volume I, part 7, page 282). The heat capacities are temperature dependent, see the Appendix.

For a given tray temperature (T_n), the mass balances over the trays and the

equilibrium relations give the mole fractions (x_n,y_n) and the flows (V_n, L_n). The duty (Q_n) then follows from the energy balance. The diabatic distillation column is simulated in this manner for given number of trays, in- and output flows, and in- and output concentrations

5.3 Objective function

The objective function for a second law optimisation is the entropy production rate, which does not consider cost:

$$\frac{dS^{\mathrm{irr}}}{dt} = BS^{\mathrm{B}} + DS^{\mathrm{D}} - FS^{\mathrm{F}} + \sum_{n=0}^{N}\left(-\frac{Q_n}{T_n}\right) + \sum_{n=0}^{N}\left(Q_n X_n^{\mathrm{HX}}\right) \tag{5.1}$$

The first three terms to the right are the change in entropy by the flows in and out of the column, which is constant in the minimisation. The fourth term is the entropy production rate from the added and removed heat, which are needed to accomplish the separation. The duty, Q_n, is the amount of heat transferred per unit of time in one heat exchanger n, and is varied in the minimisation. The fifth term $\sum Q_n X_n^{\mathrm{HX}}$ is the contribution to the entropy production from heat transfer in the heat exchangers, see De Koeijer and Rivero (2002). This term was not used before (De Koeijer et al. 2001). The symbol X_n^{HX} denotes the (average) thermal driving force for heat transfer in the heat exchanger:

$$X_n^{\mathrm{HX}} = \frac{1}{T_n} - \frac{2}{T_n^{\mathrm{u,in}} + T_n^{\mathrm{u,out}}} \tag{5.2}$$

Superscript u means the utilities (i.e. heating or cooling medium) that flows through the heat exchanger coils. The force is positive when heat is added, and negative when heat is removed. This makes the contribution of the heat exchangers positive. This heat transfer does not couple with the heat and mass transfer through the liquid/vapour interface. The variables in the minimisation are the temperatures on the trays.

5.4 Model for heat exchangers

The heat exchangers are characterised by their area of heat transfer, the flows of the utilities (i.e. heating or cooling medium), the temperatures of the utilities, and the heat transfer resistance. The equations that relate these variables are given in this section. The driving force in the heat exchangers is related to the duty by, see Sauar et al. (1996):

$$X_n^{\mathrm{HX}} = R_n^{\mathrm{HX}} Q_n \tag{5.3}$$

where R_n^{HX} is the average resistance to heat transfer of heat exchanger n. A model for R_n^{HX} is required. We apply the film model, and assume that:

- The heat exchanger is a coil, hanging above the sieve, like in Rivero (1993).
- The coil on the tray is covered with a liquid film, in which all the resistance to heat transfer is located. There are no dry spots.
- The film is not affected by the void fraction of vapour on the tray.
- The film is not affected by gas or liquid velocities.
- The conditions in the reboiler and condenser are similar to the ones in the tray heat exchangers. The same resistance model is thus used for the reboiler and condenser.

The simple model for the resistance becomes:

$$R_n^{\mathrm{HX}} = \frac{\delta}{A_n} \frac{1}{\lambda_n^{\mathrm{L}} T_n^2} \tag{5.4}$$

where δ is the constant film thickness, arbitrarily set to 10^{-5} m, λ_n^{L} is the thermal conductivity of the liquid on tray n (see the Appendix), and A_n is the area of heat exchanger n (or the area of the film covering the coil). This equation predicts heat transfer resistances from experimental data in Rivero (1993) within the same order of magnitude.

It is not necessary to determine the utilities before the minimisation. Instead, the energy balance over the heat exchangers can be used after the minimisation to design a reasonable heat exchanger network. The energy balance is:

$$Q_n = \dot{m}_n^u C_{P,n}^u \left(T_n^{\mathrm{u,in}} - T_n^{\mathrm{u,out}} \right) \tag{5.5}$$

5.5 Area distribution rules

The minimisation of the entropy production rate was carried out for four cases with different rules for area distribution. In all cases, the total transfer area ($\sum A_n$) was a result of the minimisations, where A_n obeyed one of the following area distribution rules:

1. The computationally speaking simplest rule was to take the thermal driving force over the heat exchangers constant. This choice was motivated by earlier findings for minimum entropy production in heat exchangers,

see Nummedal and Kjelstrup (2001). Equation 5.4 is then not needed in the minimisation, but is used afterwards to calculate the area on each tray. Three finite forces were used. A fourth value of the force was set equal to zero to model reversible heat transfer as a limiting case. This rule will be abbreviated as EoF, which stands for equipartition of forces.

2. In the next case, the heat exchanger area was taken as a linear function of the vapour flow of the tray. In normal practise (Douglas 1988), the tray area is linear with the vapour flow. This makes it possible to have the same pressure drop on all trays. So, the following rule was used:

$$A_n = aV_n \tag{5.6}$$

The value for the proportionality constant varied from 0.1 to 0.9 in the experimental vapour flows and areas of a diabatic column, reported by Rivero (1993). Various values in that range were used in this work. This case was motivated by an efficient use of space in the column.

3. In the third case, the area A_n was set equal on all trays. To use only one type of heat exchanger with the same area, can simplify the column construction.

4. In the fourth case, the entropy production in each heat exchanger ($Q_n X_n^{\mathrm{HX}}$) was the same for all n. This choice was motivated by the proposal of Tondeur and Kvaalen (1987) and recent work in our group, see Johannessen et al. (2002). This rule will be abbreviated as EoEP, which stands for equipartition of entropy production.

By application of Eqs. 5.3, 5.4 and one of the rules, we can find the areas of the heat exchangers. The area distribution among the heat exchangers is in focus in this work.

5.6 Calculations

5.6.1 The Monte Carlo algorithm

A Monte Carlo algorithm was developed by De Koeijer and Kjelstrup (2000), De Koeijer et al. (2001), and has now been slightly extended. The algorithm starts from either a linear temperature profile (i.e. temperature as a function of tray number) or the temperature profile of the adiabatic column. It changes, on a random tray, the temperature with a random step multiplied by a factor f. If the entropy production rate of the new profile is larger, or if the profile

is not physically realisable, the profile is rejected, and a new random step is tried on the previous profile. If the entropy production rate is lower, the new profile is accepted. This step was shown to be successful and tried again on the same tray, followed by the same check as on the previous step. The second step is the extension in comparison to De Koeijer et al. (2001), and makes the algorithm faster because it tries twice on a tray with improvement possibility. The new profile is used as the next start for a new random step on a random tray. The procedure is repeated 30000 times. The factor f is then decreased, and the procedure is repeated. The factor f decreases exponentially in 6 steps. When the factor f reaches its lowest value, the result is taken as the minimum. In order to test for a true minimum, the temperature profile is perturbed. The whole procedure is repeated again up to 1000 times. If there is no change in the course of a 2-3 hours, the procedure is stopped, and presumably a minimum is obtained.

5.6.2 *Fmincon* in *Matlab*®

Many of the nonlinear programming algorithms today are based upon the solution of the Kuhn-Tucker equations, see Nocedal and Wright (1999). The Kuhn-Tucker equations are necessary conditions for optimality for a constrained optimisation problem. In the function *fmincon* in *Matlab*® *6.1 R12.1* (The MathWorks Inc. 2001) the Kuhn-Tucker equations are implemented into a Sequential Quadratic Programming method. Each iteration consists of three main stages:

- Updating the Hessian matrix.
- Solution of a Quadratic Programming problem.
- Line search to find a suitable step.

In short, this method closely mimics Newton's method for constrained optimisation as is done for unconstrained optimisation. For more details on Sequential Quadratic Programming see Gill et al. (1981)

It is possible to minimise Eq. 5.1 just by performing an unconstrained optimisation, with given number of trays and in- and outlet concentrations and flows. This means that the only variables are the temperature on each tray. If the optimisation problem is highly nonlinear, the initial guess of the temperatures must be close to the minimum, if convergence is to be achieved. While this is tolerable in some cases, a more robust formulation can be obtained by introducing the vapour flows as an extra set of variables. This formulation

of the minimisation has proved to be less sensitive to the initial values of the variables. To ensure that the final solution fulfils the component balance, these balances are included as nonlinear constraints. Thus, we have a constrained nonlinear optimisation problem. This approach resembles the one applied to a primary steam reformer by Nummedal (2001).

5.6.3 Procedures

The minimisation of the objective function in Eq. 5.1 was first carried out with both algorithms for Rule 1. The optimum feed tray was found by minimising the entropy production rate for all possible locations, and selecting the one with least entropy production rate. The faster algorithm (*fmincon* in *Matlab*®) was next used for minimisation with Rules 2-4, with the feed tray on tray number 8. The results were generated by putting in the four rules in the simulation program for the columns. This makes the entropy production rate different for each rule with similar temperature profile. The results consisted of the temperatures, duties, mole fractions, flows, transfer areas, and entropy production rates on all trays.

As a reference for the minimisation results, the entropy production rate in adiabatic columns were calculated. The duties (Q_n) of the adiabatic columns are zero, except for reboiler and condenser. So for the given separation, the adiabatic column has a unique temperature profile, reboiler duty, and condenser duty. The heat transfer area of reboiler and condenser were taken equal.

5.7 Results

5.7.1 Reproducibility of algorithms

It was first established for Rule 1 (EoF) that the two algorithms gave the same results. Table 5.1 shows agreement within 2% in the entropy production rate for four thermal driving forces. The same feed tray was also found by both procedures. The *Matlab*® *fmincon* algorithm was, however, faster by several orders of magnitude, so we proceeded with this.

Table 5.1 shows that the entropy production rate increased with increasing thermal driving force in the heat exchanger. It was smallest for the case of reversible heat exchange ($X^{\mathrm{HX}} = 0$). Details of the solution are given below.

Table 5.1. Results of Rule 1

Force (1/K)	dS^{irr}/dt (W/K)		Area	Feed
	Monte Carlo	*fmincon*	(m^2)	tray
0	1.7215	1.6889	∞	8
0.00001	2.5308	2.4942	4.788	8
0.0001	9.3863	9.2726	0.4458	9
0.001	74.020	73.949	0.04319	9

5.7.2 Adiabatic column

Table 5.2 gives the entropy production rates and total transfer areas of the adiabatic columns at the same driving forces and feed tray locations as in Table 5.1.

Table 5.2. Adiabatic column

Force (1/K)	dS^{irr}/dt (W/K)	Area (m^2)
0	3.3629	∞
0.00001	4.081	4.342
0.0001	10.417	0.4304
0.001	74.495	0.04304

With increasing driving force, the entropy production rate increased, and the total transfer area decreased.

5.7.3 Rule 1: Constant driving force

Figure 5.2 shows the variation in the duty across the column at minimum entropy production rate with the four forces in Table 5.1.

For the case of reversible heat exchange, the behaviour was similar to the ones in De Koeijer et al. (2001). With the largest driving force, the duty was everywhere near zero, except for the last five trays. The duties for the first and last tray were respectively -19.9 10^3 and 24.8 10^3 W. Intermediate driving forces gave results between the extreme cases.

5.7.4 Rules 1-4 compared

Figure 5.3 shows the entropy production rate as a function of the total area of transfer for all heat exchangers, for the area distribution from Rules 1-4 and adiabatic column, see calculations.

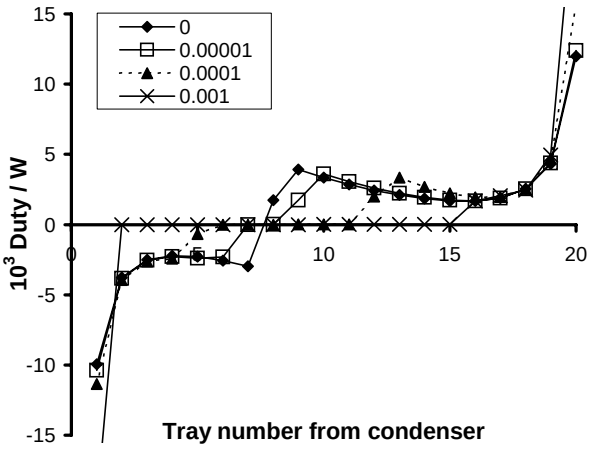

Figure 5.2. Duty as function of tray number for columns with minimum dS^{irr}/dt. The driving force for heat transfer is indicated.

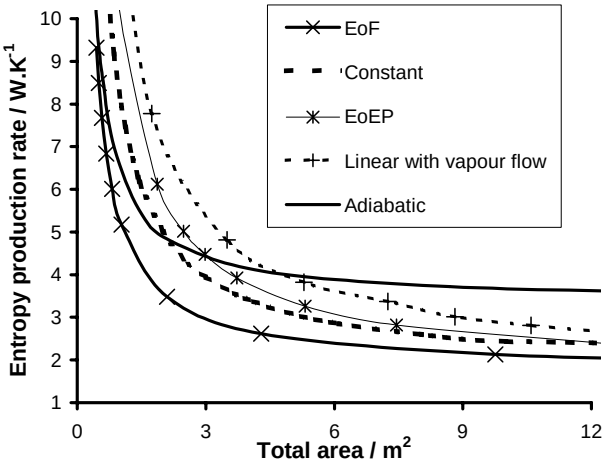

Figure 5.3. The entropy production rate vs. total area in Rule 1-4

The first rule, EoF, resulted in the lowest entropy production rate for all values of the total area of transfer. Rule 2, that used an area distribution linear with the vapour flow, had always the highest entropy production rate among the diabatic columns. The EoEP results (Rule 4) gave slightly larger values, and a near parallel curve to the one with constant area rule (Rule 3). At small transfer areas, Rules 2-4 had a larger entropy production rate than the adiabatic column. When the total area of transfer was large, the four diabatic

profiles approached each other. When the total area of transfer became small, the entropy production rates of all five cases approached infinity.

5.8 Discussion

5.8.1 The model

One premise for these results for diabatic tray distillation is the assumption of equilibrium between vapour and liquid at the outlet of each tray. Wesselingh (1997) argues that this assumption leads to results that have no connection to reality. Our research has the same overall aim as his, to introduce non-equilibrium models for simulations of distillation. This requires more work on the modelling side, however. The assumption of equilibrium at the outlet on each tray, is in the meantime an assumption that enables a first calculation of the relative role of the heat exchanger for the minimum in the total entropy production rate. Moreover, the effect of pressure drop is not taken into account in this minimisation. At large transfer areas we expect it to have a non-negligible influence.

An alternative to the model for heat transfer resistance in Eq. 5.4 is to use an empirical correlation with the dimensionless Nusselt, Reynolds and Prandtl numbers. Besides that no relation could be found in the literature for this specific type of heat exchanger, these relations only give an order of magnitude result. The model in Eq. 5.4, that corresponded to the results in Rivero (1993), was therefore preferred.

5.8.2 Rule 1: Constant driving force

We have previously reported that the diabatic column is superior to the adiabatic one in terms of its second law efficiency, see De Koeijer et al. (2001), De Koeijer and Kjelstrup (2000). This was done using a model for heat transfer in the diabatic column that corresponds to the zero driving force results of Table 5.1. We see now, that the same result holds true, even if the driving force is finite. But the relative gain is smaller, the larger the driving force is, compare Tables 5.1 and 5.2. This is understandable, since the total area for heat transfer varies. The larger the driving force, the smaller the area, the larger the entropy production rate, and the smaller the relative gain. But, the larger the transfer area is, the more expensive the column is.

By comparing the areas in Tables 5.1 and 5.2 we see that the adiabatic column had a smaller transfer area with the same driving force. This is logical because

$\sum |Q_n|$ is smaller in the adiabatic column than in the diabatic column.

There is an upper limit to the thermal force, where addition of heat exchangers has no beneficiary effect on the second law efficiency. This value is close to the value 0.001 1/K used in Table 5.1. If it is not possible to have driving forces below this value, the diabatic column has no justification. This is confirmed also by Fig. 5.2 where Rule 1 with high driving force, approaches the adiabatic column.

The reason that *Matlab's*® *fmincon* performed more accurate (see Table 5.1) than the Monte Carlo algorithm is that the Monte Carlo algorithm did not reach the same convergence as *fmincon* in the given time span.

5.8.3 Rules 1-4 compared

As was already stated, the area distribution rule with constant driving force (EoF) gave the lowest entropy production rate for all transfer areas, see Fig. 5.3. This means that the (economic) argument that a diabatic column will always cost more due to unavoidable extra heat transfer area, does not hold in general. However, a diabatic column will always be more complex than an adiabatic column, because the area is distributed over more than two heat exchangers.

The second lowest series of entropy production rates was given by the rule of constant area. So, if it is expensive to build a column with a different heat exchanger on each tray, Rule 3 could be a good alternative. Close to Rule 3 was Rule 4, with EoEP as distribution rule. The areas derived from using the EoEP rule were, however, not constant over the column. In this case, EoEP performed worse than EoF. Both equipartition theorems originate from a minimisation with specific objective function and constraints, that are not fulfilled here. We therefore expect that neither EoF nor EoEP are solutions to the minimisation problem. It is interesting however that EoF performs best. The worst performance was from the common design rule of linear vapour flows (Rule 2). So, this rule should not be used.

Figure 5.3 also shows that Rules 2-4 had a crossover with the adiabatic column. This means that not all diabatic columns have automatically a lower entropy production rate than the adiabatic column. A diabatic column should not be preferred a priori. Figure 5.3 can be used to calculate the relative reduction of entropy production for a certain amount of extra heat transfer area for various rules for area distribution. This relative reduction decreases with decreasing

driving forces. So, if extra transfer area is available, it has the highest effect in columns with large driving forces. Figure 5.2 suggests to add this extra area at the lowest and highest trays for this particular column.

The EoF area distribution rule does not necessarily give the most optimum distribution of area. We expect that if the area is also allowed to vary an even lower entropy production rate can be found. But at high driving forces, it is plausible that the minimum is not far from the one with equal driving force (Nummedal 2001, Johannessen et al. 2002).

5.8.4 Design

We have up to this point assumed that it is possible to design a heat exchanger network with utilities that can fulfil the energy balance for the heat exchangers, see Eq. 5.5. The entropy production rate is minimised independent from the choice of utilities. Given the utilities, the last two terms in the objective function, Eq. 5.1, can be replaced by $\sum_0^N \dot{m}^u C_P^u \ln\left(T_n^{\mathrm{u,out}}/T_n^{\mathrm{u,in}}\right)$. The problem then becomes which utilities to use, and how to connect the in- and outlet temperatures of the utilities. Our choice of objective function is independent of the properties of the utilities, and the design of the connections and utilities can be done afterwards.

In order to illustrate what the design task can comprise, we calculated the in- and outlet temperatures of the heat exchangers for a constant driving force of 0.0001 1/K. The utilities were water (C_P=4180 J/kg.K) and steam (C_P=2000 J/kg.K). We chose a constant flow of each utility through the heat exchangers. The values 0.3 kg/s water and 0.4 kg/s steam gave reasonable results, see Fig 5.4.

In the rectifying section the inlet temperature became lower than at the outlet, while both were at least 5-10 K below the temperature on the trays inside the column. The opposite behaviour was observed for the stripping section. This ensures that there is feasible heating in the stripping section, and feasible cooling in the rectifying section. The design demands a large variety of utility temperatures, however. These are probably not available in a plant without a heat exchanger network.

A design where the utilities flow from one heat exchanger to the next, like in Rivero (1993), was not possible with the given utilities and results. Unrealistic temperature differences around 1-2 degrees between in- an outlet of the utilities

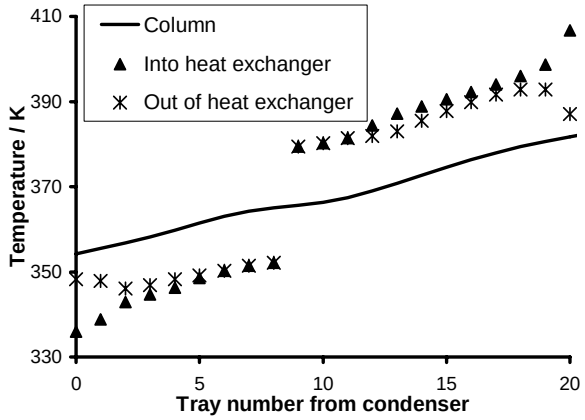

Figure 5.4. In- and outlet temperatures of water/steam for X^{HX}*=0.0001*

were obtained. Furthermore, the temperature difference between outlet and column became negligible, and the flows of utilities were not equal anymore. These results make such a design unrealistic.

It may be possible, however, to design a diabatic column with equal driving forces over the heat exchangers. Extra equipment and utilities are necessary, however, e.g. valves, pumps, compressors, heat pumps. The designing of such columns with realistic heat exchanger networks is a challenge for future research. In practise however, economical considerations must also be made, since the second law optimum does not necessarily coincide with the economical optimum.

5.9 Conclusions

In this work the effect of the heat exchangers for the minimisation of entropy production rate in diabatic columns is studied. Their effect was significant for realistic values of thermal driving forces. For large forces, or small total area, the adiabatic column was not much worse than the diabatic one, however. Out of four different candidate transfer area distributions, the one with equal forces over the heat exchangers had the lowest entropy production, for all total transfer areas investigated. It remains to be seen if the conclusions are altered by relaxing the assumption of equilibrium between liquid and vapour at the outlet of each tray. It was discussed that it is possible to design a diabatic column with minimum entropy production in connection with a heat exchanger network. The *fmincon* algorithm in *Matlab*® was superior to the Monte Carlo

algorithm for minimising entropy production rates in diabatic distillation.

Acknowledgements

The Research Council of Norway is thanked for a grant to Gelein de Koeijer. VISTA is thanked for a grant to Audun Røsjorde.

Appendix

The heat capacity for liquid and vapour, C_P^{L} and C_P^{V}, relate to the temperature as (Smith and Van Ness 1987) :

$$\frac{C_{P,i}}{R} = A_i^{C_P} + B_i^{C_P} T + C_i^{C_P} T^2 \tag{5.7}$$

The heat conductivity for the liquid is given by Reid et al. (1987):

$$\lambda_i = A_i^{\lambda} + B_i^{\lambda} T + C_i^{\lambda} T^2 \tag{5.8}$$

For a mixture the molar average of the two components is taken.

Table 5.3 gives the physical chemical properties that were used in the simulations.

Table 5.3. Physical chemical properties

Component	Benzene	Toluene
T^{boil}(K)	353.25[a]	383.78[a]
$\Delta_{\mathrm{vap}} H(T^{\mathrm{boil}})$(J/mol)	30781[a]	33201[a]
$A^{C_P^{\mathrm{V}}}$(-)	-0.206[b]	0.290[b]
$B^{C_P^{\mathrm{V}}}$(1/K)	39.064 10^{-3}[b]	47.052 10^{-3}[b]
$C^{C_P^{V}}$(1/K^2)	-13.301 10^{-6}[b]	-15.716 10^{-6}[b]
$A^{C_P^{\mathrm{L}}}$(-)	-0.747[b]	15.133[b]
$B^{C_P^{\mathrm{L}}}$(1/K)	67.96 10^{-3}[b]	6.79 10^{-3}[b]
$C^{C_P^{\mathrm{L}}}$(1/K^2)	-37.78 10^{-6}[b]	16.35 10^{-6}[b]
A^{λ}(W/m K)	1.776 10^{-1}[c]	2.03110^{-1}[c]
B^{λ}(W/m K^2)	4.773 10^{-6}[c]	-2.254 10^{-4}[c]
C^{λ}(W/m K^3)	-3.78 10^{-7}[c]	-2.47 10^{-8}[c]

[a] Sinnot et al. (1983)
[b] Smith and Van Ness (1987)
[c] Reid et al. (1987)

6 Transport Equations for Distillation of Ethanol and Water from the Entropy Production Rate

Signe Kjelstrup and Gelein de Koeijer

Norwegian University of Science and Technology
Department of Chemistry, Physical Chemistry
N-7491 Trondheim
Norway

This paper is sent in for publication

Abstract

We have derived a set of transport equations for heat and mass transfer across a liquid-vapour interface in distillation columns. The set defines overall coefficients of transport. They include one contribution from an interface, one from a vapour film, and several terms related to transport properties of a liquid film. The values were obtained by fitting the transport equations to the entropy production rate, with the thickness of the liquid film as the only adjustable parameter. They were calculated for experimental data of an adiabatic rectifying column that separates ethanol and water. The variation in the coefficients with temperature is shown. Despite the result that the liquid film was 10 times thicker than the vapour film, the coefficients had significant contributions from both films. A significant contribution from the Soret effect was also found. The driving force for mass transfer, calculated with coefficients and rates, compared well with average values, which were calculated from the experimental data. The set of equations was compared to the Maxwell-Stefan equation set. It is more detailed and can be used to asses several common approximations.

6.1 Introduction

Dynamic models of distillation require transport equations for mass and heat across a vapour-liquid interface as input. Strong arguments are given, that such models are needed also to describe the stationary state of distillation columns. A central model has been formulated by Krishnamurthy and Taylor (1985a,b), Wesselingh (1997), Taylor and Krishna (1993), Krishna and Wesselingh (1997). In this model, diffusional fluxes are calculated from the Maxwell-Stefan equations, and the heat flux from Fourier's law. The matrix of mass transfer coefficients is solved with an iterative procedure, in which the mass transfer rates become equal on both sides of the interface. The film thicknesses are variables in the procedure. Dimensionless numbers are used to find film thicknesses, for given flow patterns. Through various examples this approach has been shown useful (Krishnamurthy and Taylor 1985b, Wesselingh 1997, Taylor and Krishna 1993), and it is called the Maxwell-Stefan approach.

This work can be seen as a continuation of the efforts to find good equations of transport for distillation. The purpose of this work is to extend the Maxwell-Stefan approach. Both approaches have the entropy production in the system

as the basis for their derivation. But this property will be used in a more active way than before here, by using its value to obtain the thickness of the diffusional films. We shall put heat and mass transfer on the same basis, and define overall coefficients of transport through a liquid film, an interface and a vapour film. This will be done without knowledge of the detailed conditions at the interface. According to Alopeaus and Aittamaa (2000) it is not possible to define overall coefficients of transfer without such knowledge. Our set of equations is illustrated using experimental data from Rivero (1993) for a rectifying column that separates water and ethanol in 10 trays.

A detailed set of equations may help to assess approximations that are useful in applications, and such assessments are carried out with the cited data. One such assumption is the neglect of coupling between heat and mass transport. The assumption is often introduced with the agreement that thermal gradients are rarely high enough or sustained long enough, see e.g. Taylor and Krishna (1993), Bird et al. (1960). This assumption will be questioned for distillation.

Our set of equations does not have the independence of the frame of reference that characterises the Maxwell-Stefan equations. We can still take advantage of the expressions for the transport coefficients in this set. A short presentation of the numerical results, without the theoretical basis was already reported by De Koeijer and Kjelstrup (2002).

6.2 The system

The separation of two components in a distillation column is considered. It occurs when heat and mass are transported from the liquid phase to the vapour phase on a tray. The tray is shown in Fig. 6.1, with vapour bubbles rising in the liquid, and taking liquid droplets along. Vapour and liquid mole fractions are indicated, y and x, together with vapour and liquid flows, V, and L, respectively.

A close-up of one bubble/droplet between liquid and vapour is shown in Fig. 6.2. Mass transfer rates are denoted J_1 and J_2, and the measurable heat transfer rate is J_{q}. Superscripts L, V, or i indicate the phase in question. Our system is the region with gradients around all bubbles or droplets on a tray. Three subsystems are distinguished: the liquid film, the interface, and the vapour film. Bubble curvature is not visible on the scale chosen. We assume that all gradients in temperature, T, and chemical potential, μ_T, are in the liquid and vapour films, and across the interface. All liquid and vapour outside the

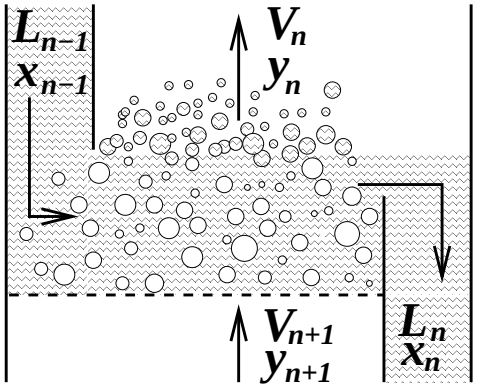

Figure 6.1. Tray in a distillation column

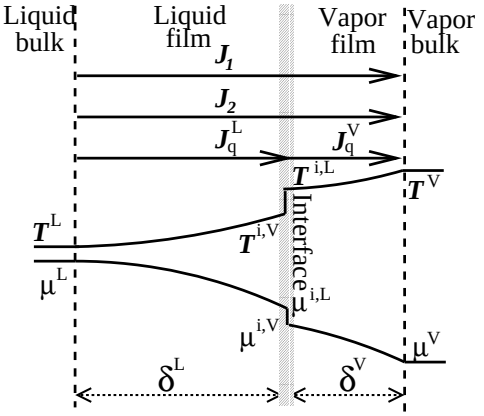

Figure 6.2. Close-up around interface

system is completely mixed. It is assumed that the extension of the gradients are the same for heat and mass transfer. For a steady state, mass transfer rates are constant throughout the region, while the heat transfer rate has a discontinuity at the interface due to different enthalpies of liquid and vapour, see the energy balance in Eq. 6.15 further on. The direction from the liquid to the vapour is taken as the positive direction, perpendicular to the interface.

The interface (or surface) is a separate open system according to Gibbs (1961). Interface coefficients lead to jumps in intensive variables across the interface. When there is equilibrium across the interface, the jumps are zero. The interface is the frame of reference for the transports. We shall further take the transfer area A and the film thicknesses δ^{L}, δ^{V}, to be the same on all trays.

6.3 The entropy production rate on a tray

All information about the transport processes is contained in the entropy production rate, since the transport equations follow from the entropy production rate. It is known that mass transport accounts for the largest part of the entropy production rate on a tray (Ray et al. 1994, Taprap and Ishida 1996, De Koeijer and Rivero 2002). Therefore, only heat and mass transfer is considered, and contributions from turbulence, pressure drop, and mixing are neglected. So, no entropy is produced outside the system. The total entropy production

is the sum of the contributions of the three subsystems in Fig. 6.2:

$$\frac{dS^{\mathrm{irr}}}{dt} = \frac{dS^{\mathrm{irr,V}}}{dt} + \frac{dS^{\mathrm{irr,i}}}{dt} + \frac{dS^{\mathrm{irr,L}}}{dt} \tag{6.1}$$

The aim is to describe all three contributions by the same variables. This is necessary to have overall coefficients defined. The critical part is to include possible interface coefficients, so we must start with an examination of the interface. The general theory behind the flux-force equations can be read in several books, see Førland et al. (2001), Kuiken (1994), Taylor and Krishna (1993), De Groot and Mazur (1985). For the interface we refer to Bedeaux and Kjelstrup (1999).

6.3.1 Interface

For a binary mixture there are in general six fluxes: three into the interface and three fluxes out of the interface. In steady state evapouration or condensation the number of independent fluxes reduces to three. The local entropy production rate (σ^{i} in J/K s m^2) is a sum of products of fluxes (J'') and forces (X^{i}). Each driving force is a sum of products of resistivities (r) and fluxes. We have:

$$\begin{aligned}
\sigma^{\mathrm{i}} =& J_q^{V\prime\prime} X_q^{\mathrm{i}} + J_1'' X_1^{\mathrm{i}} + J_2'' X_2^{\mathrm{i}} \\
X_q^{\mathrm{i}} =& r_{\mathrm{qq}}^{\mathrm{i}} J_{\mathrm{q}}^{\mathrm{V}\prime\prime} + r_{\mathrm{q1}}^{\mathrm{i}} J_1'' + r_{\mathrm{q2}}^{\mathrm{i}} J_2'' \\
X_1^{\mathrm{i}} =& r_{1\mathrm{q}}^{\mathrm{i}} J_{\mathrm{q}}^{\mathrm{V}\prime\prime} + r_{11}^{\mathrm{i}} J_1'' + r_{12}^{\mathrm{i}} J_2'' \\
X_2^{\mathrm{i}} =& r_{2\mathrm{q}}^{\mathrm{i}} J_{\mathrm{q}}^{\mathrm{V}\prime\prime} + r_{21}^{\mathrm{i}} J_1'' + r_{22}^{\mathrm{i}} J_2''
\end{aligned} \tag{6.2}$$

All fluxes are measured with the interface frame of reference. One model for these resistivities is given by kinetic theory (see section 6.6.2). The measurable heat flux was chosen as the variable in Eq. 6.2 (rather than the rate of heat transfer in the liquid) in order to include the interface resistivities. The entropy production of the interface uses, per definition, forces that are integrated over the interface (Bedeaux 1986), i.e. average forces for the region of transport. There is always a certain arbitrariness in the choice of fluxes and conjugate forces, but the entropy production rate is independent of this choice. Here, the chemical forces are the differences in chemical potential at temperature of the interface at the liquid side, divided by that temperature. These forces are for component j=1,2:

$$X_j^{\mathrm{i}} = -\frac{1}{T^{\mathrm{i,L}}} \Delta_{\mathrm{i}} \left(\mu_{j,T^{\mathrm{i,L}}} \right) \tag{6.3}$$

The thermal force $X^{\mathrm{i}}_{\mathrm{q}}$ that is conjugate to the measurable heat flux in the vapour is

$$X^{\mathrm{i}}_{\mathrm{q}} = \Delta_{\mathrm{i}} \left(\frac{1}{T} \right) \tag{6.4}$$

The differences refer to positions on each side of the interface. On the scale chosen for Fig. 6.2, the differences appear as discontinuities at the position of the interface. The entropy production rate in W/K is obtained by integrating fluxes into rates of transfer for l=1,2,q:

$$\frac{dS^{\mathrm{irr,i}}}{dt} = \int_A \sigma^i dA = \sum_l J_l X^{\mathrm{i}}_l \tag{6.5}$$

The total entropy production rate and the corresponding force-rate relations for the interface are now:

$$\begin{aligned} \frac{dS^{\mathrm{irr,i}}}{dt} =& J^{\mathrm{V}}_q X^{\mathrm{i}}_q + J_1 X^{\mathrm{i}}_1 + J_2 X^{\mathrm{i}}_2 \\ X^{\mathrm{i}}_q =& \overline{r}^{\mathrm{i}}_{\mathrm{qq}} J^{\mathrm{V}}_q + \overline{r}^{\mathrm{i}}_{\mathrm{q1}} J_1 + \overline{r}^{\mathrm{i}}_{\mathrm{q2}} J_2 \\ X^{\mathrm{i}}_1 =& \overline{r}^{\mathrm{i}}_{1\mathrm{q}} J^{\mathrm{V}}_q + \overline{r}^{\mathrm{i}}_{11} J_1 + \overline{r}^{\mathrm{i}}_{12} J_2 \\ X^{\mathrm{i}}_2 =& \overline{r}^{\mathrm{i}}_{2\mathrm{q}} J^{\mathrm{V}}_q + \overline{r}^{\mathrm{i}}_{21} J_1 + \overline{r}^{\mathrm{i}}_{22} J_2 \end{aligned} \tag{6.6}$$

Rates of transfer can be determined with higher precision from experiments data than the forces. This is the reason to express forces in terms of rates and coefficients. When the rates of transfer have been introduced, the coefficients are the resistivities divided by the area of transfer:

$$\overline{r}^{\mathrm{i}} = \frac{1}{A} r^{\mathrm{i}}(T, y) \tag{6.7}$$

These coefficients are overall resistances for the interface alone. The general word coefficient shall be used from now on for $\overline{r}$. Each coefficient is a function of the (average) temperature and vapour mole fraction. The next step is to write the entropy production rate in the vapour and liquid films with the same variables and frame of reference.

6.3.2 Films

The entropy production rate in the films are obtained in a similar manner as for the interface. But now the integration is not only over the area of transfer, but also over the film thickness. The local entropy production rate (σ^k in J/s

K m^3) gives the local driving forces as linear combinations of all fluxes for k = L,V:

$$\begin{aligned}
\sigma^k =& J_{\mathrm{q}}^{k\prime\prime} X_{\mathrm{q}}'' + J_1'' X_1'' + J_2{}'' X_2'' \\
X_{\mathrm{q}}'' =& r_{\mathrm{qq}}^k J_{\mathrm{q}}^{k\prime\prime} + r_{\mathrm{q1}}^k J_1'' + r_{\mathrm{q2}}^k J_2'' \\
X_1'' =& r_{1\mathrm{q}}^k J_{\mathrm{q}}^{k\prime\prime} + r_{11}^k J_1'' + r_{12}^k J_2'' \\
X_2'' =& r_{2\mathrm{q}}^k J_{\mathrm{q}}^{k\prime\prime} + r_{21}^k J_1'' + r_{22}^k J_2''
\end{aligned} \tag{6.8}$$

The local thermal force in a film conjugate to the measurable heat flux, $J_q^{k\prime\prime}$, is

$$X_{\mathrm{q}}'' = \frac{d}{dz}\left(\frac{1}{T}\right) \tag{6.9}$$

The local chemical driving forces in a film conjugate to the mass fluxes $J_j^{k\prime\prime}$ are, for j = 1,2:

$$X_j'' = -\frac{1}{T}\frac{d\mu_{j,T}}{dz} \tag{6.10}$$

The intensive variables do not change linearly between the liquid and vapour, neither in space nor in time. The driving forces in distillation are at their maximum value, when the vapour bubbles enter the tray, and at their minimum value when the bubbles leave the tray. An average for the driving force is somewhere between these extremes. It is assumed that there is such a representative average force for a constant area and a representative time. The integral of Eq. 6.8 for k=L,V and l=1,2,q

$$\frac{dS^{\mathrm{irr},k}}{dt} = \int_A \int_{\delta^k} \sigma^k dz dA = \sum_l J_l^k X_l^k \tag{6.11}$$

The forces X_l in Eq. 6.11 are the average forces obtained by integrating Eqs. 6.9 and 6.10 over the film thickness. The integral of flux over area gives the constant transfer rate, in a similar way as in Eq. 6.5 for the interface. By applying this to Eq. 6.8 we have the entropy production rate and the average forces for $k = L, V$:

$$\begin{aligned}
\frac{dS^{\mathrm{irr},k}}{dt} =& J_{\mathrm{q}}^k X_{\mathrm{q}}^k + J_1 X_1^k + J_2 X_2^k \\
X_{\mathrm{q}}^k =& \overline{r}_{\mathrm{qq}}^k J_{\mathrm{q}}^{\mathrm{k}} + \overline{r}_{\mathrm{q1}}^k J_1 + \overline{r}_{\mathrm{q2}}^k J_2 \\
X_1^k =& \overline{r}_{1\mathrm{q}}^k J_{\mathrm{q}}^k + \overline{r}_{11}^k J_1 + \overline{r}_{12}^k J_2 \\
X_2^k =& \overline{r}_{2\mathrm{q}}^k J_{\mathrm{q}}^k + \overline{r}_{21}^k J_1 + \overline{r}_{22}^k J_2
\end{aligned} \tag{6.12}$$

The coefficients, $\overline{r}$, in these equations are overall coefficients of the film in question. The resistance coefficient is equal to the resistivity (r) multiplied by the film thickness, divided by the area of transfer.

$$\overline{r}^{\mathrm{L}} = \frac{\delta^{\mathrm{L}}}{A} r^{\mathrm{L}}(T,x) \qquad\qquad \overline{r}^{\mathrm{V}} = \frac{\delta^{\mathrm{V}}}{A} r^{\mathrm{V}}(T,y) \tag{6.13}$$

6.3.3 Combining the contributions

The total entropy production is the sum of three contributions. From Eqs. 6.1, 6.6, and 6.12 we have:

$$\begin{aligned}\frac{dS^{\mathrm{irr}}}{dt} =& J_{\mathrm{q}}^{\mathrm{V}}\left(X_{\mathrm{q}}^{\mathrm{V}} + X_{\mathrm{q}}^{\mathrm{i}}\right) + J_{\mathrm{q}}^{\mathrm{L}} X_{\mathrm{q}}^{\mathrm{L}} + J_1\left(X_1^{\mathrm{V}} + X_1^{\mathrm{i}} + X_1^{\mathrm{L}}\right) \\ &+ J_2\left(X_2^{\mathrm{V}} + X_2^{\mathrm{i}} + X_2^{\mathrm{L}}\right)\end{aligned} \tag{6.14}$$

We are now in a position to eliminate J_q^{L} using the energy balance for the interface:

$$J_{\mathrm{q}}^{\mathrm{L}} = J_{\mathrm{q}}^{\mathrm{V}} + J_1 \Delta_{\mathrm{vap}} H_1 + J_2 \Delta_{\mathrm{vap}} H_2 \tag{6.15}$$

Equation 6.15 is introduced into Eq. 6.14:

$$\begin{aligned}\frac{dS^{\mathrm{irr}}}{dt} =& J_{\mathrm{q}}^{\mathrm{V}}\left(X_{\mathrm{q}}^{\mathrm{L}} + X_{\mathrm{q}}^{\mathrm{V}} + X_{\mathrm{q}}^{\mathrm{i}}\right) + J_1\left(X_1^{\mathrm{V}} + X_1^{\mathrm{i}} + X_1^{\mathrm{L}} + \Delta_{\mathrm{vap}} H_1 X_{\mathrm{q}}^{\mathrm{L}}\right) \\ &+ J_2\left(X_2^{\mathrm{V}} + X_2^{\mathrm{i}} + X_2^{\mathrm{L}} + \Delta_{\mathrm{vap}} H_2 X_{\mathrm{q}}^{\mathrm{L}}\right) \\ =& J_{\mathrm{q}}^{\mathrm{V}} X_{\mathrm{q}} + J_1 X_1 + J_2 X_2\end{aligned} \tag{6.16}$$

The last equation contains the three rates of transfer that we started out with in the entropy production for the interface. Each rate of transfer is multiplied with a force that is an average for the transport region. The conjugate driving forces to the three rates are:

$$\begin{aligned}X_{\mathrm{q}} =& X_{\mathrm{q}}^{\mathrm{V}} + X_{\mathrm{q}}^{\mathrm{i}} + X_{\mathrm{q}}^{\mathrm{L}} \\ X_1 =& X_1^{\mathrm{V}} + X_1^{\mathrm{i}} + X_1^{\mathrm{L}} + \Delta_{\mathrm{vap}} H_1 X_{\mathrm{q}}^{\mathrm{L}} \\ X_2 =& X_2^{\mathrm{V}} + X_2^{\mathrm{i}} + X_2^{\mathrm{L}} + \Delta_{\mathrm{vap}} H_2 X_{\mathrm{q}}^{\mathrm{L}}\end{aligned} \tag{6.17}$$

The entropy production remains the same, whether we choose this or other representations. The form that is chosen, is motivated by practical considerations. In the present case, the search for a definition of overall coefficients motivated the choice. Expressions for the average forces in Eq. 6.17 shall next be obtained.

6.4 Transport equations with overall coefficients

The forces in Eq. 6.17 and their corresponding rates should map all (most) of the dissipation in a good model. From Eq. 6.16 the following coefficient-rate products are derived for the driving forces:

$$\begin{aligned}\frac{dS^{\mathrm{irr}}}{dt} &= J_{\mathrm{q}}^{\mathrm{V}} X_{\mathrm{q}} + J_1 X_1 + J_2 X_2 \\ X_{\mathrm{q}} &= \overline{r}_{\mathrm{qq}} J_{\mathrm{q}}^{\mathrm{V}} + \overline{r}_{\mathrm{q1}} J_1 + \overline{r}_{\mathrm{q2}} J_2 \\ X_1 &= \overline{r}_{1\mathrm{q}} J_{\mathrm{q}}^{\mathrm{V}} + \overline{r}_{11} J_1 + \overline{r}_{12} J_2 \\ X_2 &= \overline{r}_{2\mathrm{q}} J_{\mathrm{q}}^{\mathrm{V}} + \overline{r}_{21} J_1 + \overline{r}_{22} J_2 \end{aligned} \tag{6.18}$$

Now $\overline{r}$ is an overall coefficient for vapour film, interface and liquid film. In order to determine these coefficients, Eqs. 6.6, and 6.12 are introduced into Eq. 6.17. For the driving force of component 1, the result is:

$$\begin{aligned} X_1 = &\left(\overline{r}_{\mathrm{q1}}^{\mathrm{i}} + \overline{r}_{\mathrm{q1}}^{\mathrm{V}} + \overline{r}_{\mathrm{q1}}^{\mathrm{L}} + \overline{r}_{\mathrm{qq}}^{\mathrm{L}} \Delta_{\mathrm{vap}} H_1\right) J_{\mathrm{q}}^{\mathrm{V}} + \\ &\left(\overline{r}_{11}^{\mathrm{i}} + \overline{r}_{11}^{\mathrm{L}} + \overline{r}_{11}^{\mathrm{V}} + 2\Delta_{\mathrm{vap}} H_1 \overline{r}_{\mathrm{q1}}^{\mathrm{L}} + \Delta_{\mathrm{vap}} H_1^2 \overline{r}_{\mathrm{qq}}^{\mathrm{L}}\right) J_1 + \\ &\left(\overline{r}_{12}^{\mathrm{i}} + \overline{r}_{12}^{\mathrm{L}} + \overline{r}_{12}^{\mathrm{V}} + \Delta_{\mathrm{vap}} H_2 \overline{r}_{\mathrm{q1}}^{\mathrm{L}} + \Delta_{\mathrm{vap}} H_1 \overline{r}_{\mathrm{q2}}^{\mathrm{L}} + \Delta_{\mathrm{vap}} H_1 \Delta_{\mathrm{vap}} H_2 \overline{r}_{\mathrm{qq}}^{\mathrm{L}}\right) J_2 \end{aligned} \tag{6.19}$$

The coefficients in this equation are $\overline{r}_{11}$, $\overline{r}_{12}$, and $\overline{r}_{1\mathrm{q}}$. Similar derivations are done for X_2 and X_{q}, in order to obtain the other coefficients. In this manner we obtain all overall coefficients as combinations of the coefficients of the two films and interface:

$$\begin{aligned} \overline{r}_{\mathrm{qq}} &= \overline{r}_{\mathrm{qq}}^{\mathrm{i}} + \overline{r}_{\mathrm{qq}}^{\mathrm{V}} + \overline{r}_{\mathrm{qq}}^{\mathrm{L}} \\ \overline{r}_{\mathrm{q1}} &= \overline{r}_{1\mathrm{q}} = \overline{r}_{\mathrm{q1}}^{\mathrm{i}} + \overline{r}_{\mathrm{q1}}^{\mathrm{V}} + \overline{r}_{\mathrm{q1}}^{\mathrm{L}} + \overline{r}_{\mathrm{qq}}^{\mathrm{L}} \Delta_{\mathrm{vap}} H_1 \\ \overline{r}_{\mathrm{q2}} &= \overline{r}_{2\mathrm{q}} = \overline{r}_{\mathrm{q2}}^{\mathrm{i}} + \overline{r}_{\mathrm{q2}}^{\mathrm{V}} + \overline{r}_{\mathrm{q2}}^{\mathrm{L}} + \overline{r}_{\mathrm{qq}}^{\mathrm{L}} \Delta_{\mathrm{vap}} H_2 \\ \overline{r}_{11} &= \overline{r}_{11}^{\mathrm{i}} + \overline{r}_{11}^{\mathrm{V}} + \overline{r}_{11}^{\mathrm{L}} + 2\Delta_{\mathrm{vap}} H_1 \overline{r}_{\mathrm{q1}}^{\mathrm{L}} + \Delta_{\mathrm{vap}} H_1^2 \overline{r}_{\mathrm{qq}}^{\mathrm{L}} \\ \overline{r}_{22} &= \overline{r}_{22}^{\mathrm{i}} + \overline{r}_{22}^{\mathrm{V}} + \overline{r}_{22}^{\mathrm{L}} + 2\Delta_{\mathrm{vap}} H_2 \overline{r}_{2\mathrm{q}}^{\mathrm{L}} + \Delta_{\mathrm{vap}} H_2^2 \overline{r}_{\mathrm{qq}}^{\mathrm{L}} \\ \overline{r}_{12} &= \overline{r}_{21} = \overline{r}_{12}^{\mathrm{i}} + \overline{r}_{12}^{\mathrm{V}} + \overline{r}_{12}^{\mathrm{L}} + \Delta_{\mathrm{vap}} H_2 \overline{r}_{\mathrm{q1}}^{\mathrm{L}} + \Delta_{\mathrm{vap}} H_1 \overline{r}_{\mathrm{q2}}^{\mathrm{L}} + \Delta_{\mathrm{vap}} H_1 \Delta_{\mathrm{vap}} H_2 \overline{r}_{\mathrm{qq}}^{\mathrm{L}} \end{aligned} \tag{6.20}$$

The coefficients refer to the same region of transport. In this formulation, gradients in temperature and concentration therefore have the same extension. The overall coefficients are not just a sum of the corresponding film and interface coefficients. Only the main thermal coefficient $\overline{r}_{\mathrm{qq}}$ is such a sum. The terms that contain heats of vapourisation, $\Delta_{\mathrm{vap}} H_j$, originate from the energy balance, that was used to eliminate the rate of heat transfer in the liquid. The

main coefficients $\overline{r}_{11}$ and $\overline{r}_{22}$, and the coupling coefficient $\overline{r}_{12}$ depend therefore on the coupling between heat and mass transport in the liquid phase. An assumption of equilibrium across the interface, means that coefficients with superscript i are zero. Neglect of coupling between heat and mass transfer in the liquid, removes terms that contain $\overline{r}^{\mathrm{L}}_{\mathrm{q}1}$ and $\overline{r}^{\mathrm{L}}_{\mathrm{q}2}$. If these assumptions both apply, we are left with:

$$\begin{aligned}
\overline{r}_{\mathrm{qq}} &= \overline{r}^{\mathrm{V}}_{\mathrm{qq}} + \overline{r}^{\mathrm{L}}_{\mathrm{qq}} \\
\overline{r}_{\mathrm{q}1} &= \overline{r}_{1\mathrm{q}} = \overline{r}^{\mathrm{L}}_{\mathrm{qq}} \Delta_{\mathrm{vap}} H_1 \\
\overline{r}_{\mathrm{q}2} &= \overline{r}_{2\mathrm{q}} = \overline{r}^{\mathrm{L}}_{\mathrm{qq}} \Delta_{\mathrm{vap}} H_2 \\
\overline{r}_{11} &= \overline{r}^{\mathrm{V}}_{11} + \overline{r}^{\mathrm{L}}_{11} + \Delta_{\mathrm{vap}} H_1^2 \overline{r}^{\mathrm{L}}_{\mathrm{qq}} \\
\overline{r}_{22} &= \overline{r}^{\mathrm{V}}_{22} + \overline{r}^{\mathrm{L}}_{22} + \Delta_{\mathrm{vap}} H_2^2 \overline{r}^{\mathrm{L}}_{\mathrm{qq}} \\
\overline{r}_{12} &= \overline{r}_{21} = \overline{r}^{\mathrm{V}}_{12} + \overline{r}^{\mathrm{L}}_{12} + \Delta_{\mathrm{vap}} H_1 \Delta_{\mathrm{vap}} H_2 \overline{r}^{\mathrm{L}}_{\mathrm{qq}}
\end{aligned} \tag{6.21}$$

The coefficients in Eq. 6.21 are equivalent to the ones from the Maxwell-Stefan equations plus Fourier's law, which is the normal way of describing interface transport, see also Appendix A.

6.5 Transfer rates, transfer area and film thickness ratio

The mass transfer rates are calculated from mass balances over the vapour phase on a tray:

$$J_{j,n} = V_n y_{j,n} - V_{n+1} y_{j,n+1} \tag{6.22}$$

The heat transfer rate across *the vapour film* is also calculated from variables of the vapour phase on a tray. From an energy balance over the vapour phase in the tray, we obtain:

$$\begin{aligned}
J^{\mathrm{V}}_{\mathrm{q}} = &(T^{\mathrm{V}}_{n+1} - T^{\mathrm{V}}_{n}) \frac{1}{2} (V_n \left[y_{n,1} C^{\mathrm{V}}_{P,1} + y_{n,2} C^{\mathrm{V}}_{P,2} \right] + \\
&V_{n+1} \left[y_{1,n+1} C^{\mathrm{V}}_{P,1} + y_{2,n+1} C^{\mathrm{V}}_{P,2} \right])
\end{aligned} \tag{6.23}$$

The temperature difference is multiplied with a term that can also be perceived as the average heat capacity of the vapour, as it ascends on a tray.

The transfer area is the interface area of all bubbles/droplets on a tray. This can be estimated by the average diameter of a bubble or droplet, d, the void fraction, ϵ, and the volume of the mixture on the tray V^{mix}:

$$A = \frac{8\pi\epsilon}{d} V^{\mathrm{mix}} \tag{6.24}$$

The film thickness of a layer can be estimated from divergence of the energy flux across the interface. We assume that there is one film in each phase, for conduction of heat and mass, undisturbed by hydrodynamic flow conditions.

$$\nabla J''_{\mathrm{e}} = \nabla(J''_{\mathrm{q}} + J''_1 H_1 + J''_2 H_2) = 0 \tag{6.25}$$

When the heats of transfer (De Groot and Mazur 1985) are constant, this gives:

$$0 = -\lambda \frac{d^2T}{dz^2} + \left[J''_1 \frac{dH_1}{dT} + J''_2 \frac{dH_2}{dT} \right] \frac{dT}{dz} \tag{6.26}$$

We solve the film thickness from the last equation for $k = L, V$:

$$\delta^k \approx \frac{\lambda^k}{J''_1 \frac{dH_1^k}{dT} + J''_2 \frac{dH_2^k}{dT}} \tag{6.27}$$

In the approximation in Eq. 6.27 it was assumed that

$$\int_o^{\delta} \left(\frac{dT}{dz} \right)^{-1} d\frac{dT}{dz} = 1 \tag{6.28}$$

The assumption is not always good, since δ^k in Eq. 6.27 may be negative. The ratio of film thicknesses may be more accurate:

$$\frac{\delta^{\mathrm{L}}}{\delta^{\mathrm{V}}} = \frac{\lambda^{\mathrm{L}}}{\lambda^{\mathrm{V}}} \frac{J_1 C^{\mathrm{V}}_{P,1} + J_2 C^{\mathrm{V}}_{P,2}}{J_1 C^{\mathrm{L}}_{P,1} + J_2 C^{\mathrm{L}}_{P,2}} \tag{6.29}$$

With Eqs. 6.24 and 6.29, two of the three unknowns A, δ^{V}, δ^{L} are known. We choose here the liquid film thickness as the adjustable parameter.

6.6 Overall coefficients from experimental data

Equations for the resistivities r^{i}, r^{L} and r^{V} are given below. Once resistivities, interface area and film thicknesses are known, the corresponding average coefficient for the region can then be calculated from Eq. 6.20.

6.6.1 Vapour and liquid resistivities

The resistivities for diffusion in the vapour and liquid phases were obtained partly from the Maxwell-Stefan equations for interdiffusion, see Appendix A. We used the expressions for Maxwell-Stefan resistivities given by Taylor and Krishna (1993), Krishna and Wesselingh (1997). Table 6.1 gives an overview of expressions for the resistivities in the vapour and liquid films. The Soret coefficient in the vapour is neglected, because it is much smaller than the one in the liquid, see Hafskjold et al. (1993). There are 3 independent resistivities for each film.

Table 6.1. Resistivities in the films

	Liquid film	Vapour film	Unit
r_{11}	$\frac{Rx_2}{x_1 c^{\mathrm{L}} \text{Đ}_{12}^{\mathrm{L}}} + \frac{{r_{1\mathrm{q}}^{\mathrm{L}}}^2}{r_{\mathrm{qq}}}$	$\frac{Ry_2}{y_1 c^{\mathrm{V}} \text{Đ}_{12}^{\mathrm{V}}}$	$\frac{\mathrm{mol^2\,K}}{\mathrm{s\,J\,m}}$
r_{12}	$-\frac{x_1}{x_2} r_{11}^{\mathrm{L}}$	$-\frac{y_1}{y_2} r_{11}^{\mathrm{V}}$	$\frac{\mathrm{mol^2\,K}}{\mathrm{s\,J\,m}}$
r_{22}	$-\frac{x_1}{x_2} r_{12}^{\mathrm{L}}$	$-\frac{y_1}{y_2} r_{12}^{\mathrm{V}}$	$\frac{\mathrm{mol^2\,K}}{\mathrm{s\,J\,m}}$
r_{qq}	$\frac{1}{\lambda^{\mathrm{L}} T^2}$	$\frac{1}{\lambda^{\mathrm{V}} T^2}$	$\frac{\mathrm{K\,J}}{\mathrm{s\,m}}$
$r_{1\mathrm{q}}$	$-x_2 r_{\mathrm{qq}}^{\mathrm{L}} \mathbb{S}_T R T^2$	0	$\frac{\mathrm{K\,mol}}{\mathrm{s\,m}}$
$r_{2\mathrm{q}}$	$-\frac{x_1}{x_2} r_{1\mathrm{q}}^{\mathrm{L}}$	0	$\frac{\mathrm{K\,mol}}{\mathrm{s\,m}}$

6.6.2 Interface resistivities

The interface resistivities (also called the jump coefficients) are given by kinetic theory (Bedeaux et al. 1992, Cipolla Jr. et al. 1974). In this theory, the interface has a thickness of approximately one Knudsen layer, i.e. one mean free path. The resistivities refer to this thickness. The theory applies to atoms and conditions that are closer to the triple point than to the critical point in a pure system (Røsjorde et al. 2001). The expressions for a binary mixture, corrected for misprints in Bedeaux et al. (1992), are:

$$
\begin{aligned}
r_{\mathrm{qq}}^{\mathrm{i}} =& \frac{\sqrt{\pi}}{4 c^V R \left(T^V\right)^2 v_{mp}} \\
& \left\{ 1 + \frac{104}{25\pi} \left\{ \left(\frac{y_1 \lambda_1^V}{\lambda^V} \right)^2 \left[1 + \frac{c_2^V}{c_1^V} \sqrt[4]{\frac{M_1}{M_2}} \right] + \left(\frac{y_2 \lambda_2^V}{\lambda^V} \right)^2 \left[1 + \frac{c_1^V}{c_2^V} \sqrt[4]{\frac{M_2}{M_1}} \right] \right\} \right\} \\
r_{11}^{\mathrm{i}} =& \frac{R\sqrt{\pi}}{16 c^V v_{mp}} \left\{ 1 + 32 \left[\sigma_1^{-1} + \frac{1}{\pi} - \frac{3}{4} \right] \left[1 + \frac{c_2^V}{c_1^V} \sqrt[4]{\frac{M_1}{M_2}} \right] \right\} \\
r_{22}^{\mathrm{i}} =& \frac{R\sqrt{\pi}}{16 c^V v_{mp}} \left\{ 1 + 32 \left[\sigma_2^{-1} + \frac{1}{\pi} - \frac{3}{4} \right] \left[1 + \frac{c_1^V}{c_2^V} \sqrt[4]{\frac{M_2}{M_1}} \right] \right\} \\
r_{\mathrm{q1}}^{\mathrm{i}} =& r_{1\mathrm{q}}^{\mathrm{i}} = \frac{\sqrt{\pi}}{8 c^V T^V v_{mp}} \left\{ 1 + \frac{16 y_1 \lambda_1^V}{5\pi\lambda^V} \left[1 + \frac{c_2^V}{c_1^V} \sqrt[4]{\frac{M_1}{M_2}} \right] \right\} \\
r_{\mathrm{q2}}^{\mathrm{i}} =& r_{2\mathrm{q}}^{\mathrm{i}} = \frac{\sqrt{\pi}}{8 c^V T^V v_{mp}} \left\{ 1 + \frac{16 y_2 \lambda_2^V}{5\pi\lambda^V} \left[1 + \frac{c_1^V}{c_2^V} \sqrt[4]{\frac{M_2}{M_1}} \right] \right\}
\end{aligned}
$$

$$r_{12}^{\mathrm{i}} = r_{21}^{\mathrm{i}} = \frac{R\sqrt{\pi}}{16 c^V v_{mp}} \tag{6.30}$$

These resistivities are all positive. In the expression for the resistivities, v_{mp} is the average of the most probable velocities of the two components (in m/s):

$$v_{mp} = \frac{1}{c^{\mathrm{V}}} \left(c_1^{\mathrm{V}} \sqrt{\frac{2RT^{\mathrm{V}}}{M_1}} + c_2^{\mathrm{V}} \sqrt{\frac{2RT^{\mathrm{V}}}{M_2}} \right) \tag{6.31}$$

The condensation coefficient(σ_j, $j = 1, 2$) is the fraction of molecules of component j that stays in the interface after collision. The rest bounces back after collision. The condensation coefficient has been found to vary largely with system and conditions (Marek and Straub 2001). We have chosen 0.8 for both components. The choice is not critical, because it will be shown that the excess entropy production rate of the interface with these coefficients is small in the studied columns.

6.7 Calculations

Experimental column data were taken from Rivero (1993). He measured all compositions, vapour and liquid rates and the temperatures in the liquid on all 10 trays in a rectifying column that separated ethanol and water. Also the entropy production rates were calculated. The vapour temperature was not measured and we assumed that the vapour temperature was the same as the temperature of the liquid flow that left the tray, i.e. $T_n^{\mathrm{V}} = T_n^{\mathrm{L}}$. The volume of the mixture on each tray was V^{mix}=2.0 10^{-3} m^3. A void fraction of 0.7, and a bubble diameter of 10^{-2} m was assumed, see De Koeijer and Kjelstrup (2002). This gave an area of transfer of 3 m^2, and a film thickness ratio around 10 from Equation 6.29. The resistivities on a tray were found for the appropriate composition and temperature using expressions in Table 6.1, and data referred to in Appendix B.

An initial guess was made for the liquid film thickness, and the solver function in MS Excel was used to minimise the squared difference between the entropy production from experimental data, and the entropy production calculated from transfer rates and coefficients, Eq. 6.18. The only adjustable variable in this fit was the liquid film thickness. By minimising the sum of squares, the liquid film thickness was determined, and the other variables accordingly. With the above parameters, the liquid film thickness was 2.0 10^{-3} m. The main data are reported with this set.

6.8 Results

De Koeijer and Kjelstrup (2002) have reported in a short form some of these calculations already. A full report is now given. The contributions to the entropy production rate are plotted in Figs. 6.3 and 6.4 as functions of tray number. Figure 6.3 shows that mass transfer can explain most of its value. Transfer of ethanol explains 68 % of the total, and transfer of water 32 % of the total. Heat transfer accounts for only 0.04 % of the total entropy production rate. The entropy production rate calculated from experimental results is also shown in Fig. 6.3.

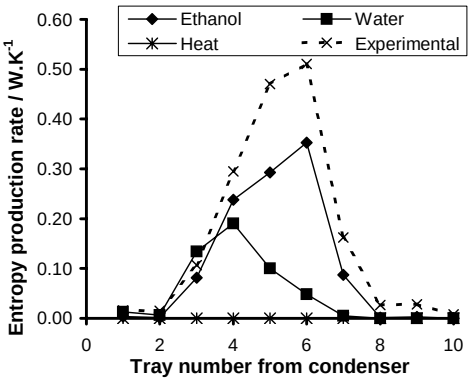

Figure 6.3. Entropy production rate from Rivero (1993) and of Eq. 6.18

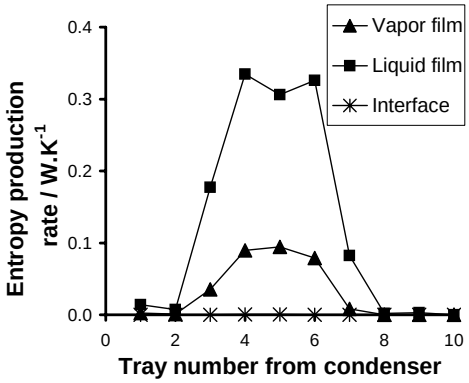

Figure 6.4. Entropy production rate in vapour film, interface, and liquid film

The contributions from the subsystems are compared in Fig. 6.4. The results is that 80 % of the entropy production rates takes place in the liquid film, and the rest in the vapour film (20 %). The contribution of the interface is only 0.05 %.

Figure 6.5 gives the main coefficient for transfer of component 1 in the two films, $\overline{r}_{11}$, as a function of average liquid temperature on the trays. The coefficient $\overline{r}_{11}$ has the highest value of all coefficients and gives therefore the most important contribution to the entropy production rate. The liquid coefficients are relatively large, much larger than the vapour coefficients. The maximum vapour contribution is 18 % at 360 K for $\overline{r}_{11}$. The contribution of the heat-mass coupling coefficients, $\overline{r}_{jq}$ is 6.5 % at the lowest temperature, 351 K. The interface coefficients are not seen with the scale that is used.

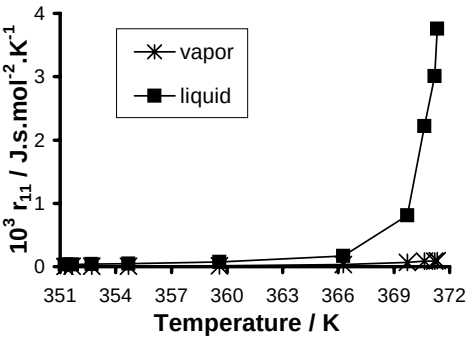

Figure 6.5. Vapour an liquid contributions to $\overline{r}_{11}$

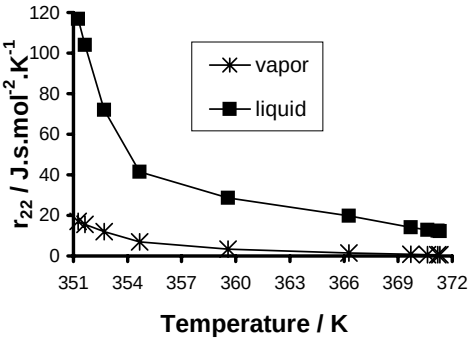

Figure 6.6. Vapour an liquid contributions to $\overline{r}_{22}$

Figure 6.6 gives the main coefficient for transfer of component 2 in the films, $\overline{r}_{22}$, as a function of average liquid temperature on the trays. The coefficient $\overline{r}_{22}$ has a larger relative contribution from the vapour than $\overline{r}_{11}$, but it is in general smaller. The contribution of the heat-mass coupling coefficients, $\overline{r}_{jq}$, was 4.0 % at the lowest temperature, 351 K.

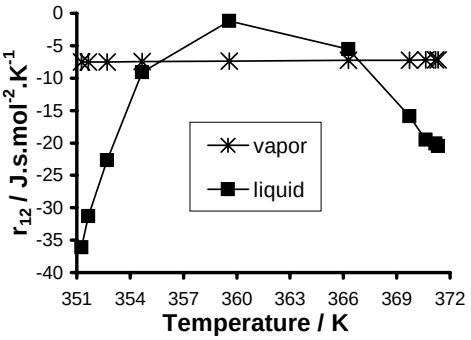

Figure 6.7. Vapour an liquid contributions to $\overline{r}_{12}$

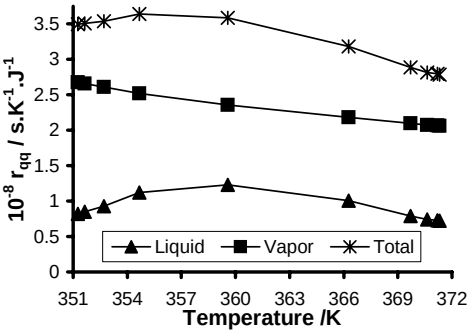

Figure 6.8. Vapour an liquid contributions to $\overline{r}_{\mathrm{qq}}$

Figure 6.7 gives the coupling coefficient $\overline{r}_{12}$ for transfer of the two components. The coefficient $\overline{r}_{12}$ is shown as a function of average liquid temperature on the trays. The coefficient is vapour dominated in the middle of the column and liquid dominated in the ends. There is a maximum in the liquid contribution, while the vapour contribution is rather constant. The coupling coefficients $\overline{r}_{jq}$ contribute up to 10.9 % to $\overline{r}_{12}$ at 371 K.

The main coefficient of heat transfer $\overline{r}_{qq}$ is shown in Figure 6.8. The contributions from the liquid film and vapour film to this coefficient are shown as a function of average liquid temperature on the tray. The vapour contribution is larger than the liquid contribution.

Figure 6.9 shows the role of the Soret coefficient on all trays. On tray 1, all coefficients ($\overline{r}_{11}$, $\overline{r}_{22}$, $\overline{r}_{12}$) have a significant contribution from the Soret coefficient. In contrast, on tray 6 there is only a small contribution. After tray 6 the contributions changes sign and becomes larger, because the Soret coefficient changes sign around the temperature and concentration on tray 6. The contribution to $\overline{r}_{12}$ has a minimum at tray 5. The contributions to $\overline{r}_{11}$ and $\overline{r}_{22}$ vary anti-symmetrically.

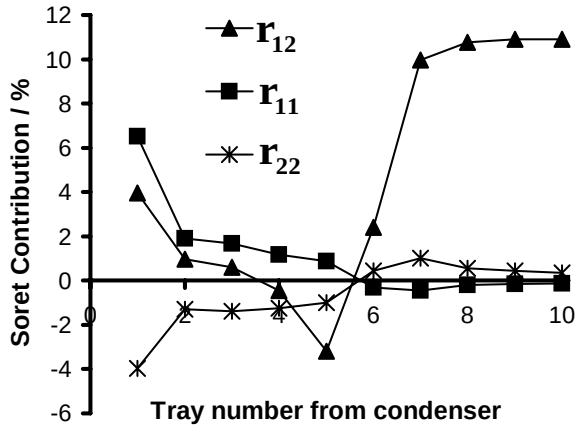

Figure 6.9. Soret contribution to coefficient coefficients as function of tray number

6.9 Discussion

6.9.1 Entropy production rate

An explanation for the location of the irreversibilities and their origin is first of interest. Most of the entropy production rate is located in the centre of the column, see Figs. 6.3 and 6.4. This can be explained by the particular rectifying column that is used. At trays that are situated below the condenser, the entropy production rate is small, because the most important coefficient, the main coefficient of ethanol transport $\overline{r}_{11}$ is small. At trays where $\overline{r}_{11}$ is large, there is not much separation work done, because the most important

driving force is small (see Fig. 6.10 below). The entropy production is thus in the middle part, where most of the separation takes place.

The experimental error in the mole fractions gives an error in the entropy production rate of ± 0.02 W/K. This means that the experimental and theoretical entropy production fall in each others confidence intervals in Fig. 6.3. The resulting close fit is surprising, considering the approximations that we have used, namely those of a constant area of transfer, constant film thicknesses throughout the column, and the fact that the fit was obtained with only one adjustable parameter (the liquid film thickness). The true entropy production may contain other contributions than the ones we considered, for instance from pressure variation and mixing. We are, however, able to predict the *variation* in the entropy production rate along the trays rather well. This lends support to the assumption that most of the entropy production is indeed due to coupled heat and mass transport. Other authors (Ray et al. 1994, Taprap and Ishida 1996) have concluded the same, but with different expressions for the irreversibilities.

Figure 6.3 showed that transfer of both ethanol and water gives significant contributions. This must be so for distillation, which is a typical process of interdiffusion. The contribution from heat transfer is small, in agreement with other studies by Ray et al. (1994). But even if this true, one must not conclude that the coupling between heat and mass transfer is unimportant, cf. Figure 6.9. In general, the entropy production does not depend very much on the coupling coefficient, see Førland et al. (2001). In the present case, we have the entropy production in terms of rates and coefficients:

$$\frac{dS^{\mathrm{irr}}}{dt} = \overline{r}_{11} J_1^2 + \overline{r}_{22} J_2^2 + \overline{r}_{\mathrm{qq}} {J_{\mathrm{q}}^{\mathrm{V}}}^2 + 2\overline{r}_{12} J_1 J_2 + 2\overline{r}_{1\mathrm{q}} J_1 J_{\mathrm{q}}^{\mathrm{V}} + 2\overline{r}_{2\mathrm{q}} J_2 J_{\mathrm{q}}^{\mathrm{V}} \quad (6.32)$$

The first three terms on the right hand side are positive, as all main coefficients are positive, see Figs. 6.5, 6.6, and 6.8. The fourth term is also positive, because in binary adiabatic distillation the mass transfer rates have opposite signs on all trays, and because $\overline{r}_{12}$ is negative. However, the last two terms nearly cancel each other, because $\overline{r}_{1\mathrm{q}}$ and $\overline{r}_{2\mathrm{q}}$ are positive and have the same order of magnitude. Even if the entropy production is not sensitive to the coupling coefficients, the forces and the transfer rates are. The contribution of the Soret effect on the thermal force in Eq. 6.18 was on average 50 %.

Figure 6.4 shows that the vapour and liquid phases both contribute significantly to the entropy production rate, in spite of the liquid film being 10 times larger than the vapour film. The entropy production per length of film is around 5

times larger in the vapour. In this analysis, the interface need not be considered as a source of entropy production. One explanation for this is that the rates of transfer are so moderate in distillation that the assumption of equilibrium across the interface is a good one. But the result depends of course entirely on the validity of rate coefficients from kinetic theory. These coefficients for the vapour film are derived for ideal gases close to the triple point (or triple line), and most likely do not apply to non-ideal systems. We can therefore only conclude that *ideal systems* have negligible coefficients for the interface. Possible consequences of this for the rate equations are discussed further below.

6.9.2 The overall coefficients

The overall resistance coefficients for mass transfer must be understood on the background of their interdependency. The main coefficients to mass transfer $\overline{r}_{11}$ and $\overline{r}_{22}$ were plotted in Figs. 6.5 and 6.6. The coefficients vary in opposite manners along the column, due to their interdependency introduced by the Gibbs-Duhem equation, see Table 6.1. The large variation in the main coefficients is avoided in the Maxwell-Stefan equations.

A smaller variation is seen in $\overline{r}_{12}$, see Fig. 6.7 and Table 6.1. In ideal liquid mixtures, the coefficient $\overline{r}_{12}$ will show a monotonic variation with the concentration, and a good estimate is obtained by the Wilke-Chang equation combined with the Vignes equation (Taylor and Krishna 1993). For the liquid ethanol-water mixture this was not the case, however. The Maxwell-Stefan diffusion coefficients did not show a monotonic behaviour in the experimental data from Tyn and Calus (1975). There is maximum in the liquid contribution in Fig. 6.7 due to non-ideal behaviour. So, the normal method could not be used. The alternative equation for this specific mixture is given in Appendix B. In contrast, the vapour contribution is rather constant due to the choice of model, see Appendix B.

The film thicknesses were calculated, assuming hydrodynamically undisturbed films. They were found, by fitting a theoretical expression for the entropy production rate (where the thicknesses entered) to values calculated from experimental results. We have assumed that the entropy production rate has only contributions from mass and heat transfer, while other contributions may also be present. This means that *maximum values* for the thicknesses were found. It is therefore not surprising that our values appear to be on the large side of those reported elsewhere in Taylor and Krishna (1993), Alopeaus and Aittamaa (2000). We explain this by our neglect of other contributions to the

entropy production rate, and to hydrodynamic effects.

A film thickness ratio of 10 means that the liquid should dominate the coefficients, see Fig. 6.4. A close inspection shows, however, that the liquid contribution is not systematically the largest contribution to all coefficients. The main coefficients for mass transfer, $\overline{r}_{11}$ and $\overline{r}_{22}$, are dominated by the liquid, but the coefficient of heat transfer $\overline{r}_{\mathrm{qq}}$ is largest in the vapour phase, see Fig. 6.8. The coupling coefficient $\overline{r}_{12}$ showed a mixed behaviour. It is therefore not correct to speak about one phase-control for heat and mass transfer. In order for a single phase to dominate totally, a thickness ratio much larger than 10, or much smaller than 0.1, is necessary.

It is possible to estimate the film thicknesses by other methods than ours. We took the film thicknesses for mass and heat transfer to be the same. This is not only for simplicity, but also because we know that the coupling coefficients for heat and mass influence the film thicknesses. The film thickness of Eq. 6.27 resembles the expression that is found from the Lewis number ($Le = \lambda/\rho C_P Đ_{12}$). The Lewis number gives the ratio of heat transfer and mass transfer film thicknesses in cases when coupling coefficients are zero. With our data, the Lewis number varied from 4 to 8 in the vapour, and from 17 to 48 in the liquid. A ratio of 10 between the liquid and vapour is possible from these numbers, but a difference is indicated for heat and mass transfer.

De Koeijer and Rivero (2002) gave a qualitative argument for the presence of a non-negligible coupling effect between heat and mass transfer in distillation. They arrived at this conclusion by analysing a diabatic column. The results in Fig. 6.9 quantify their conclusion. The Soret coefficients may give a non-negligible contribution to the overall coefficients in Eq. 6.20. This conclusion does not depend on the values for the transfer area, or of the film thicknesses, because these variables are common to all coefficients. The ratio between the thicknesses is important, however, since the Soret effects in the vapour are smaller than in the liquid (Hafskjold et al. 1993). A shift in the film thickness ratio from 10 to 1, will make the coefficients more vapour dominant. The importance of the coupling between heat and mass transfer decreases accordingly.

6.9.3 The average driving forces

The driving forces for transport, like in Eq. 6.19, are averages over the time that the bubbles and droplets reside on the tray, as well as over the transport path

between liquid and vapour. Once the overall coefficients have been determined, the forces can be calculated from Eq. 6.18. This calculation used a constant transfer area, constant film thicknesses and constant transfer rates. The force can also be estimated as an arithmetic average of the minimum and maximum driving force on a tray. The maximum driving force exists at the entrance between L_{n-1} and V_{n+1}, while the minimum force exists at the exit between L_n and V_n. If equilibrium is reached on a tray, the minimum value is zero. An arithmetic average can be justified, when there is a linear variation in the intensive variables in Fig. 6.1. The average driving force of mass transport is from Eq.(17), see also De Koeijer and Rivero (2002):

$$X_j = \frac{1}{2} R \ln \frac{x_{j-1}\gamma_j P_j^*(T_{n-1}^{i,\mathrm{L}})}{y_{j+1}P_{n+1}^{\mathrm{V}}} \frac{x_j \gamma_j P_j^*(T_n^{i,\mathrm{L}})}{y_j P_n^{\mathrm{V}}} \tag{6.33}$$

The term with the thermal driving force over the liquid film in Eq. 6.17 can be neglected. A corresponding expression for the average thermal force can be written.

Figure 6.10 gives the driving force for ethanol transport on all trays as calculated from Eq. 6.33 and from Eq. 6.18 or 6.19. The two results were similar, they followed each other rather well along the column. The agreement was less good, but still reasonable for the driving force for water transfer, see Fig. 6.11. Because ethanol transfer was the largest contributor to the entropy production, it is reasonable that the fitting procedure will fit best the force for ethanol transport. Differences in Figs. 6.10 and 6.11 reflect the goodness of the averaging procedures and the model used.

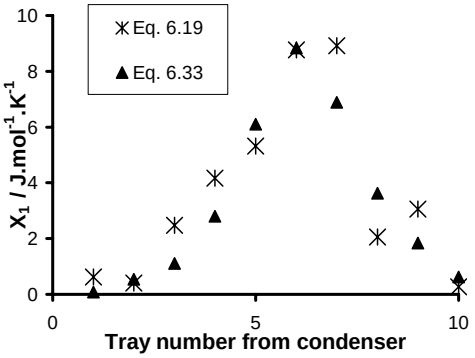

Figure 6.10. Driving force X_1

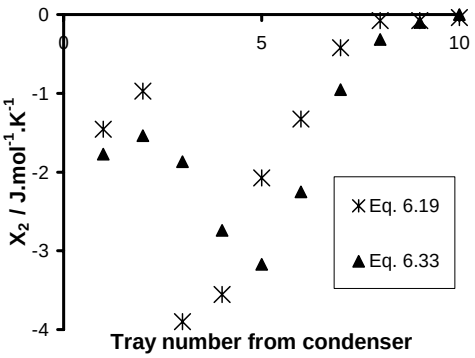

Figure 6.11. Driving force X_2

The thermal force is very probably much less well predicted by an average

procedure, since we do not have temperature measurements in the vapour to use. The term that contains the thermal force and transfer rate is also very small compared to the other two, and less suitable for a similar examination as this one.

6.9.4 Non-equilibrium modelling

Our set of equations, using Eq. 6.20, can be reduced to the Maxwell-Stefan approach of Taylor and Krishna (1993) when the interface coefficients and Soret coefficients are zero. The first step in this direction is done in Eq. 6.21. The Maxwell-Stefan equations of transport give convenient descriptions of multicomponent diffusion. They are independent of the choice of frame of reference for the fluxes, and their coefficients are in many cases remarkably independent of the concentration (Krishna and Wesselingh 1997). In the particular case studied here, a concentration dependence was seen, however.

Our formulation needs the interface as the frame of reference, as explained previously. One advantage of the Maxwell-Stefan's formulation is lost by introducing this particular frame of reference. We gain on the other hand, a common basis that makes possible an inclusion of more terms, as they are deemed necessary. The interface might be rate limiting to transport in non-ideal systems. This is not known, but it is now feasible to include this, if necessary. We can still take advantage of expressions for diffusion coefficients in the Maxwell-Stefan equations, as was shown.

Rate equations are needed in dynamic modelling of distillation. We have described above a procedure that can describe better, but not yet fully, the coupling of heat and mass transfer, in distillation. This is the main difference between our work, and other available methods. We have chosen a particular estimate for transfer area and film thicknesses, but these estimates can be improved. Equation 6.18 is constructed in such a way that this is possible.

So far, the temperature profile of the column is best modelled by the temperature that corresponds to the equilibrium of the outlet liquid mole fractions on the tray. It will be interesting to see whether a better estimate can be obtained, with a thermal force that include the Soret effect in the liquid. This has not been possible to test with the available data.

6.10 Conclusions

A set of equations for heat- and mass transfer in distillation has been derived in a systematic manner from the entropy production rate of the trays in a distillation column. The equations were illustrated by experimental data from distillation of ethanol and water. The description was able to model the variation in the entropy production over the trays that was calculated from experimental data. This result was obtained with an estimated transfer area and film thickness ratio, and one fitting variable: the liquid film thickness. The fitting procedure was based on the entropy production. Six overall coefficients for transport of heat and mass across the phase boundary were presented, and discussed on the basis of the experimental data. Heats of vapourisation contributed to the coupling coefficients, making these non-negligible. The coefficients include contributions from the liquid as well as the vapour phase and the interface. While the actual contributions from the interface was negligible with the kinetic theory model for these contributions, the interface does play a role in defining proper boundary conditions. Further attention should be given to the thermal force and its role in predicting the column temperature profile.

Acknowledgements

Dick Bedeaux is thanked for suggesting to use Eq. 6.27. The Research Council of Norway is thanked for a grant to Gelein de Koeijer.

Appendix: Resistivities in the interface frame of reference

The entropy production rate does not change when the frame of reference is changed for the fluxes. This property is useful to derive relations between our coefficients and other ones. The Maxwell-Stefan equations are convenient, since they do not depend upon the choice for frame of reference. These are our starting point. They are written for an interface frame of reference, with an interface velocity u^{i}. In an isothermal system, the entropy production rate can be written:

$$\sigma = c_1(u_1 - u^{\mathrm{i}})\left(-\frac{1}{T}\frac{d\mu_{1,T}}{dz}\right) + c_2(u_2 - u^{\mathrm{i}})\left(-\frac{1}{T}\frac{d\mu_{2,T}}{dz}\right) \tag{6.34}$$

where u_j are component velocities. The flux equations that follow from this formulation of the entropy production rate are the Maxwell-Stefan equations:

$$\begin{aligned} -\frac{c_1}{T}\frac{d\mu_{1,T}}{dz} =& \frac{r_{11}}{T}(u_1 - u^{\mathrm{i}}) + \frac{r_{12}}{T}(u_2 - u^{\mathrm{i}}) \\ -\frac{c_2}{T}\frac{d\mu_{2,T}}{dz} =& \frac{r_{21}}{T}(u_1 - u^{\mathrm{i}}) + \frac{r_{22}}{T}(u_2 - u^{\mathrm{i}}) \end{aligned} \tag{6.35}$$

The rate equations are constructed so that Onsager reciprocal relations hold. Because the sum of the left hand side of these equations is zero (Gibbs-Duhem's equation), and because the coefficients are dependent, the coefficients (in J.s/m^5) are related:

$$r_{11} = -r_{12} = -r_{21} = r_{22} \tag{6.36}$$

By filling in Eq. 6.36 into 6.35, the velocity of the frame of reference drops out, and leaves a set that is independent of the frame of reference. With the Maxwell-Stefan equations from Krishna and Wesselingh (1997) the coefficients r are directly related to the Maxwell-Stefan diffusion coefficient:

$$r_{11} = RT\frac{x_1 x_2}{c\text{Đ}_{12}} \tag{6.37}$$

In order to compare with our work, the flux in the interface frame of reference is defined for j=1,2 as:

$$J_j'' = c_j(u_j - u^{\mathrm{i}}) \tag{6.38}$$

By filling in Eq. 6.38 and 6.37 into 6.35, we get the force equations in the interface frame of reference:

$$-\frac{1}{T}\frac{d\mu_{1,T}}{dz} = \frac{Rx_2}{cx_1\text{Đ}_{12}}J_1'' + \frac{R}{c\text{Đ}_{12}}J_2'' \tag{6.39}$$

$$-\frac{1}{T}\frac{d\mu_{2,T}}{dz} = \frac{R}{c\text{Đ}_{12}}J_1'' + \frac{Rx_1}{cx_2\text{Đ}_{12}}J_2'' \tag{6.40}$$

This derivation shows that both approaches are in principle the same. Next, non-isothermal systems are considered. The Maxwell-Stefan equation for the first component in a binary mixture with a temperature gradient is described by Kuiken (1994):

$$-\frac{x_1}{RT}\frac{d\mu_{1,T}}{dz} = \frac{x_1 x_2\left(u_1^{\mathrm{T}} - u_2^{\mathrm{T}}\right)}{\text{Đ}_{12}} \tag{6.41}$$

where u_j^T are the augmented component velocities that incorporate the contribution of thermal diffusion. By separating the isothermal and thermal velocities, we have

$$-\frac{x_1}{RT}\frac{d\mu_{1,T}}{dz} = \frac{x_1 x_2 \left(u_1 - u_2\right)}{Đ_{12}} + x_1 x_2 s_T \left(1 + \frac{d\ln\gamma_1}{d\ln x_1}\right)\frac{dT}{dz} \tag{6.42}$$

In terms of the driving force for component 1, this is:

$$X_1'' = \frac{R x_2 J_1''}{x_1 c Đ_{12}} - \frac{R J_2''}{c Đ_{12}} - x_2 \mathbb{S}_T R T^2 X_\mathrm{q}'' \tag{6.43}$$

with the experimental Soret coefficient s_T in

$$\mathbb{S}_T = s_T \left(1 + \frac{d\ln\gamma_1}{d\ln x_1}\right) \tag{6.44}$$

The force in Eq. 6.18 can be rewritten:

$$X_1'' = \left(r_{11} - \frac{{r_{1\mathrm{q}}}^2}{r_{\mathrm{qq}}}\right) J_1'' + \left(r_{12} - \frac{r_{1\mathrm{q}} r_{2\mathrm{q}}}{r_{\mathrm{qq}}}\right) J_2'' + \frac{r_{1\mathrm{q}}}{r_{\mathrm{qq}}} X_\mathrm{q}'' \tag{6.45}$$

A comparison of the Eqs. 6.43 and 6.45 gives the resistivities in Table 6.1. So, also for non-isothermal systems, it is shown that both descriptions are in principle the same.

Finally, the experimentally measured Soret coefficients s_T from Kolodner et al. (1988) is rewritten in our terms. They found the Soret coefficient from the gradient in mole fraction at zero mass transfer rate:

$$\left(\frac{dx_1}{dz}\right)_{J_1=0} = -s_T x_1 x_2 \frac{dT}{dz} \tag{6.46}$$

This condition is rewritten as:

$$\begin{aligned} X_1'' &= \frac{r_{1\mathrm{q}}}{r_{\mathrm{qq}}} X_\mathrm{q}'' \\ -\frac{1}{T}\frac{d\mu_{1,T}}{dz} &= \frac{r_{1\mathrm{q}}}{r_{\mathrm{qq}}}\frac{d(1/T)}{dz} \\ \frac{dx_1}{dz} &= \frac{r_{1\mathrm{q}}}{R r_{\mathrm{qq}}}\frac{1}{T^2}\frac{dT}{dz}\left(1 + \frac{d\ln\gamma_1}{d\ln x_1}\right)^{-1} \end{aligned} \tag{6.47}$$

The resistivity ratio $r_{1\mathrm{q}}/r_{\mathrm{qq}}$ is connected to the Soret coefficient by these equations. From these equations, the coefficients in Table 6.1 are derived.

Appendix: Estimating resistivities

The vapour-liquid equilibrium properties were calculated using the integrated Clausius-Clapeyron equations for a regular solution with the Margules equation for the activity coefficients. The Margules parameters were 1.6711 and 0.9006 (see DECHEMA data series Gmehling and Onken (1977)). Densities and molar volumes for the vapour phase were calculated from the ideal gas law. For the liquid phase we assumed constant density and molar volumes. The thermal conductivity was taken from Reid et al. (1987) who tabulated λ in the form:

$$\lambda_j = A_j^{\lambda} + B_j^{\lambda} T + C_j^{\lambda} T^2 + D_j^{\lambda} T^3 \tag{6.48}$$

The conductivity of a vapour mixture was the molar average one. For the thermal conductivity of a liquid mixture, Yano et al. (1988) recommended the following Filipov equation:

$$\lambda = w_1 \lambda_1 + w_2 \lambda_2 - 0.45 w_1 w_2 |\lambda_1 - \lambda_2| \tag{6.49}$$

The heat capacities for the liquid and vapour, C_P^{L} and C_P^{V}, were taken from Smith and Van Ness (1987). As a function of temperature, they are for j=1,2:

$$\frac{C_{P,j}}{R} = A^{C_{P,j}} + B^{C_{P,j}} T + C^{C_{P,j}} T^2 + \frac{D^{C_{P,j}}}{T^2} \tag{6.50}$$

The Maxwell-Stefan diffusion coefficients were calculated from the experimental data (Tyn and Calus 1975) using the formulation from Kuiken (1994):

$$Đ_{12}^{\mathrm{L}} = D_{12} \left(1 + \frac{\partial \ln \gamma_1}{\partial \ln x_1} \right)^{-1} \tag{6.51}$$

A polynomial of the third degree in mole fraction and second degree in temperature was assessed to be sufficient to describe the experimental data for the diffusion coefficient. The model was created by starting with the suggested polynomial including all cross combinations, i.e. 11 terms. Then a linear regression was performed and the term with the highest p-value was taken out of the model. This was done until all p-values were below 10^{-7}. The result was a polynomial with only 4 terms and a constant:

$$10^9 Đ_{12}^{\mathrm{L}} = 1.15 + \frac{T - 305}{50} \left(1.66 + 18.4 x_1 - 35.7 x_1^2 + 17.7 x_1^3 \right) \tag{6.52}$$

The Fuller relation was used for $Đ_{12}^{\mathrm{V}}$, as proposed by Taylor and Krishna (1993):

$$Đ_{12}{}^{\mathrm{V}} = 1.013\, 10^{-2} T^{1.75} \frac{\sqrt{\frac{M_1 + M_2}{M_1 M_2}}}{P \left(\sqrt[3]{V_1^{\mathrm{dif}}} + \sqrt[3]{V_2^{\mathrm{dif}}} \right)^2} \tag{6.53}$$

Kolodner et al. (1988) measured the Soret coefficient of a liquid water/ethanol mixture in the range from 283-313 K and 0.05-0.6 in ethanol mole fraction. The experimental results showed a shift in sign, i.e. a highly non-ideal behaviour. A model for the s_T was presented, suitable for extrapolation:

$$10^3 s_T = \left(2.493 - \frac{T}{39.661}\right)\left(1 - 3.190\left(\tanh\left(\frac{w - 0.2387}{0.1668}\right)^3\right)^{1/3}\right) \quad (6.54)$$

The temperature is given in K and w is the weight fraction of ethanol. Table 7.2 gives an overview of the constants that are used.

Table 6.2. Physical chemical properties

Component	Ethanol	Water	Reference
T^{boil}(K)	351.45	373.73	Sinnot et al. (1983)
ρ^{L}(kg/m^3)	789	998	Sinnot et al. (1983)
$\Delta_{\mathrm{vap}}H(T^{\mathrm{boil}})$ (J/mol)	38770	40683	Sinnot et al. (1983)
$A^{C_P^{\mathrm{V}}}$(-)	3.518	3.470	Smith and Van Ness (1987)
$B^{C_P^{\mathrm{V}}}$(1/K)	20.001 10^{-3}	1.450 10^{-3}	Smith and Van Ness (1987)
$C^{C_P^{\mathrm{V}}}$(1/K^2)	-6.002 10^{-6}	-	Smith and Van Ness (1987)
$D^{C_P^{\mathrm{V}}}$(K^2)	-	0.121 10^5	Smith and Van Ness (1987)
$A^{C_P^{\mathrm{L}}}$(-)	33.866	8.712	Smith and Van Ness (1987)
$B^{C_P^{\mathrm{L}}}$(1/K)	-172.60 10^{-3}	1.25 10^{-3}	Smith and Van Ness (1987)
$C^{C_P^{\mathrm{L}}}$(1/K^2)	349.1710^{-6}	-0.18 10^{-6}	Smith and Van Ness (1987)
$A^{\lambda^{\mathrm{V}}}$(W/m.K)	-7.797 10^{-3}	7.341 10^{-3}	Reid et al. (1987)
$B^{\lambda^{\mathrm{V}}}$(W/m.K^2)	4.167 10^{-5}	-1.013 10^{-5}	Reid et al. (1987)
$C^{\lambda^{\mathrm{V}}}$(W/m.K^3)	1.214 10^{-8}	1.8017 10^{-7}	Reid et al. (1987)
$D^{\lambda^{\mathrm{V}}}$(W/m.K^4)	-5.184 10^{-11}	-9.100 10^{-11}	Reid et al. (1987)
$A^{\lambda^{\mathrm{L}}}$(W/m.K)	2.629 10^{-1}	-3.838 10^{-1}	Reid et al. (1987)
$B^{\lambda^{\mathrm{L}}}$(W/m.K^2)	-3.847 10^{-4}	3.374 10^{-3}	Reid et al. (1987)
$C^{\lambda^{\mathrm{L}}}$(W/m.K^3)	2.211 10^{-7}	-3.667 10^{-6}	Reid et al. (1987)
V^{dif}	90.96	113.79	Taylor and Krishna (1993)

7 Entropy Production Minimisation of a SO_2 Converter

Gelein de Koeijer, Eivind Johannessen, and Signe Kjelstrup

Norwegian University of Science and Technology
Department of Chemistry, Physical Chemistry
N-7491 Trondheim
Norway

This paper will be sent in for publication

Abstract

The entropy production rate of a SO_2 converter is minimised by changing simultaneously the heights of four catalytic beds, temperature differences across five intermediate heat exchangers, and the distribution of area available for heat exchange. The inlet temperature, inlet pressure, inlet composition, outlet temperature, and outlet composition were kept constant in the minimisation. In comparison to a standard converter, 16.7 % of the entropy production rate due to reaction, pressure drop, and heat transfer could be saved. This can appear as higher quality heat output, or less area of transfer required for heat exchange. The optimum operating conditions indicate that the reaction can be carried out under milder thermal conditions than in the standard converter. We found that the requirement for catalyst, as measured by the total bed height, decreases with area available for heat transfer, from 2.4 m at 2000 m^2 to 1.7 m at 6000 m^2. So, there is a large improvement potential for this process.

7.1 Introduction

Optimisation of reactors in chemical industry is studied intensively, since a reactor is most often the central unit around which a plant is designed. A good reactor design is crucial for the performance of other units. We have chosen to consider a simple and well studied reactor system, namely the oxidation of sulphur dioxide (SO_2) to sulphur trioxide (SO_3) in packed beds. The system is part of the sulphuric acid synthesis system, a well proven technology, see Zeisberg (1911), Fogler (1992), Mueller (1994). There is a large variety of optimisation problems of interest for this system: high yield by Chartrand and Crowe (1969), return on investment by Doering and Gaddy (1980), and operating and investment cost of heat exchangers by Ostrovsky et al. (1990), to mention some.

In view of the demands worldwide on higher energy efficiency and smaller emissions of carbon dioxide, we have chosen to minimise the entropy production rate (or exergy loss or lost work) of reactor systems. This is equivalent to maximise the second law energy efficiency. We have so far worked mostly on method development with that purpose (Kjelstrup et al. 1999b, Kjelstrup and Island 1999, Kjelstrup et al. 1998, 2000, Nummedal et al. 2001, 2002, Johannessen et al. 2002). Some simplifications have been introduced, i.e. we

have always assumed plug flow conditions. It is not enough to study the reaction alone. The optimum solution changes considerably, when the heat exchange in the system is taken into account. The method development has now reached a stage that it is possible to test it on a real system.

The technology studied here consists of four catalytic beds and five heat exchangers (Lurgi GmbH 1990). Some standard operating conditions are chosen and used to define our reference system. The objective function is the entropy production rate of the beds and the heat exchangers, and the problem we want to examine is the following: Given that we keep the most important inlet and outlet conditions constant, is it possible to find a new path of operation that has minimum entropy production rate? The reason why we keep inlet and outlet conditions fixed is that we want an answer that effects up- and downstream processes in the plant as little as possible. The variables of the minimisation are realistic: The temperature differences between the outlet and inlet of the heat exchangers, the heights of the catalytic beds, and the areas available for heat transfer in the heat exchangers.

We shall indeed see that it is possible to find a state of operation that has a significant lower entropy production rate. The maximum gain solution is interestingly also characterised by milder thermal conditions in the reactor. This may be beneficial for the durability of the catalyst. A trade-off situation shall also be demonstrated between heat exchanger design and amount of catalyst used. The requirement for catalyst amounts, as measured by the bed heights, decreases namely with area available for heat transfer. Furthermore, chemical equilibrium is not necessarily reached at the outlet of each catalyst bed. In addition we will see that when fewer variables are allowed to vary, a smaller gain is obtained.

7.2 The system

7.2.1 Introduction

In the system sulphur dioxide is oxidised. This is an important step in the production of sulphuric acid. Sulphur dioxide is a toxic gas, so governments have imposed strict regulations on the amount and the concentration of sulphur dioxide outputs to the environment. An important aspect of sulphur dioxide oxidation units is thus to keep the outlet concentration of sulphur dioxide below acceptable levels. Sulphur dioxide, diluted in air, is oxidised to sulphur

trioxide according to:

$$SO_2(g) + \frac{1}{2}O_2(g) \rightleftarrows SO_3(g) \qquad \text{(I)}$$

A vanadium pentoxide catalyst is used. The product, sulphur trioxide, is afterwards dissolved in water producing sulfuric acid, which is an important bulk chemical.

A low enough concentration of sulphur dioxide cannot be reached in one adiabatic catalytic bed. Therefore, more beds with intermediate cooling are needed. The intermediate cooling is done with heat exchangers. We chose a reactor system design with four beds and five heat exchangers. In most literature 4 or 5 beds are reported. The system is shown in Figure 7.1.

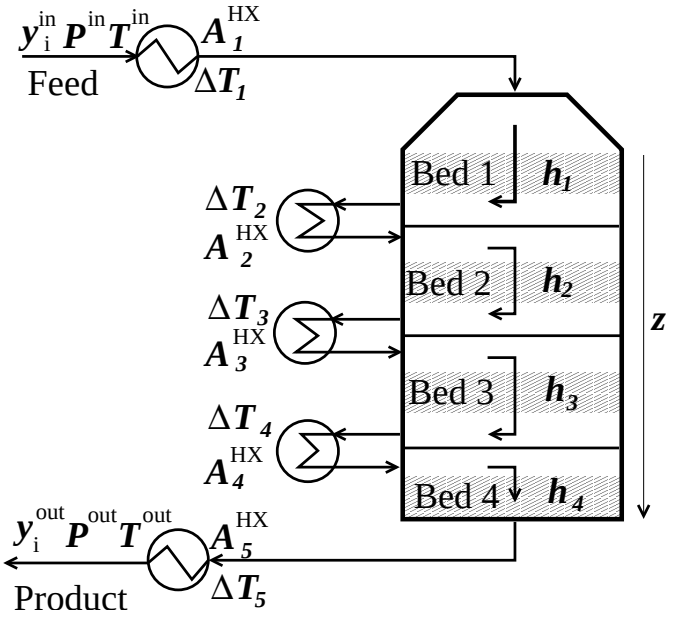

Figure 7.1. Sketch of the reactor system

Inlet and outlet parameters, as well as some other parameters for the reactor, are given in Table 7.1. The parameters are arbitrary, but representative for an industrial reactor system (Målsnes and Rostad 1998). We consider them as fixed in the present study.

Table 7.1. Parameters

Parameter	Description	Value
d^{bed}	Diameter bed	6 m
d^{part}	Particle diameter	8 mm
ρ^{bed}	Bed density	450 kg/m^3
ϵ	Bed porosity	0.26
T^{in}	Inlet temperature	333 K
P^{in}	Inlet pressure	1.3 10^5 Pa
$y^{in}_{SO_2}$	Inlet mole fraction SO_2	0.075
$y^{in}_{SO_3}$	Inlet mole fraction SO_3	0
$y^{in}_{O_2}$	Inlet mole fraction O_2	0.1
$y^{in}_{N_2}$	Inlet mole fraction N_2	0.825
F^{in}	Initial molar flow	480 mol/s
η	Gas viscosity	3.7 10^{-5} Pa s

7.2.2 Conservation equations for the catalyst beds

We use a plug flow model for the catalyst beds. This model considers only transport by convection in the z-direction, i.e. from the top of the first bed to the bottom of the fourth bed. There is a flat gas velocity profile and no radial gradients in the beds. Heterogeneous effects due to diffusion and reaction inside the catalyst pellets are neglected. Each bed is adiabatic.

We want to model the state of the reacting stream as it moves from the inlet at $z = 0$ to the outlet at $z = h_n$ (n =1, 2, 3, 4). The state is fully specified by the temperature (T), pressure (P) and chemical composition. The composition of the reacting mixture can be described with a single variable; the conversion of SO_2 in reaction I. This is a standard way to keep track of the composition in plug flow reactors (see for instance Fogler (1992)). The conversion of SO_2 in reaction I is defined as

$$\chi = \frac{\text{moles of } SO_2 \text{ consumed by reaction I}}{\text{moles of } SO_2 \text{ initially}} \tag{7.1}$$

The molar flow rates, F_i, and the mole fractions, y_i, become then

$$F_i = F^{in}_{S0_2} \, (\theta_i + \nu_i \, \chi \,) \tag{7.2}$$

and

$$y_i = \frac{F_i}{F_{tot}} = \frac{\theta_i + \nu_i \, \chi}{\theta_{tot} - \frac{1}{2} \, \chi} \tag{7.3}$$

respectively. Here, $i = SO_2$, O_2, SO_3, N_2, superscript in means values at the inlet of the first bed, ν_i is the stoichiometric coefficient of component i, and

$$\theta_i = \frac{F_i^{\text{in}}}{F_{\text{SO}_2}^{\text{in}}} \qquad \theta_{\text{tot}} = \frac{F_{\text{tot}}^{\text{in}}}{F_{\text{SO}_2}^{\text{in}}} \tag{7.4}$$

The state variables are governed by conservation equations. These are the energy balance, the momentum balance and the mole balance, see for instance Fogler (1992) for a derivation. The energy balance is

$$\frac{dT}{dz} = \frac{\pi}{4} (d^{\text{bed}})^2 \, \rho^{\text{bed}} \, \frac{r_{\text{SO}_2} \, (-\Delta_{\text{R}} H \,)}{\sum_i F_i \, C_{P,i}} \tag{7.5}$$

Here, $\Delta_{\text{R}} H$ is the heat of reaction, r_{SO_2} is the rate of reaction I, and $C_{P,i}$ is the heat capacity of component i.

Ergun's equation is used to describe the pressure drop:

$$\frac{dP}{dz} = -\left(\frac{150 \, \eta}{(d^{\text{bed}})^2} \, \frac{(1-\epsilon)^2}{\epsilon^3} + \frac{1.75 \, \rho^{\text{in}} \, v^{\text{in}}}{d^{\text{bed}}} \, \frac{1-\epsilon}{\epsilon^3} \right) v \tag{7.6}$$

Here, η is the gas viscosity, ρ^{in} is the initial density of the gas, v^{in} is the initial gas velocity, and v is the gas velocity.

Finally, the mole balance is

$$\frac{d\chi}{dz} = \frac{\pi}{4} \, d_{\text{bed}}^2 \, \frac{\rho_{\text{bed}}}{F_{\text{SO}_2}^{\text{in}}} \, r_{\text{SO}_2} \tag{7.7}$$

We use the heat capacities, the enthalpy of reaction and the reaction rate expressions given by Fogler (1992), pages 438-440. All variables have been converted to SI units. Details are given in the Appendix.

7.2.3 The heat exchangers

We use the same values for the properties of all heat exchangers. The following parameters were fixed: The diameter of the heat exchanger tube ($d^{\text{HX}} = 0.03$ m), the number of tubes ($N = 1000$), and the Fanning friction factor ($f = 0.005$). These choices lead to reasonable overall heat transfer coefficients, between 10 and 50 W/K.m^2 for gas-gas type heat exchangers (Sinnot et al. 1983). These values are representative for a shell and tube heat exchanger where the reaction mixture flows turbulently on the tube side.

A linear relation is used between the average driving force X_m^{HX}, and the total heat transferred (the duty), Q_m, of heat exchanger number m, see De Koeijer et al. (2002b).

$$X_m^{\mathrm{HX}} = R_m^{\mathrm{HX}} Q_m \tag{7.8}$$

The average driving force is

$$X_m^{\mathrm{HX}} = \frac{2}{T_m^{\mathrm{u,out}} + T_m^{\mathrm{u,in}}} - \frac{2}{T_m^{\mathrm{out}} + T_m^{\mathrm{in}}} \tag{7.9}$$

The superscript u refers to the utility, i.e cooling or heating medium. The proportionality constant R_m^{HX} can be seen as an average resistance to heat transfer. The resistance to heat transfer is located in the gas film that covers the heat exchanger pipes, giving:

$$R_m^{\mathrm{HX}} = \frac{\delta}{A_m^{\mathrm{HX}}} \frac{1}{\lambda_m \overline{T}_m^2} \tag{7.10}$$

The film thickness of the gas layer, δ, was set to 10^{-3} m (Taylor and Krishna 1993), and A_m^{HX} is the area of transfer. The thermal conductivity of the gas, λ, depends on the average temperature, see the Appendix.

For a given duty and area of transfer, the average driving force in the heat exchanger is calculated by introducing Eq. 7.10 into 7.8:

$$X_m^{\mathrm{HX}} = \frac{\delta Q_m}{A_m^{\mathrm{HX}} \overline{T}_m^2 \lambda_m} \tag{7.11}$$

From knowledge of the number of tubes and the diameter of the tubes, the average velocity of the gas in the tubes $\overline{v}_m$ is:

$$\overline{v}_m = \frac{4 F_m R \overline{T}_m}{N \pi (d^{\mathrm{HX}})^2 P_m^{\mathrm{in}}} \tag{7.12}$$

Here, F_m is the total molar flow, R is the gas constant, and P_m^{in} is the pressure at the entrance of the heat exchanger. We should have used the average pressure in the heat exchanger, but using P_m^{in} enables a calculation without iterations with a negligible error. The average density of the gas $\overline{\rho}_m$ is:

$$\overline{\rho}_m = \frac{P_m^{\mathrm{in}} \overline{M}_m}{R \overline{T}_m} \tag{7.13}$$

where $\overline{M}_m$ is the average molecular weight of the gas mixture. The length of the tubes L_m^{HX} in the heat exchangers is:

$$L_m^{\mathrm{HX}} = \frac{A_m^{\mathrm{HX}}}{\pi d^{\mathrm{HX}} N} \tag{7.14}$$

The pressure difference (outlet minus inlet), $\Delta_m P^{\mathrm{HX}}$, over heat exchanger m is:

$$\Delta_m P^{\mathrm{HX}} = -4f \frac{L_m^{\mathrm{HX}}}{d^{\mathrm{HX}}} \frac{1}{2} \overline{\rho}_m \overline{v}_m^2 \tag{7.15}$$

The pressure difference is necessary for the calculation of the entropies, (Eq. 7.30), that define the objective function.

7.2.4 The reference reactor system

In order to have a meaningful optimisation, one needs to define a reference. A reference reactor system was chosen, using the variables of Table 7.1 as a basis. The height of the catalytic beds were all set to 0.6 m. The reference reactor system had a heat exchanger network in which the heats, taken away in heat exchanger number 2, 4, and 5, were used for heating the feed with heat exchanger number 1. Four of the five duties of the heat exchangers were thus related:

$$Q_1 + Q_2 + Q_4 + Q_5 = 0 \tag{7.16}$$

The temperature differences between the outlet and the inlet of the heat exchangers, $\Delta_m T$, were 374.54, -90, -80, -55, and -214 K, respectively. So, negative sign means cooling. The areas of transfer of the heat exchangers were taken as 1743.8, 581.2, 512.5, 181.3, and 981.2 m^2. The total area of transfer was then 4000 m^2. This total area was used as a constraint on the minimisation. The restriction on the duties was not maintained in the minimisation.

The equations of the reactor system were solved (see Sections 7.2.2 and 7.2.3), and the following results were obtained. The outlet temperature of the reference reactor was 486.22 K, and the outlet mole fraction of SO_2 was 1.839 10^{-3}. The duties of the heat exchangers were 5.58, -1.45, -1.27, -0.87, and -3.26 MW, respectively (negative sign means cooling). The outlet temperature and mole fraction of SO_2, obtained in this manner, were used as constraints.

7.3 The minimisation problem

7.3.1 The objective function

The objective function is the entropy production rate dS^{irr}/dt of the reactor system:

$$\frac{dS^{\mathrm{irr}}}{dt} = \sum_{n=1}^{4} \left(\frac{dS_n^{\mathrm{irr,bed}}}{dt} \right) + \sum_{m=1}^{5} \left(\frac{dS_m^{\mathrm{irr,HX}}}{dt} \right) \tag{7.17}$$

The first sum on the right hand side is the contribution due to the reaction and pressure drop in the beds. The second sum is due to heat transfer and pressure drop in the heat exchangers. The contribution from bed number n was obtained from the entropy balance over the bed:

$$\frac{dS_n^{\mathrm{irr,bed}}}{dt} = F_n^{\mathrm{out}} S_n^{\mathrm{out}} - F_n^{\mathrm{in}} S_n^{\mathrm{in}} \tag{7.18}$$

The contribution to the entropy production rate from heat exchanger m was obtained from the entropy balance over the heat exchanger:

$$\frac{dS_m^{\mathrm{irr,HX}}}{dt} = F_m(S_m^{\mathrm{out}} - S_m^{\mathrm{in}}) + F_m^u(S_m^{\mathrm{u,out}} - S_m^{\mathrm{u,in}}) \tag{7.19}$$

Here, superscript u means properties of the unknown utility, which cools or heats the reaction mixture on the shell side of the heat exchangers.

The entropy production rate due to heat transfer is also approximately equal to the product of average force and total heat transferred. The following expression from a diabatic column applies (De Koeijer and Rivero 2002):

$$Q_m X_m^{\mathrm{HX}} = \frac{Q_m}{\overline{T}_m} + F_m^u(S_m^{\mathrm{u,out}} - S_m^{\mathrm{u,in}}) \tag{7.20}$$

By introducing Eq. 7.20 into Eq. 7.19 we have an expression for the entropy production rate in the heat exchangers, that does not dependent on knowledge of the utility:

$$\frac{dS_m^{\mathrm{irr,HX}}}{dt} = F_m(S_m^{\mathrm{out}} - S_m^{\mathrm{in}}) - \frac{Q_m}{\overline{T}_m} + Q_m X_m^{\mathrm{HX}} \tag{7.21}$$

The term $Q_m X_m^{\mathrm{HX}}$ is the contribution from heat transfer perpendicular to the area of transfer. In case of zero pressure drop the first and second term on the right hand side of Eq. 7.21 would cancel. But this is not the case here, and Eq. 7.21 is therefore a convenient description.

By introducing Eqs. 7.21 and 7.18 into Eq. 7.17 the objective function is obtained:

$$\frac{dS^{\mathrm{irr}}}{dt} = F^{\mathrm{out}} S^{\mathrm{out}} - F^{\mathrm{in}} S^{\mathrm{in}} - \sum_{m=1}^{5} \frac{Q_m}{\overline{T}_m} + \sum_{m=1}^{5} Q_m X_m^{\mathrm{HX}} \tag{7.22}$$

The calculation of entropies is explained in the Appendix. The explicit expressions for X_m^{HX} or R_m^{HX} were introduced in the objective function as explained before. An objective function has thus been formulated without explicit reference to the cooling and heating media around the reactor.

7.3.2 Choice of variables and constraints

Three sets of variables were allowed to vary in the minimisation. These were:

1. The height of the beds, h_n (n =1, 2, 3, 4). These were also used in optimisation studies by Chartrand and Crowe (1969), Doering and Gaddy (1980). The heights can be changed to a certain extent in an already existing reactor systems during the replacement of the deactivated catalyst. This makes them a practical variable. Since catalyst costs money (Doering and Gaddy 1980), these variables have a direct economical significance.

2. The transfer areas of the heat exchangers, A_m (m =1, 2, 3, 4, 5). By varying them, we automatically allowed the driving forces to vary, see Eq. 7.11. We chose the transfer areas and not the forces, because the areas are always positive. They are thus convenient properties for the minimisation algorithm. Like the catalyst, transfer area costs money, and has therefore also a direct economic significance.

3. The temperature differences of the reaction mixture between out- and inlet of the heat exchangers, ΔT_m (m =1, 2, 3, 4, 5). They correspond to the duties of the heat exchangers. They are relatively easy to manipulate with the choice of utilities, but might have a significant effect on the heat exchanger network. We did not consider this effect here.

This choice of variables enables us to optimise the reactor system without reference to utilities (cooling and heating media) and heat exchanger network. Additional variables like number of beds, number of heat exchangers, bed porosity, inlet conditions, outlet conditions, diameter of the bed, etc. may be studied in a similar manner.

The main constraints were on the mole fractions at the inlet and the outlet, and the inlet molar flow rate, F^{in}. These constraints fixed the chemical production to that of the reference case. The inlet temperature and pressure, T^{in} and P^{in}, and the outlet temperature, T^{out}, were also kept constant. In this way the up- and downstream processes are disturbed as little as possible. The bed diameter, the bed density and the bed porosity were constant. The sum of bed heights, $\sum_{n=1}^{4} h_n$, was less than or equal to the total height in the reference reactor. In other words, we afforded the weight for a height of 2.4 m, but not more and preferably less. A similar constraint was put on the sum of transfer

areas, $\sum_{m=1}^{5} A_m$. The outlet pressure, P^{out}, is a function of the height of the beds and area of transfer, which were variables in the minimisation. The outlet pressure was therefore allowed to vary.

7.4 Calculations

7.4.1 The mathematical method

The minimisation problem is a constrained nonlinear programming problem. We used the *Matlab® 6.1* function *fmincon* to solve it. The same function has been used earlier to minimise the entropy production rate of distillation by De Koeijer et al. (2002b) and reactors by Nummedal et al. (2001, 2002). *Fmincon* uses a sequential quadric programming method to solve our problem. We refer to The MathWorks Inc. (2001) for details on the algorithms in *fmincon*. In addition to the constraints described in Section 7.3.2, we included upper and lower bounds on the variables. The temperature differences over the heat exchangers were allowed to vary from -700 to 700 K, the bed heights from 0 to 2.4 m, and the transfer areas from 1 to 10000 m^2. This was done to prevent the algorithm from crashing by trying unfeasible values.

In order to check for multiple minima and the reliability of the minimum that is reported, we used different starting vectors. The first starting vector was always the reference. Secondly, perturbed versions of the reference were used. Finally, perturbed versions of the minima were tried. The perturbations were done on all variables. The main ones were to set a height or temperature difference to zero, and to rescale the transfer areas. For the minimisations that served the purpose of comparison with the reference reactor 20-30 different starting points were tried. By varying the total transfer area, the results of a previous minimum was used and 5-10 perturbations were tried. Furthermore, a random choice of starting vectors was made over a period of two weeks for selected cases. Several hundreds initial variable vectors were tried. Most vectors caused the algorithm to crash. Among those which converged, the optimum was the same as the one found directly using the reference reactor to start.

Depending on the initial values, it took the algorithm 1000-10000 iterations to find a minimum. The algorithm needed a high accuracy of the simulation of the system (10^{-6}) and minimisation (10^{-10}) to converge to a satisfactory minimum.

7.4.2 The calculation procedure

The conservation equations were solved for the reference reactor, and used to establish the boundary conditions for the optimisation. The input and output from the reference reactor to the optimisation were given above.

A general study was first performed, when all three sets of variables were varied simultaneously as described above. A minimum was found, and studied in more detail. The sum of all areas of transfer was less or equal to the value of the reference reactor (4000 m^2) in this calculation. In the next set of calculations, the upper limit of the total transfer area varied from 1000 to 6000 m^2. In the end further restrictions were introduced in order to gain more insight, and show alternative optimisations.

7.5 Results and discussion

7.5.1 Entropy production rates

Figure 7.2 shows the entropy production rate as a function of the sum of areas of transfer ($\sum_{m=1}^{5} A_m$) of the reactor system with minimum entropy production rate (solid line) and with the entropy production rate of the reference reactor system (triangle).

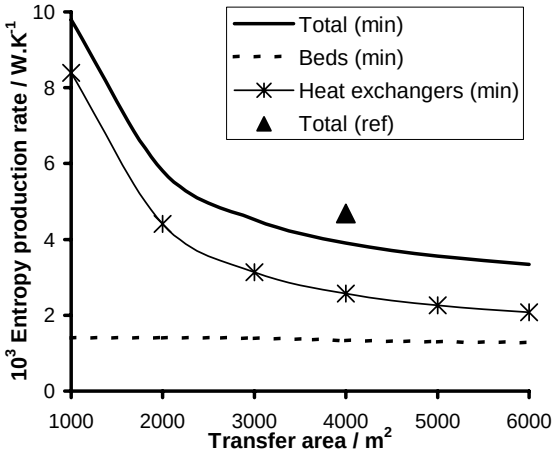

Figure 7.2. Entropy production rate of the contributions of the minimum vs transfer area, including reference

The reduction in entropy production rate from the reference state to the state

of minimum entropy production was 16.7 % at 4000 m^2. This means that the reference reactor system has a large potential for saving energy. This is the main result of this work. The second law energy efficiency (Smith and Van Ness 1987) increased from 0.31 of the reference to 0.42 of the minimum. The reason for the large relative difference in efficiency is that the maximum obtainable work from this system (1.97 MW) was in the same order of magnitude as the entropy production rate times reference temperature (298.15 K).

Figure 7.2 gives also the contributions to the entropy production rate. The total entropy production rate (solid line) is the sum of contributions from the reaction and pressure drop in catalytic beds (thick dashed line), and heat transfer and pressure drop in the heat exchangers (thin line with cross). The total entropy production rate was roughly parallel to the contribution of the heat exchangers. So, the contribution from the heat exchangers was the most important part in Eq. 7.22. This means that the variation in the entropy production rate must be explained by the contribution of the heat exchangers. The contribution of the beds to the entropy production decreased very little with increasing area of transfer (from 1400 W/K at 1000 m^2 to 1270 W/K at 6000 m^2), see Figure 7.2.

The value of the entropy production rate was roughly inversely proportional to the transfer area. This is reasonable. At zero area of transfer, the entropy production rate would be infinite. At infinite transfer area the entropy production rate due to heat exchange went to zero. Only the contributions of reaction and pressure drop remained.

By drawing a straight line parallel with the area axis, through the point that represents the reference system, we see from Figure 7.2 that the same production and entropy production can be maintained, but with 1200 m^2 less area of transfer area. This may be an interesting alternative to improve the energy efficiency; to save instead on the area of transfer. The details of this solution were however not further investigated.

7.5.2 Temperature and concentration profiles for a given total transfer area

The variables that characterised the state of minimum entropy production are shown in more detail in Fig. 7.3. The figure applies to a total transfer area of 4000 m^2. The temperature and SO_2 mole fraction profiles through the reactor are shown and compared to the profiles of the reference system.

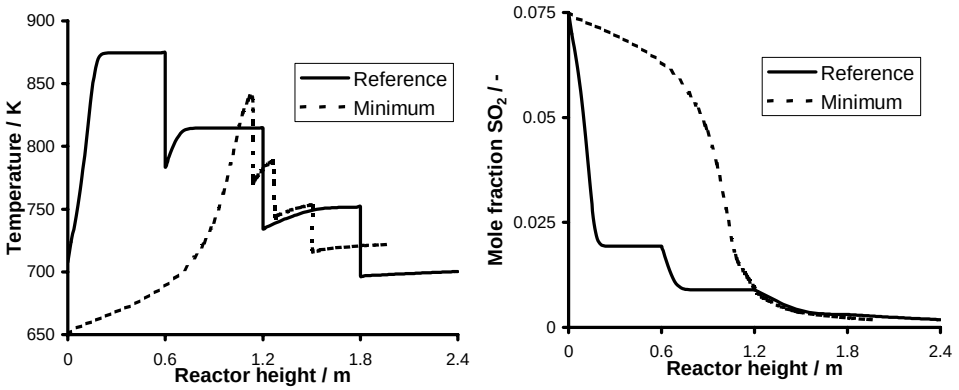

(a) Temperature

(b) Mole fraction SO_2

Figure 7.3. Temperature and mole fraction profiles of the optimised and reference reactors

The profiles of the reference system were typical for a conventional SO_2 oxidation reactor system, see Mueller (1994). The reacting mixture reached equilibrium (characterised by flat profiles) well before the end of each bed. This gives the reactor system a possibility to cope with deactivating catalyst. From the mole fraction profile, there seemed to be little reacted in the last bed. However, there was a significant relative conversion, since $p_{SO_2}/p^{\text{in}}_{SO_2,4}$ reached 0.40 in the last bed.

In the state of minimum entropy production rate, equilibrium was only nearly reached at the outlet of each bed. This is expected in an optimisation that had catalyst height as a variable; reaching the equilibrium state in this respect means a waste of catalyst. Extra catalyst would only cause unnecessary pressure drop. So, Figure 7.3 show that there was excess catalyst in the reference reactor. The total bed height decreased from 2.4 m in the reference state to 1.98 m in the state of minimum entropy production rate.

The fact that one did not reach equilibrium at the outlet of a bed made the reactor system more sensitive to deactivation of catalyst, however. The SO_2 mole fraction profiles show that the production was now more uniformly distributed. More importantly, this state of operation had a lower maximum temperature in the reactor, and the high temperature region is smaller. In summary, the catalyst was overall exposed to milder conditions, meaning that

the catalyst will deactivate slower than in the reference case. So, the optimum case did not only have a higher second law energy efficiency, but probably also longer catalyst lifetime. An excess bed height may thus be less important.

The profiles as shown in Fig. 7.3 did not change much by varying the sum of transfer areas. Their qualitative behaviour was maintained. The only quantitative exceptions were the heights and transfer areas (or forces) as we will discuss later on.

A temperature-conversion diagram with the equilibrium and maximum reaction rate lines is a common way to illustrate this type of processes (Mueller 1994, Lurgi GmbH 1990). For the sake of comparison this diagram with the lines of the reference and minimum is also given in this work.

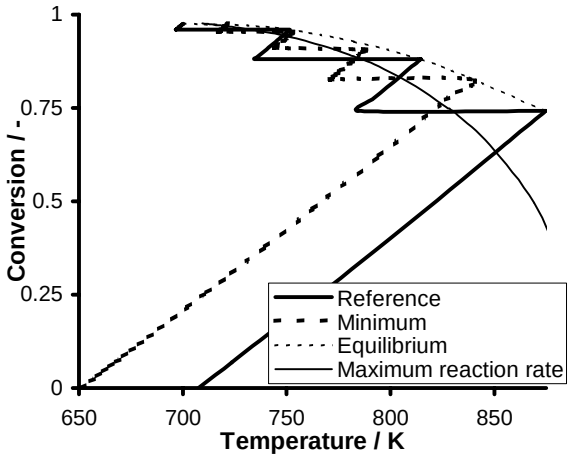

Figure 7.4. Conversion as a function of temperature of reference and minimum

We know from Fig. 7.3 that the turning points of the reference reactor must lie on the equilibrium line. But we see now that the turning points of the minimum were nearly on the equilibrium line. So, the mixtures of the minimum came very close to equilibrium at the end of the beds.

7.5.3 Heat exchanger conditions and bed heights as a function of area of transfer

The values of the variables were investigated as a function of area of transfer. Figure 7.5 gives the temperature differences between out- and inlet of the heat

exchangers for different total transfer areas in the state of minimum entropy production rate. We see that these temperature differences were not affected much by the varying transfer area. Their values showed some scatter. We explain this by numerical inaccuracies, due to the flatness of the solution surface around the minimum, see also section 7.5.5.

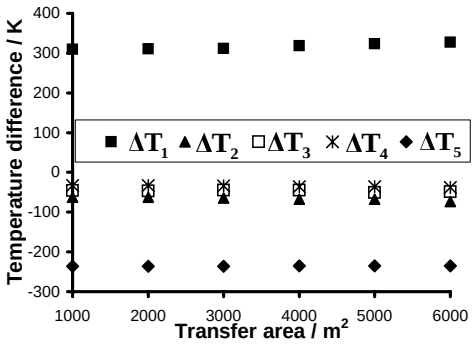

Figure 7.5. Temperature differences in the state of minimum entropy production

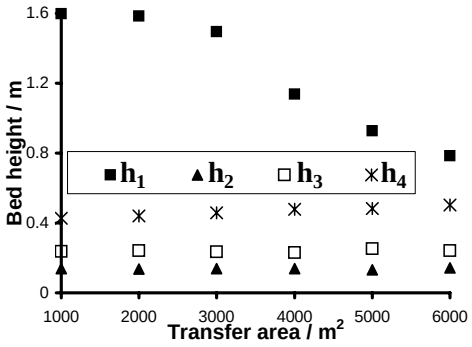

Figure 7.6. Bed heights in the state of minimum entropy production

Figure 7.6 gives the heights corresponding to Figure 7.5. The height of the first bed decreased with the transfer area, while the others increased slightly. Mueller (1994) recommended however single bed heights between 0.2 and 1.0 m. Above 4000 m^2, the state of minimum entropy production did not break with this recommendation significantly. But above, the height of the first bed became too large. Moreover, the sum of the heights was 2.4 m when the total area is below 2000 m^2, and decreased to 1.7 m when the total area becomes 6000 m^2. The reason for this lies in the total amount of heat transferred, which was larger at larger transfer area. This means that the system had a larger flexibility, which made it easier to operate closer to maximum reaction rate, see Fig. 7.4. That this was indeed the case is confirmed by the higher entropy production rate of the reaction per kg catalyst at larger transfer area.

Figure 7.7 gives the driving force for heat transfer, corresponding to Fig. 7.6. All driving forces decreased in absolute value with the transfer area and tended to zero at infinite transfer area, as expected.

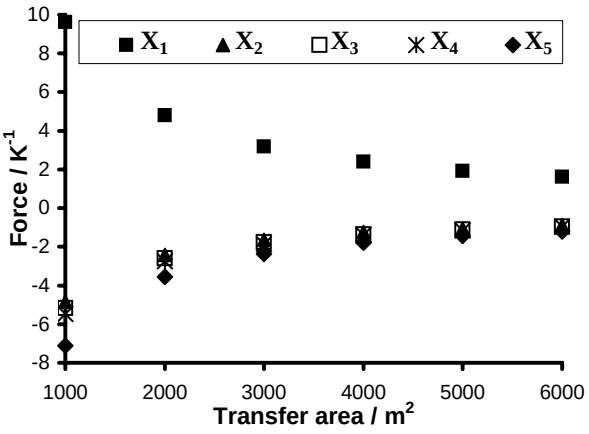

Figure 7.7. Driving forces in the state of minimum entropy production

7.5.4 Further restrictions of the variables

In order to see how sensitive the minimum solution was to the set of variables chosen, the minimisation was carried out with subsets of the variables. A more practical motivation for doing this is to provide guidelines for improving a reactor system if a total optimisation is not possible. This situation can occur during a shut-down, replacement of deactivated catalyst, or redesign of the heat exchangers. In the first calculation, only the bed heights were varied. In the second case, only the transfer areas of the heat exchanger were varied. Finally, the variations of the temperature differences were studied.

By varying the bed heights only, the entropy production was reduced by 4.2 % (4490 W/K) compared to the reference case. The resulting heights for minimum entropy production rate were 0.250, 0.175, 0.465, and 0.580 m for bed numbers 1-4. The sum of the heights of those four beds was smaller than 2.4 m. So, the reactor system require less catalyst than the reference case. The entropy production rate decreased by only 3.6 % when the transfer area distribution alone was allowed to vary. The areas became 2247, 386, 349, 199, and 819 m^2. A variation of the temperature differences, gave a 12.4 % reduction in the entropy production rate in comparison with the reference reactor. The temperature differences were respectively 213.3, 121.6, -118.3, -45.2, and -237.6 K. The first two heat exchangers were used for heating, and the first bed did not perform any reaction due to the low temperature difference over the first heat exchanger.

To vary only one of the variables may thus be fruitful. The temperature differences had by far the largest impact on the reduction in entropy production in this reactor system. The heights as a variable came second, and the area distribution had the least impact. But the results of the single variable set minimisations were distinctly different from the ones found when all variables were included, see Figs. 7.5-7.7.

The last case we investigated was the one with constant average forces across the heat exchangers. This is motivated from the good results in De Koeijer et al. (2002b) for diabatic distillation by applying this rule. For a reactor system with 4000 m^2 the constant driving force was 2.08 10^{-4} 1/K, and the minimum entropy production rate was 4039.53 W/K. The reduction was 13.8 % compared to the reference value. This is also a significant reduction, which is in accordance with the result obtained for diabatic distillation columns.

7.5.5 Final comments

An interesting question is now how to turn the reductions in entropy production rate into benefits? Since entropy is a measure of quality of energy, a lower entropy production rate means higher quality outlets and/or lower quality inlets. A good example of a benefit is a higher outlet temperature of the heating medium. As already mentioned, less transfer area could also be a benefit. The benefits will however depend on the other processes in the plant. Further research should be done to investigate all possible benefits systematically.

The expression for the entropy production rate in the objective function was found starting from the entropy balances of the different parts. This means that the different parts of the process were taken as black boxes. The entropy production rate per unit of volume, as given by a flux-force product from irreversible thermodynamics

$$\frac{dS_n^{\mathrm{irr,bed}}}{dt} = \frac{\pi}{4}\, d_{\mathrm{bed}}^2\, \rho_{\mathrm{bed}} \int_0^{h_n} r_{\mathrm{SO_2}} \left(-\frac{\Delta_{\mathrm{R}} G}{T}\right) dz \tag{7.23}$$

is an alternative used by Johannessen and Kjelstrup (2002), Kjelstrup and Island (1999), Kjelstrup et al. (1999a), but may be unnecessarily complicated. More detailed information can be obtained from the flux-force expression, for instance information on the local behaviour of the driving force, $(-\Delta_{\mathrm{R}} G/T)$. In this work, we choose the simpler way to express the entropy production rate, Eq. 7.18, because the computations became faster.

The multidimensional surface around the minimum was flat: Several other

minima with entropy productions very close (< 0.3 W/K) to the reported ones were found, but with different values for the variables. The maximum differences were 2.5 K for the temperature differences, 0.013 m for the heights, and 16 m^2 for the transfer areas. This is the reason for the scatter of the variables in Figures 7.5- 7.7.

It is interesting to compare the results obtained here, to the results obtained for diabatic distillation columns in De Koeijer et al. (2002b). A diabatic tray distillation column has heat exchangers in connection with several trays. A similar figure as Figure 7.2 was presented for distillation. In both processes, the contribution to the entropy production rate of heat transfer was modelled by $Q_m X_m^{\mathrm{HX}}$. The main conclusion of the work on distillation is that the heat exchangers have a significant influence on the state of minimum entropy production rate. The same conclusion is made for this reactor system, see Fig. 7.2. Here a non-equilibrium model was used, however, while the distillation columns were modelled with the assumption of equilibrium between the outlet flows from a tray.

7.6 Conclusion

We have shown that the entropy production rate of a typical SO_2 converter in the industry can be reduced by 16.7 % in comparison with a reference system. This was obtained by changing bed heights, area distribution between intermediate heat exchangers, and inlet and outlet temperatures from the heat exchangers. Inlet and outlet conditions to the surrounding equipment were not altered. The state of operation that has minimum entropy production rate is characterised by milder thermal conditions. The calculations also show that the amount of catalyst used, can be lowered if the area of the heat exchangers is increased. If one chooses to operate with the same entropy production as the reference case, the results can be used to find a smaller area for heat exchange.

It is interesting to note that even for well proven technology, it seems possible to find new modes of operation that do not alter the output, but results in better overall energy economy for the part studied.

Acknowledgements

The Research Council of Norway is thanked for a grant to De Koeijer and Johannessen. Målsnes and Rostad from Outokumpu Norzink AS are thanked for the valuable discussions. Leiv Eiriksson Nyfotek AS is thanked for travel

money.

Appendix

The reaction rate, $r_{\mathrm{SO_2}}$, is given by Fogler (1992):

$$r_{\mathrm{SO_2}} = k_{\mathrm{r}}\sqrt{\frac{P_{\mathrm{SO_2}}}{P_{\mathrm{SO_3}}}}\left[P_{\mathrm{O_2}} - \left(\frac{P_{\mathrm{SO_3}}}{P_{\mathrm{SO_2}}K_{\mathrm{P}}}\right)^2\right] \tag{7.24}$$

where:

$$k_{\mathrm{r}} = 9.8692\,10^{-3}\exp\left(\frac{-97782}{T} - 110.1\ln T + 848.1\right) \tag{7.25}$$

and

$$K_{\mathrm{P}} = 0.003142\exp\left(\frac{98359}{RT} - 11.24\right) \tag{7.26}$$

Below $\chi = 0.05$, the reaction rate at $\chi = 0.05$ was used. This is recommended by Fogler (1992) because Eq. 7.24 gives to high reaction rate in that region.

Fogler (1992), page 403, reported the heat capacities as a function of temperature in the form:

$$C_{P,i} = A_i^{C_P} + B_i^{C_P}T + C_i^{C_P}T^2 \tag{7.27}$$

Here, $A_i^{C_P}$, $C_i^{C_P}$, and $C_i^{C_P}$ are coefficients given in Table 7.2.

With these heat capacities, the heat of reaction was:

$$\begin{aligned}\Delta_{\mathrm{R}}H =& \Delta_{\mathrm{R}}H(T^{\mathrm{ref}}) - 6.5415(T - T^{\mathrm{ref}}) + \\ & \frac{0.0205165}{2}(T^2 - T^{\mathrm{ref}\,2}) - \frac{10.007\,10^{-6}}{3}(T^3 - T^{\mathrm{ref}\,3})\end{aligned} \tag{7.28}$$

The heat of reaction at reference temperature, 700 K, was taken as -98787.5 J/mol.

The thermal conductivity was taken from Reid et al. (1987) who tabulated λ in the form:

$$\lambda_i = A_i^{\lambda} + B_i^{\lambda}T + C_i^{\lambda}T^2 + D_i^{\lambda}T^3 \tag{7.29}$$

The thermal conductivity and heat capacity of a vapour mixture was the molar average one. The coefficients are given in Table 7.2.

The absolute entropies of a gas, required for Eqs. 7.18 and 7.21, were calculated with:

$$S = \sum_i y_i \left(S_i^{\text{ref}} + \int_{T^{\text{ref}}}^{T} \frac{C_{P,i}}{T} dT \right) - R \sum_i y_i \ln y_i - R \ln \frac{P}{P^{\text{ref}}} \qquad (7.30)$$

The reference pressure was 1.013 10^5 Pa. The reference entropies at 298.15 K in the gas phase can be found in Table 7.2, and were taken from Weast and Astle (1982).

Table 7.2. Heat capacity coefficients, thermal conductivity coefficients and reference entropies

Component	SO_2	SO_3	O_2	N_2
A^{C_P}(J/mol.K)	30.178	35.634	23.995	26.159
B^{C_P}(J/mol.K^2)	42.452^{-3}	71.722^{-3}	17.507 10^{-3}	6.615 10^{-3}
C^{C_P}(J/mol.K^3)	-18.218 10^{-6}	-31.539 10^{-6}	-6.628 10^{-6}	-2.889 10^{-7}
A^{λ}(W/m.K)	-8.086 10^{-3}	-6.683 10^{-3}	-3.273 10^{-3}	3.919 10^{-3}
B^{λ}(W/m.K^2)	6.344 10^{-5}	7.07710^{-5}	9.966 10^{-5}	9.816 10^{-5}
C^{λ}(W/m.K^3)	-1.382 10^{-8}	-1.968 10^{-8}	-3.743 10^{-8}	-5.067 10^{-8}
D^{λ}(W/m.K^3)	2.303 10^{-12}	1.256 10^{-12}	9.7312 10^{-11}	1.504 10^{-11}
S^{ref}(J/mol.K)	248.488	256.185	204.994	191.47

8 Conclusions and Outlook

8.1 Overall conclusions

The entropy production rates of diabatic distillation columns and a SO_2 converter were minimised. This means that the second law efficiency of large energy users is maximised. So, this type of optimisation serves the need of making development sustainable. For defining the entropy production rate irreversible thermodynamics was useful. The minimum entropy production could be investigated accurately due the availability of fast computers and good optimisation procedures.

With the objective functions, variables, and constraints used in Chapter 5, the entropy production rate in distillation could be reduced up to 50 %. The second law efficiency in Eq. 1.1 increased from 0.57 of the adiabatic column to 0.73 of the diabatic column at the limit of reversible heat transfer. The reduction of the SO_2 converter was 16.7 % in Chapter 7. The reductions are large, and show that there is still a large improvement potential for these processes. To achieve such reductions their operation had to be changed. In distillation heat exchangers were added. For the SO_2 converter, the heights of the catalytic beds, the transfer areas of the heat exchangers, and temperature differences over the heat exchangers were redistributed.

The theory on diabatic distillation was developed further by applying the theory of irreversible thermodynamics. The systematic character of irreversible thermodynamics enabled us to derive for various assumptions different equations for the entropy production rate. The ones we started with were derived by Sauar et al. (1997) and De Koeijer et al. (2002a). For the purpose of Chapter 2, we needed an equation that enabled an analytical solution of the Euler-Lagrange minimisation. After improving the use of the Gibbs-Duhem equation of Sauar et al. (1997), and neglecting the liquid contribution in De Koeijer et al. (2002a), we obtained Eq. 2.2 for the driving force of mass transport. The corresponding equation for the entropy production rate contained only one product of average driving force and flow. It performed satisfactory for equilibrium columns separating ideal mixtures. Furthermore, it led to the desired solution of the Euler-Lagrange minimisation, see Eqs. 3.21 and 3.22. However, we found that this equation did not perform satisfactorily for the experimental results of a column separating the non-ideal mixture water-ethanol, see Fig. 4.6. We needed to extend it to an equation with three force-flow products. Furthermore, a more accurate equation for the driving force for mass trans-

port was derived, see Eq. 4.7. It included the activity coefficients, and both liquid and vapour contributions. A similar improvement was observed for the equation for the measurable heat flow through the interface. In Chapters 2 and 3 the contribution to the entropy production rate from heat transfer through the interface was neglected. This was based on an equation where the temperature gradients in the liquid were neglected, see De Koeijer et al. (2002a). This assumption was removed, and a new equation was derived in Chapter 4, Eq. 4.9. The relative contribution of the measurable heat flow to the total entropy production rate decreased from less than 8% to 0.6% by improving the equation. The Soret effect (or thermal diffusion) was shown to be significant in Chapter 6. The average thermal driving force over the interface and films is still uncertain. The best estimate we have is Eq. 4.6, but it was not assessed with the experimental data.

Following the reversible column of Fonyo (1974a) and the diabatic column of Rivero (1993), we give a sketch of a diabatic distillation column at minimum entropy production rate. The sketch is shown in Fig. 8.1.

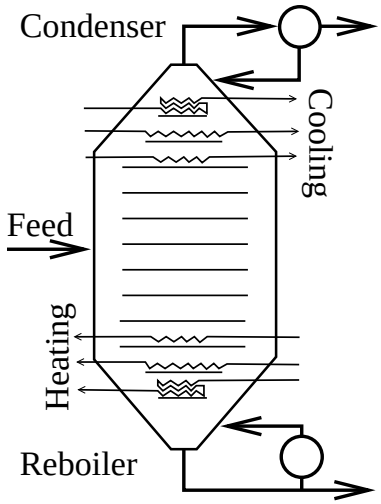

Figure 8.1. Sketch of an optimum diabatic distillation column

The sketch is based on the results of Chapter 5 with reasonable thermal driving forces over the heat exchangers (10^{-3}-10^{-4} 1/K). The duty profiles in Fig. 5.2 indicated that heat exchangers are necessary for trays near the top and bottom. The larger the driving force, the fewer heat exchangers are necessary, but the more entropy is produced. The transfer area and duty decrease the further

away from reboiler or condenser the heat exchanger is. To avoid problems with uneven pressure drop, weeping, and flooding (Douglas 1988), the diameter of the column should decrease at the top and bottom trays. For every single column the details of the optimum operation will of course be different, but we believe that some general characteristics are described with the sketch.

8.2 Estimate of possible savings

In the introduction in Chapter 1 it was said that increasing the energy efficiency of distillation can be a significant factor for increasing the overall energy efficiency of society and sustainability level of development. We are now able to qualify this statement. Figure 5.3 shows that even with the contribution of the heat exchangers diabatic distillation has a large improvement potential with respect to energy efficiency. The benefit of a reduction in entropy production rate lies in a lower inlet and/or higher outlet temperature of the utilities. As most of the utilities are fixed as inlets, a higher outlet temperature is probably preferred. By using this higher outlet temperature somewhere else in the plant the steam generation of the plant can be reduced. Say that we can reduce the contribution to the steam generation of distillation with 20 %. This can be seen as direct fuel saving. Humphrey and Siebert (1992) says that 40 % of the equivalent of 3 million barrels of crude oil per day is used by distillation in the USA, i.e. a possible saving of $3 * 0.4 * 0.2 = 0.24$ million barrels per day. Since Humphrey and Siebert (1992) gave numbers from 1991, we continue to do so. Given the total USA oil demand of 17.04 million barrels a day (Energy Information Administration 2002), this means a reduction of 1.4 %. If this saving is similar for the whole world, it is possible to reduce oil production with 0.84 million barrels per day[1]. In order to give an idea, this is the same as 42 % of the oil production of Norway[2]. As the use of crude oil and CO_2 emissions are related, we expect that CO_2 emissions can be reduced in the same order.

This estimate is rough, and requires that all distillation columns in the world are built diabatically. But on the other hand we might have been conservative in the possible reduction, and we did not take possible reduction of entropy production rate in all reactive processes into account. Concluding, the numbers tell that the methods and results presented in this thesis can contribute to substantial energy savings.

[1]World oil production in 1991 was 60.207 million barrels a day (Energy Information Administration 1999)

[2]Norwegian oil production in 1991 was 1.890 million barrels a day (Energy Information Administration 1999)

8.3 The method

With the results from Sauar (1998), Nummedal (2001), and the ones presented in this thesis, we can construct and exemplify a method. The aim of this method is to show how the thermodynamically optimum operations of distillation columns and reactors can be determined. The elements of the method follow common practise, see e.g. Bejan (1996), Biegler et al. (1997), Kjelstrup et al. (1998):

- The first step is to determine the system and the system boundaries. If the system is complex and/or large, we have learned to start with a simpler or smaller one, in order to gain experience and insight. This was for example done for distillation where the contribution of the heat exchangers was not taken into account at first in Chapters 2 and 3, but added later in Chapter 5. Another example is found in Kjelstrup et al. (2000) and Nummedal et al. (2002). In the first work only the contribution of the reaction was minimised, and in the latter the contribution from heat exchange was added.
- A decision on the purpose of the minimization must be addressed. Is a realisable design the main purpose, or is it more knowledge and insight? In the first case the entropy balance in Eq. 1.8 over the system as a black box may hold. This was done for the catalytic beds in Chapter 7. Irreversible thermodynamics can provide insight and knowledge on the system (see e.g. Ch. 6), but needs more information.
- The system can now be modelled. From our experience several assumptions must be made. Irreversible thermodynamics allows us to do this in a systematic manner (see also overall conclusions further on). In the thesis, this is illustrated by moving from the assumption of equilibrium between the flows leaving the tray in Chapters 2, 3, and 5 to the non-equilibrium models in Chapters 4, 6, and 7.
- The objective function, here the entropy production rate of the system, must be determined at this stage. Nummedal (2001) and Sauar (1998) use the sum of flux-force products from irreversible thermodynamics. The most extended type of objective function in this thesis is the combination of entropy balances (Eq. 1.8) and flux-force products from irreversible thermodynamics (Eq. 1.4), like in Chapters 5 and 7.
- The next step is to determine the constraints and variables. In the cases we studied, constraints were mainly on in- and outlet properties, while

the variables were operation properties. If an applicable design is pursued like in Chapter 7, the constraints and variables need to have a direct connection to the design, e.g. transfer areas, bed heights. It is also possible to choose variables without a direct connection to the design, e.g. the driving forces in Chapter 5, and idealised temperature in Johannessen et al. (2002), Johannessen and Kjelstrup (2002). The realisability in terms of design can be determined afterwards, see e.g. Fig. 5.4. We learned to look for alternative descriptions of the variables and constraints. An example is the choice between driving force and transfer area in Chapter 7. We choose the transfer area as variable, because it is always positive. Also introducing extra variables and constraints for increasing convergence of the minimisation procedure should be investigated. This is for example done in Chapter 5 by adding the energy balance as constraints, and the vapour flows as variables.

- In this thesis 5 different minimization procedures were used: Euler-Lagrange with irreversible thermodynamics (analytical, Ch. 2 and Sauar (1998)), Equal Thermodynamic Distance (analytical, Ch. 3), Powell's procedure (numerical, Ch. 3), Monte Carlo procedure (numerical, Ch. 2, 3, and 5), and the function *fmincon* in *Matlab*® 6.1 (numerical, Ch. 5, 7 and Nummedal (2001)). The latter was for distillation columns and reactors the fastest and most accurate. Which procedure to choose depends on the complexity of the system, objective function, variables and constraints. Simple problems can often be solved analytically (Sauar 1998, Bejan 1996). More complicated problems need a numerical procedure, like Powell's procedure and the function *fmincon* in *Matlab*®. If the solution is very non-linear and/or dependent on the starting point, a certain randomness should be introduced, like in the Monte Carlo procedure. Randomness increases however the calculation time.
- At last, the entropy production rate can be minimised. A critical assessment and redefinition of the system's objective function, constraints, variables, and minimisation procedure is always necessary. The minimum needs to be explored, not only to check whether there are minima lower than the ones already found (as observed in Ch. 7), but also because the interaction between the phenomena producing entropy can change with the constraints. This insight might lead to better results. Chapters 5 and 7 showed for example that by increasing the total amount of transfer area of the heat exchangers the reduction of entropy production rate increased even more.
- The last step of this method is to design the optimised system. Especially

if the solution is not directly realisable from the choice of variables, this is a challenge, as illustrated in Chapter 5.

8.4 Outlook

There is not yet much experience with the last element of the method: the final design of the systems at minimum entropy production rate. Chapters 5, 7, Johannessen et al. (2002) and Johannessen and Kjelstrup (2002) contain first proposals on how to do this. More research should be done on how the potential reduction in entropy production rate can be converted fully into energy savings. The optimisation method could for example be extended with the design of the most optimum heat exchanger network, see e.g. Biegler et al. (1997).

To understand the transport phenomena in optimum diabatic distillation better (see also section 4.4.1), the minimisation of entropy production rate should be done with a set of non-equilibrium transport equations. Chapters 4 and 6 show that the set should include at least the Soret effect, and preferably the interface. The importance of these effects can then be investigated quantitatively. Their role in multi-component distillation should also be investigated. Furthermore, a model for the thermal resistance in the heat exchangers should be tested with experimental data. Chapter 5 gives a first proposal. Finally, a complete model should be tested and adjusted with experiments on pilot plant scale, like Rivero (1993). In a pilot plant advanced process control should be used, which was also suggested by Humphrey and Siebert (1992). Time dependent factors as fouling, start-up/shut-down should be investigated before the design of the pilot-plant. Afterwards, a full economic evaluation can be done for the industrial scale process. If the Net Present Value (Park and Sharp-Bette 1990) of the project is larger than zero it should be done. Governments can have an influence in this decision by means of subsidies and regulations.

A comparison of diabatic distillation columns with Heat Integrated Distillation Columns (HIDiC, Nakaiwa et al. (2001)), Petlyuk columns (King 1980), and Secondary Reflux and Vapourisation (SRV, Mah et al. (1977)) columns will be interesting for further research. All types can namely have a higher energy efficiency than conventional adiabatic distillation columns. Beside taking the optimisation of diabatic distillation as a single project, minimisation of entropy production rate of a whole plant is a challenge.

Nomenclature

A	Transfer area (m^2)
a	Proportionality constant (1/m)
B	Bottom (mol/s)
c	Concentration (mol/m^3)
C_P	Heat capacity (J/mol.K)
C_σ	Constant pressure coexistence heat capacity (J/K)
D	Distillate (mol/s)
D	Fick's diffusion coefficient in Ch. 6 (m^2/s)
Đ	Maxwell-Stefan diffusion coefficient (m^2/s)
d	Diameter (m)
dS^{irr}/dt	Entropy production rate (J/s.K)
Ex	Exergy (J/mol)
F	Feed (mol/s)
F	Flow in Ch. 7 (mol/s)
f	Fanning friction factor (-)
G	Gibbs energy (J/mol)
H	Enthalpy (J/mol)
I	Value of constraint (mol/s or J/mol K)
J	Transfer rate or flow (mol/s or J/s)
J''	Flux (various)
J''_{q}	Measurable heat flux ($J/s.m^2$)
K_{P}	Reaction rate constant (-)
k_{r}	Reaction rate constant (mol/s.kg.Pa)
L	Liquid flow (mol/s)
ℓ	Phenomenologic coefficient (various)
$d\mathcal{L}$	Thermodynamic length ($\sqrt{J/K}$)
Le	Lewis number (-)
$\dot{m}$	Mass flow of utility (kg/s)
M	Molar mass (kg/mol)
M	Number of search directions in Powell's algorithm in Ch. 3 (-)
N	Number of trays (-)
P	Pressure (Pa)
Q	Duty (J/s)
R	Gas constant (J/mol.K)
R^{HX}	Heat transfer resistance (s/J.K)
R^2	Correlation coefficient (-)

r	Resistivity (various)
r	Reaction rate in Ch. 7 (mol/s.kg)
$\overline{r}$	Resistance (various)
S	Entropy (J/mol K)
$\mathbb{S}_T$	Soret coefficient (1/K)
s_T	Experimental Soret coefficient (1/K)
T	Temperature (K)
$\tilde{\mathbf{T}}$	Temperature profile (K)
$\tilde{\mathbf{u}}$	Search direction (-)
u	Component velocity (m/s)
V	Vapour flow (mol/s)
$\mathbb{V}$	Volume (m^3)
V^{mix}	Volume of mixture on tray (m^3)
V^{dif}	Diffusion volume (Taylor and Krishna 1993)
v	Velocity (m/s)
v_{mp}	Most probable velocity (m/s)
$\dot{W}$	Work (J/s)
w	Weight fraction (-)
X	Driving force conjugate to flow (J/mol.K or 1/K)
X''	Local force conjugate to flux (various)
x	Liquid mole fraction (-)
y	Vapour mole fraction (-)
$\overline{\text{y}}$	Average Gibbs-Duhem vapour mole fraction ratio, see Eqs. 2.3 and 4.10 (-)
Z	Extensive variables of the system (various)
z	Distance (m)

Greek

γ	Activity coefficient (-)
δ	Film thickness (m)
$\Delta\dot{E}x$	Exergy loss (J/s)
$\Delta_{\text{vap}}H$	Heat of vapourisation (J/mol)
ϵ	Void fraction/porosity (-)
η	Efficiency (-)
η	Viscosity in Ch. 7 (Pa.s)
Θ	Flow fraction (-)
λ	Thermal conductivity (W/m K)
λ	Lagrange multiplier in Ch. 2 and 3 (mol/s or J/mol K)

μ	Chemical potential (J/mol)
ν	Stoichiometric coefficient (-)
ξ	Definition introduced in Eq. 3.7 (W/K)
ρ	Density (kg/m^3)
Σ	Largest decrease in Powell's algorithm (J/s K)
σ	Local entropy production rate (J/s.K.m^3 or W/K m^2)
σ_j	Condensation coefficient in Ch. 6 (-)
$\dot{\phi}$	Molar flow (mol/s)
χ	Conversion (-)
ω	Non-ideality parameter (-)

Super- and subscripts

I	First law of thermodynamics
II	Second law of thermodynamics
B	Bottom
b	Benzene
boil	Boiling
cond	Condenser
cool	Cooling water
D	Distillate
E	See Eq. 3.7
e	Energy
e	Ethanol in Ch. 4
F	Feed
HX	Heat exchanger
i	Component number (subscript)
i	Interface in Ch. 6 (superscript)
ii	Imperfect insulation
j	Component number in Ch. 6
k	Liquid or vapour
l	Phenomenon number
L	Liquid
M	Number of search directions in Powell's algorithm in Ch. 3 (-)
m	Heat exchanger number in Ch. 7
m	Phenomenon number in Ch. 1
N	Total number of trays
n	Tray or bed number
part	Particle

q	Measurable heat
R	Reaction
reb	Reboiler
ref	Reference
T	At constant temperature (subscript)
T	Augmented with thermal diffusion (superscript in Ch. 6)
t	Toluene
tot	Total
u	Utilities, i.e. heating or cooling medium
V	Vapour
vap	Vapourisation
w	Water
0	Reference state (298.15 K, 1.013 10^5 Pa)
$*$	Saturation
$\overline{x}$	Average of property x
$\dot{x}$	Property x per second

Bibliography

Agrawal, R. and Fidbowski, Z. 1996. On the use of intermediate reboilers in the rectifying section and condensers in the stripping section of a distillation column. *Industrial & Engineering Chemistry Research* **35**(8), 2801–2807.

Agrawal, R. and Fidbowsky, Z. 1998. Are thermally coupled distillation columns always thermodynamically more efficient for ternary distillation?. *Industrial & Engineering Chemistry Research* **37**(8), 3444–3454.

Alopeaus, V. and Aittamaa, J. 2000. Appropriate simplifications in calculation of mass transfer in a multicomponent rate-based distillation tray model. *Industrial & Engineering Chemistry Research* **39**(11), 4336–4345.

Andresen, B. and Salamon, P.: 2000. Distillation optimized by thermodynamic geometry. *Entropie*. Vol. 36. pp. 4–10.

Bedeaux, D. 1986. Nonequilibrium thermodynamics and statistical physics of surfaces. *Advances in chemical physics* **64**, 47–109.

Bedeaux, D. and Kjelstrup, S. 1999. Transfer coefficients for evaporation. *Physica A* **270**, 413–426.

Bedeaux, D., Smit, J., Hermans, L. and Ytrehus, T. 1992. Slow evaporation and condensation. 2. A dilute mixture. *Physica A* **182**, 388–418.

Bedeaux, D., Standaert, F., Hemmes, K. and Kjelstrup, S. 1999. Optimization of processes by equipartition. *Journal of Non-Equilibrium Thermodynamics* **24**, 242–259.

Bejan, A.: 1996. *Entropy Generation Minimization. The Method of Thermodynamic Optimization of Finite-Size Systems and Finite-Time Processes*. CRC Press. New York.

Biegler, L. T., Grossmann, I. E. and Westerberg, A. W.: 1997. *Systematic Methods of Chemical Process Design*. Prentice Hall.

Bird, R. B., Stewart, W. E. and Lightfoot, E. N.: 1960. *Transport Phenomena*. John Wiley & Sons.

Chartrand, G. and Crowe, C. 1969. The optimization of the catalytic oxidation of sulphur dioxide in a multi-bed reactor. *The Canadian Journal of Chemical Engineering* **47**, 269–301.

Cipolla Jr., J. W., Lang, H. and Loyalka, S.: 1974. Temperature and partial pressure jumps during evaporation and condensation of a multicomponent mixture. *Rarefied Gas Dynamics*. Vol. II. DFVLR-Press, Portz-Wahn. pp. F.4–1– F.4–10.

De Groot, S. R. and Mazur, P.: 1985. *Non-Equilibrium Thermodynamics*. Dover. London.

De Koeijer, G.: 1997. *Thermodynamic analysis of the sequencing, feed tray, and interstage heat exchanger location in multi component distillation.* Master's thesis. Delft University of Technology, Laboratory for Phase Equilibria and Applied Thermodynamics. Julianalaan 136, Delft, The Netherlands.

De Koeijer, G. and Kjelstrup, S. 2000. Minimizing entropy production in binary tray distillation. *International Journal of Applied Thermodynamics* **3**(3), 105–110.

De Koeijer, G. and Kjelstrup, S.: 2002. Application of rate equations for heat and mass transfer to distillation of ethanol and water. Accepted for publication in proceedings of ESCAPE12, The Hague, The Netherlands.

De Koeijer, G. and Rivero, R. 2002. Entropy production and exergy loss in experimental distillation columns. *in preparation.*

De Koeijer, G., Kjelstrup, S., Salamon, P., Siragusa, G. and Hoffmann, M. S. K.: 2001. Comparison of entropy production rate minimization methods for binary diabatic tray distillation. *in* A. Ozturk and Y. Gogus (eds), *Proceedings of ECOS 2001.* Vol. II. Istanbul, Turkey. pp. 667–677. ISBN 975-97568-2-2.

De Koeijer, G., Kjelstrup, S., van der Kooi, H. J., Gross, B., Knoche, K. F. and Andersen, T.: 1999. Positioning heat exchangers in binary tray distillation using isoforce operation. *in* M. Ishida, G. Tsatsaronis, M. Moran and H. Kataoka (eds), *Proceedings of ECOS 1999.* Tokyo, Japan. pp. 471–476. ISBN4-9980762-0-5.

De Koeijer, G., Kjelstrup, S., van der Kooi, H. J., Gross, B., Knoche, K. F. and Andersen, T. 2002a. Positioning heat exchangers in binary tray distillation using isoforce operation. *Energy Conversion and Management* **43**(9-12), 1571–1581.

De Koeijer, G., Røsjorde, A. and Kjelstrup, S.: 2002b. The role of heat exchangers in optimum diabatic distillation columns. Accepted for publication in proceedings of ECOS 2002, Berlin, Germany.

Demirel, Y. and Sandler, S. 2001. Linear-nonequilibrium thermodynamics for coupled heat and mass transport. *International Journal of Heat and Mass Transfer* **44**, 2439–2451.

Doering, F. and Gaddy, J. 1980. Optimization of the sulfuric acid process with a flowsheet simulator. *Computers & Chemical Engineering* **4**, 113–122.

Douglas, J.: 1988. *Conceptual Design of Chemical Processes.* McGraw-Hill.

Energy Information Administration: 1999. World crude oil production. Website. http://www.eia.doe.gov/pub/international/ieapdf/t02_02.pdf (accessed March 2002).

Energy Information Administration: 2002. Annual U.S. energy supply and demand. Website. http://www.eia.doe.gov/emeu/steo/pub/pdf/a1tab.pdf (accessed March 2002).

Fogler, H.: 1992. *Elements of Chemical Reaction Engineering.* 2nd. edn. Prentice-Hall, New York.

Fonyo, Z. 1974a. Thermodynamic analysis of rectification I. Reversible model of rectification. *International Chemical Engineering* **14**(1), 18–27.

Fonyo, Z. 1974b. Thermodynamic analysis of rectification II. Finite cascade models. *International Chemical Engineering* **14**(2), 203–210.

Førland, K. S., Førland, T. and Kjelstrup, S.: 2001. *Irreversible Thermodynamics. Theory and Application.* 3rd edn. Tapir. Trondheim, Norway.

Gani, R. and Bek-Pedersen, E. 2000. Simple new algorithm for distillation column design. *AIChE Journal* **46**(6), 1271–1274.

Gibbs, J. W.: 1961. *Collected Works, 2 vols.* Dover. London.

Gill, P., Murray, W. and Wright, M. H.: 1981. *Practical Optimization.* Academic Press. London.

Gmehling, J. and Onken, U. (eds): 1977. *Vapor-Liquid Equilibrium Data Collection - Chemistry Data Series.* DECHEMA.

Hafskjold, B. and Ratkje, S. K. 1995. Criteria for local equilibrium in a system with transport of heat and mass. *Journal of Statistical Physics* **78**, 463–494.

Hafskjold, B., Ikeshoji, T. and Ratkje, S. 1993. On the molecular mechanism of thermal diffusion in liquids. *Molecular Physics* **80**(6), 1389–1412.

Humphrey, J. and Siebert, A. 1992. Separation technologies: An opportunity for energy savings. *Chemical Engineering Progress* **88**(3), 32–41.

Johannessen, E. and Kjelstrup, S.: 2002. Entropy production minimization in plug flow fixed-bed reactors: Theoretical limit and practical approximation. Accepted for publication in proceedings of ECOS 2002, Berlin, Germany.

Johannessen, E., Nummedal, L. and Kjelstrup, S. 2002. Minimizing the entropy production in heat exchange. *International Journal of Heat and Mass Transfer.* in print.

Kauchali, S., McGregor, C. and Hildebrandt, D. 2000. Binary distillation re-visited using the attainable region theory. *Computers & Chemical Engineering* **24**, 231–237.

King, C.: 1980. *Separation Processes.* 2nd. edn. McGraw-Hill, New York.

Kjelstrup Ratkje, S., Sauar, E., Hansen, E., Lien, K. and Hafskjold, B. 1995. Analysis of entropy production rates for design of distillation columns. *Industrial & Engineering Chemistry Research* **34**(9), 3001–3007.

Kjelstrup, S. and Bedeaux, D.: n.d.. *Irreversible Thermodynamics of Heterogeneous Systems.* in preparation.

Kjelstrup, S. and De Koeijer, G. 2002. Transport equations for distillation of ethanol and water from the entropy production rate. *to be published.*

Kjelstrup, S. and Island, T. V. 1999. The driving force distribution for minimum lost work in a chemical reactor close to and far from equilibrium. II. Oxidation of SO_2. *Industrial & Engineering Chemistry Research* **38**(8), 3051–3055.

Kjelstrup, S., Bedeaux, D. and Sauar, E.: 1999a. Distribution of driving forces in process design. *in* M. Ishida, G. Tsatsaronis, M. Moran and H. Kataoka (eds), *Proceedings of ECOS 1999*. Tokyo, Japan. pp. 70–75. ISBN4-9980762-0-5.

Kjelstrup, S., Island, T. V., Sauar, E. and Bedeaux, D.: 1998. Fremgangsmåte for optimalisering av entropiporoduksjon i en eller flere kjemiske reaktorer. Norwegian patent number 311286. Filed 17 June 1998; Accepted 12 November 2001.

Kjelstrup, S., Johannessen, E., Røsjorde, A., Nummedal, L. and Bedeaux, D. 2000. Minimizing the entropy production for the methanol producing reaction in a methanol reactor. *International Journal of Applied Thermodynamics* **3**(4), 147–153.

Kjelstrup, S., Sauar, E., Bedeaux, D. and van der Kooi, H. 1999b. The driving force distribution for minimum lost work in a chemical reactor close to and far from equilibrium. I. Theory. *Industrial & Engineering Chemistry Research* **38**(8), 3046–3050.

Koehler, J., Poellmann, P. and Blass, E. 1995. A review on energy calculations for ideal and nonideal distillations. *Industrial & Engineering Chemistry Research* **34**(4), 1003–1020.

Kolodner, P., Williams, H. and Moe, C. 1988. Optical measurements of the Soret coefficient of ethanol/water solutions. *Journal of Chemical Physics* **88**(10), 6512–6524.

Kotas, T.: 1995. *The Exergy Method of Thermal Plant Analysis*. reprint edn. Krieger Publishing Company.

Krishna, R. and Wesselingh, J. 1997. The Maxwell-Stefan approach to mass transfer. *Chemical Engineering Science* **52**(6), 861–911.

Krishnamurthy, R. and Taylor, R. 1985a. A nonequilibrium stage model of multicomponent separation processes. Part I: Model description and method of solution. *AIChE Journal* **31**(3), 449–456.

Krishnamurthy, R. and Taylor, R. 1985b. A nonequilibrium stage model of multicomponent separation processes. Part II: Comparison with experiment. *AIChE Journal* **31**(3), 456–465.

Kuiken, G.: 1994. *Thermodynamics of Irreversible Thermodynamics*. John Wiley and Sons. Chichester, England.

Le Goff, P., Cachot, T. and Rivero, R. 1996. Exergy analysis of distillation processes. *Chemical Engineering Technology* **19**, 478–485.

Linnhoff, B. and Smith, R. 1979. The thermodynamic efficiency of distillation. *Institution of Chemical Engineers Symposium Series* (56(Distillation, Vol. 1)), 2.1/47–2.1/73.

Liu, X. and Qian, J. 2000. Modeling, control, and optimization of ideal internal thermally coupled distillation columns. *Chemical Engineering & Technology* **23**(3), 235–241.

Lurgi GmbH: 1990. H_2SO_4 atlas. POB 111231, D-6000, Frankfurt am Main, Germany.

Mah, R., Jr., J. N. and Wodnik, R. 1977. Distillation with secondary reflux and vaporization: A comparative evaluation. *AIChE Journal* **23**(5), 651–658.

Marek, R. and Straub, J. 2001. Analysis of the evaporation coefficient and the condensation coefficient of water. *International Journal of Heat and Mass Transfer* **44**, 39–53.

Meadows, D. H. and Randers, J.: 1972. *The Limits to growth: A report for the Club of Rome's project on the predicament of mankind.* Universe Books.

Meadows, D. H., Meadows, D. L. and Randers, J.: 1992. *Beyond the limits : Confronting global collapse, envisioning a sustainable future.* Earthscan Publications.

Miller, O. 1935. Sur l'énergie libre du distillat comme mesure de l'efficacité de l'appareil distillatoire. *15me Congrès de Chimie Industrielle* pp. 352–363. Bruxelles.

Målsnes, A. and Rostad, K.: 1998. Personal communication. Outokumpu Norzink AS, Odda, Norway.

Mueller, H.: 1994. *Ullmann's Encyclopedia of Industrial Chemistry.* Vol. A25. VCH Verlagsgesellschaft. chapter Sulfuric Acid and Sulphur Trioxide, pp. 635–703.

Nakaiwa, M., Huang, K., Naito, K., Endo, A., Akiya, T., Nakane, T. and Takamatsu, T. 2001. Parameter analysis and optimization of ideal heat integrated distillation columns. *Computers & Chemical Engineering* **25**(4-6), 737–744.

Nocedal, J. and Wright, S. J.: 1999. *Numerical Optimization.* Springer-Verlag. New York.

Nulton, J. D. and Salamon, P. 2001. Optimality in multi-stage operations with asymptotically vanishing cost. *SIAM Journal of Optimization.* submitted.

Nulton, J., Salamon, P., Andresen, B. and Anmin, Q. 1985. Quasistatic processes as step equilibrations. *Journal of Chemical Physics* **83**(1), 334–338.

Nummedal, L.: 2001. *Entropy Production Minimization of Chemical Reactors and Heat Exchangers.* PhD thesis. Norwegian University of Science and Technology, Department of Chemistry, Trondheim, Norway. ISBN 82-471-5350-5, ISSN 0809-103x.

Nummedal, L. and Kjelstrup, S. 2001. Equipartition of forces as a lower bound on the entropy production in heat exchange. *International Journal of Heat and Mass Transfer* **44**, 2827–2833.

Nummedal, L., Costea, M., Røsjorde, A., Johannessen, E. and Kjelstrup, S.: 2001. Minimization of the entropy production in the ammonia reactor. *in* A. Ozturk and Y. Gogus (eds), *Proceedings of ECOS 2001.* Vol. II. Istanbul, Turkey. pp. 697–704. ISBN 975-97568-2-2.

Nummedal, L., Røsjorde, A., Johannessen, E. and Kjelstrup, S.: 2002. Minimization of the entropy production in the primary steam reformer. Accepted for publication in proceedings of ESCAPE12, The Hague, The Netherlands.

Ostrovsky, G., Ostrovsky, M. and Mikhailow, G. 1990. Discrete optimization of chemical processes. *Computers & Chemical Engineering* **14**(1), 111–117.

Park, C. S. and Sharp-Bette, G. P.: 1990. *Advanced Engineering Economics.* Wiley.

Pitzer, K. and Brewer, L.: 1961. *Thermodynamics.* McGraw-Hill.

Press, W. H., Vetterling, W. T., Teukolsky, S. A. and Flannery, B. P.: 1992. *Numerical Recipes in C.* Cambridge University Press.

Ray, S. and Sengupta, S. 1996. Irreversibility analysis of a sieve tray in a distillation column. *International Journal of Heat and Mass Transfer* **39**(7), 1535–1542.

Ray, S., Panja, A. and Sengupta, S. 1994. Irreversibility analysis of a separation system using sieve tray distillation column. *Chemical Engineering Science* **49**(9), 1472–1477.

Reid, R. C., Prausnitz, J. M. and Poling, B. E.: 1987. *The Properties of Gases and Liquids.* 4th edn. McGraw-Hill.

Rivero, R.: 1993. *L'Analyse d'Exergie: Application à la Distillation Diabatique et aux Pompes à Chaleur à Absorption.* PhD thesis. Institut National Polytechnique de Lorraine, Nancy, France.

Rivero, R.: 1995. Exergy simulation of a distillation tower: Diabatic stripping column. *in* Y. Gogus, A. Ozturk and G. Tsatsaronis (eds), *Proceedings of ECOS 1995.* Vol. 1. Istanbul. pp. 163–167. ISBN975-7475-07-6.

Rivero, R. 2001. Exergy simulation an optimization of adiabatic and diabatic binary distillation. *Energy* **26**, 561–593.

Rivero, R., Cachot, T. and Le Goff, P.: 1993. Exergy analysis of adiabatic and diabatic distillation columns: An experimental study. *in* P. Pilavaci (ed.), *Energy Efficiency in Process Technology.* Elsevier Applied Science Publisher, Ltd.. London. pp. 1254–1267. ISBN 1-85861-019-2.

Røsjorde, A., Kjelstrup, S., Bedeaux, D. and Hafskjold, B. 2001. Nonequilibrium molecular dynamics simulations of steady-state heat and mass transport in condensation: II. Transfer coefficients. *Journal of Colloid and Interface Science* **240**, 355–364.

Ruppeiner, G. 1995. Riemannian geometry in thermodynamic fluctuation theory. *Reviews of Modern Physics* **67**(3), 605–659.

Salamon, P. and Nulton, J. 1998. The geometry of separation processes: A horse-carrot theorem for steady flow systems. *Europhysics Letters* **42**(5), 571–576.

Sauar, E.: 1998. *Energy efficient process design by equipartition of forces: With applications to distillation and chemical reaction.* PhD thesis. Department of Physical Chemistry, Norwegian University of Science and Technology. Trondheim, Norway. ISBN 82-471-0276-5, ISSN 0802-3271.

Sauar, E., Kjelstrup Ratkje, S. and Lien, K. M.: 1995. Process optimisation by equipartition of forces. Applications to distillation columns. *in* Y. Gogus, A. Ozturk and G. Tsatsaronis (eds), *Proceedings of ECOS 1995.* Vol. 2. pp. 413–418. ISBN 975-7475-08-4, Istanbul, Turkey.

Sauar, E., Kjelstrup, S. and Lien, K. M. 1996. Equipartition of forces: A new principle for process design and operation. *Industrial & Engineering Chemistry Research* **35**(11), 4147–4153.

Sauar, E., Rivero, R., Kjelstrup, S. and Lien, K. M. 1997. Diabatic column optimization compared to isoforce columns. *Energy Conversion and Management* **38**(15-17), 1777–1783.

Schaller, M., Hoffmann, K. H., Siragusa, G., Salamon, P. and Andresen, B. 2001. Numerically optimized performance of diabatic distillation columns. *Computers & Chemical Engineering* **25**(11-12), 1537–1548.

Sinnot, R., Coulson, J. and Richardson, J.: 1983. *An Introduction to Chemical Engineering Design.* Vol. 6 of *Chemical Engineering.* Pergamon Press.

Smith, J. and Van Ness, H.: 1987. *Introduction to Chemical Engineering Thermodynamics.* 4th edn. McGraw-Hill, Inc.

Taprap, R. and Ishida, M. 1996. Graphic exergy analysis of processes in distillation column by energy-utilization diagrams. *AIChE Journal* **42**(6), 1633–1641.

Taylor, R. and Krishna, R.: 1993. *Multicomponent Mass Transfer.* Wiley. New York.

The MathWorks Inc.: 2001. Version 6.1.0.450 release 12.1. CD-ROM. Website: http://www.mathworks.com/products/matlab/ (accessed March 2002).

Tondeur, D. and Kvaalen, E. 1987. Equipartition of entropy production. An optimality criterion for transfer and separation processes. *Industrial & Engineering Chemistry Research* **26**(1), 50–56.

Tyn, M. T. and Calus, W. F. 1975. Temperature and concentration dependence of mutual diffusion coefficients of some binary liquid systems. *Journal of Chemical Engineering Data* **20**(3), 310–316.

UNFCCC: 1997. Kyoto protocol to the united nations framework convention on climate change. Kyoto, Japan. Website: http://unfccc.int/text/resource/docs/cop3/07a01.pdf (accessed March 2002).

Weast, R. C. and Astle, M. J. (eds): 1982. *CRC Handbook of Chemistry and Physics.* 62nd edn. CRC Press. Boca Raton, Florida.

Wesselingh, J. A. 1997. Non-equilibrium modelling of distillation. *Chemical Engineering Research and Design (Trans IChemE)* **75**(A), 529–538.

World Commission on Environment and Development: 1987. *Our Common Future.* Oxford University Press. Chairman: Gro Harlem Brundtland.

Yano, R., Fukuda, Y. and Hashi, T. 1988. Thermal conductivity measurements of water-ethanol solutions by the laser-induced transient grating method. *Chemical Physics* **124**, 315–319.

Zeisberg, F. 1911. The thermal problem in contact sulphuric acid manufacture. *Transactions of the American Electrochemical Society* **36**, 187–194.

Zemp, R., de Faria, S. and de L. Oliveira Maia, M. 1997. Driving force distribution and exergy loss in the thermodynamic analysis of distillation columns. *Computers & Chemical Engineering* **21, Suppl.**, S523–S528.

A C-code for Monte Carlo procedure

Introduction

For enabling reproduction of the results of the Monte Carlo procedure in Chapters 2, 3, and 5, the ANSI C-code is given in this appendix. For using this algorithm one needs some basic knowledge about programming in C. The code calls several times the function 'column()'. This function simulates the column. An array of temperatures 'T[]' is used, which is a global variable in the program. It calculates the vapour flows 'V[]', liquid flows 'L[]', heat exchanger duties 'Q[]', and the total entropy production 'totalentropyproduction', which are also global variables. Comments that explain the code are set between '/*' and '*/', as used in C, and refer to code below. The compiling command was 'gcc <filename> -lm'.

C-code

```
void minimize()
{
/* The local variables are defined */
int randomtray, randomsign, i, j, k, l;
double randomstep, maximumTstep, Tchange, minimumentropyproduction, power;

/* A factor is introduced that determines the maximum size of the temperature step. It
enables adjustment of the precision in a simple manner*/
maximumTstep=0.0000001;

/*Before the algorithm starts, a simulation of the starting column must have been done.
The minimum entropy production rate is set to the entropy production rate of the starting
column.*/
minimumentropyproduction=totalentropyproduction;

/* The temperatures of the column with minimum entropy production rate are set equal to
the ones from the starting column*/
for(i=0; i<=Ntray; i++)
{
Tminimum[i]=T[i];
}

/* The minimisation starts. The values of the counters l, k, and i can be used for adjusting
duration and accuracy of the algorithm*/
for(l=0;l<50;l++)
{
for(k=6;k>2;k--)
{
for(i=0;i<30000;i++)
{

/* the value of the random tray, random step, random sign, and power are set zero, which
```

```
is good custom in programming C*/
randomtray=0;
randomstep=0;
randomsign=0;
power=0;

/*The integer value of the random tray is determined with the function rand(), which has a maximum high value RANDMAX. Ntray is the total number of trays and is a global variable.*/
randomtray=(int)((double)(rand())/(double)(RANDMAX)*(double)(Ntray-1))+1;

/* the temperature of tray number 1 should not be altered. So if the random tray has the value 1, it is set to 2. Some randomness is lost here*/
if(randomtray==1)
{
randomtray=2;
}

/* For an exponential decrease of the step, it is multiplied with the variable power (factor f in the chapters). Power is determined from the counter k.*/
power=0.01*pow(10,(double)(k));

/* the size of the step is calculated*/
randomstep=power*maximumTstep*((double)(rand())/(double)(RANDMAX));

/* The sign of the step is determined randomly*/
randomsign=(int)((double)(rand())/(double)(RANDMAX)+0.5);
if(randomsign==0)
{
randomsign=-1;
}

/* The step is added to temperature of randomtray*/
Tchange=T[randomtray];
T[randomtray]=Tchange+(double)(randomsign)*randomstep;

/*A switch for checking whether the simulation is feasible is introduced. If the switch is zero the column is feasible. If it is unity the column is unfeasible. This switch is also be used in the function column() for avoiding the return of unfeasible results to minimize()*/
physicalfeasibilityswitch=0;

/* The column is simulated. The global variable T[] is used for calculating the global variables V[], L[], x[], y[], HeatExchangerDuty[], and totalentropyproduction./*
column();

/*The function column allows the vapour and liquid flows to be less then zero. If this is the case the feasibility switch is set unity*/
for(j=0; j<=Ntray; j++)
{
```

```
if(L[j]<0 || V[j]<0)
{
physicalfeasibilityswitch=1;
}
}

/* If the entropy production rate of the recently simulated column is lower than the previ-
ously found lowest value (or of the value of the starting column if this is the first time a value
lower than that one is found), and if the column is feasible, the temperatures and duties of
the minimum are set to the recently simulated one. In the next iteration, a new step will be
tried on this temperature profile.*/
if(totalentropyproduction<minimumentropyproduction && physicalfeasibilityswitch==0)
{
minimumentropyproduction=totalentropyproduction;

for(j=0; j<=Ntray+1; j++)
{
/*Tminimum[] is also a global variable*/
Tminimum[j]=T[j];
}

/* The step that gave a lower entropy production rate is applied on the same tray, with
the same check afterwards. This increases the algorithm but the random character is de-
creased*/
T[randomtray]=T[randomtray]+(double)(randomsign)*randomstep;

physicalfeasibilityswitch=0;

column();

for(j=0; j<=Ntray; j++)
{
if(L[j]<0 || V[j]<0)
{
physicalfeasibilityswitch=1;
}
}

if(totalentropyproduction<minimumentropyproduction && physicalfeasibilityswitch==0)
{

minimumentropyproduction=totalentropyproduction;

for(j=0; j<=Ntray+1; j++)
{
Tminimum[j]=T[j];
}

}
```

```
/* If the entropy production rate of the recently simulated one is not lower than the minimum entropy production rate, the step is reversed and the original temperature profile is restored. */
else
{

Tchange=T[randomtray];
T[randomtray]=T[randomtray]-(double)(randomsign)*randomstep;
}

}
else
{
Tchange=T[randomtray];
T[randomtray]=Tchange-(double)(randomsign)*randomstep;
}

}
}

/* after one part minimization(the for-loops with counters i and k) is done the intermediate result is saved. This enables a quick restart of the algorithm at the point it stopped or crashed. First the temperature must be set to the one of the minimum that is found up to now*/
for(i=0; i<=Ntray; i++)
{
T[i]=Tminimum[i];
}

/* The column with minimum entropy production rate is simulated again.*/
column();

/* For having a unique filename for each time the results are saved, the file gets the value of the entropy production in its name*/
sprintf(filename,"minimumEntrprod%.0f",totalentropyproduction*1000000000000);

/*The file is opened*/
if((minimumdata= fopen(filename,"w")) == NULL)
{
printf("could not open file \n");
fclose(minimumdata);
}
else
{

/* The global variables of the minimum are saved */
fprintf(minimumdata,"trayno T Q S L V x y \n");
for(i=0; i<=Ntray+1; i++)
```

```
{
fprintf(minimumdata,"%d %9.8f ",i,T[i]);
fprintf(minimumdata,"%11.8f ",HeatExchangerDuty[i]);
fprintf(minimumdata,"%11.8f %11.8f ",L[i],V[i]);
fprintf(minimumdata,"%11.8f %11.8f \n",x[i],y[i]);
}
fclose(minimumdata);
}

/* The value of the minimum entropy production is relaxed by a factor 1.2. So the first step
that has feasible results will be the next minimum. In this way the temperature profile is
perturbed. The next step in the for-loop with counter l is started afterwards.*/

minimumentropyproduction=1.2*minimumentropyproduction;
}
}
```

B *Matlab*® code for *fmincon* procedure

Introduction

The *Matlab*® codes of the four main files of the procedure used in Chapter 7 are given here in order to enable reproduction of the results. Moreover, it can serve as a guideline for writing *Matlab*® codes for optimising other applications, see also The MathWorks Inc. (2001). The first file is called 'optimize.m' and is the file that contains the *fmincon* function and the starting point. In the function *fmincon* 'EP.m' and 'constraints.m' are called. 'EP.m' returns the entropy production rate, and 'constraints.m' the value of the constraints. In 'EP.m' the function 'simulate.m' is called. This function simulates the reactor system with the four beds and five heat exchangers. For understanding the code, knowledge of *Matlab*® is required. Some comments are included after the %-symbol. The names used here are as close as possible to the ones used in Chapter 7. The only exception is EP, which is entropy production rate. Otherwise, P is pressure, T is temperature, xi is conversion, y is mole fraction, F is flow.

Matlab® code

Optimize.m

```
close all
clear all

global k iter

format short e

% The name of the RunDump file
```

```
k.RDfile = 'RunDumpA';

% All variables and constraint are put in or returned from fmincon in
% scaled form in order to increase convergence.
k.Scales.T = 1000;
k.Scales.EP = 5000;
k.Scales.ySO2 = 0.05;
k.Scales.height = 0.01;
k.Scales.area = 100000;
k.Scales.DeltaT = 700;

% Starting point of the variables is given. As an example the
% reference values are given
DeltaT =1e3*[0.37454 -0.0900 -0.080 -0.055 -0.214];
heights = [0.6 0.6 0.6 0.6 ];
areas = [1743.75 581.25 512.50 181.25 981.25];
variables0 = [DeltaT heights areas];

% The values of constraint are given here
k.Settings.ySO2 = 0.00183932159311;
k.Settings.T = 4.862150269147006e+02;
k.Settings.sumheights = 2.4;
k.Settings.sumareas = 4000;

% Counter for number of times entropy production rate is calculated is initialised.
k.count = 0;

% Simulating the reactor system with starting point
iter = simulate([variables0]);

% See below for explanation of these quantities
A = [];
B = [];
Aeq = [];
Beq = [];

% Lower and upper bounds on the variables
LB(1) = -700;
UB(1) = 700;
LB(2) = -700;
UB(2) = 700;
LB(3) = -700;
UB(3) = 700;
LB(4) = -700;
UB(4) = 700;
LB(5) = -700;
UB(5) = 700;
LB(6) = 0;
UB(6) = 2.4;
```

```
LB(7) = 0;
UB(7) = 2.4;
LB(8) = 0;
UB(8) = 2.4;
LB(9) = 0;
UB(9) = 2.4;
LB(10) = 1;
UB(10) = 10000;
LB(11) = 1;
UB(11) = 10000;
LB(12) = 1;
UB(12) = 10000;
LB(13) = 1;
UB(13) = 10000;
LB(14) = 1;
UB(14) = 10000;

%Numerical optimisation
OPTIONS = optimset('Diagnostics', 'on', 'Display', 'iter', 'MaxFunEvals', 1e10,'MaxIter',
1e10, 'TolCon', 1E-10, 'TolFun', 1E-10, 'LargeScale', 'off');

[Optimalvariables, MinEP, EXITFLAG, OUTPUT, LAMBDA, GRAD] = fmincon('EP',
variables0, A, B, Aeq, Beq, LB, UB,'constraints', OPTIONS);

%Right hand side
%
% FMINCON Finds the constrained minimum of a function of several variables.
% FMINCON solves problems of the form:
% min F(X) subject to: A*X <= B, Aeq*X = Beq (linear constraints)
% X C(X) <= 0, Ceq(X) = 0 (nonlinear constraints)
% LB <= X <= UB
%
% LB and UB defines a set of lower and upper bounds on the design
% variables, X, so that the solution is in the range LB <= X <=
% UB. Use empty matrices for LB and UB if no bounds exist. Set
% LB(i) = -Inf if X(i) is unbounded below; set UB(i) = Inf if X(i)
% is unbounded above. (Set LB = [] and/or UB = [] if no bounds exist)
%
% The function 'constraints' should return the vectors C and Ceq,
% representing the nonlinear inequalities and equalities
% respectively, when called with feval: [C, Ceq] =
% feval(constraints,X). FMINCON minimizes FUN such that C(X) <= 0 and
% Ceq(X) = 0.
%
% 'EP' is a function that returns the total entropy
% production of a reactor as a function of the variables.
%
% variables0 is the inital value of the variables.
%
```

```
%Left hand side
%
% Optimalvariables contains the values of the variables that gives the minimum
% entropy production if it is minimized with respect to the variables.
%
% MinEP is the minimum entropy production.
%
% EXITFLAG :
% > 0 then FMINCON converged to a solution X.
% 0 then the maximum number of function evaluations was reached.
% < 0 then FMINCON did not converge to a solution.
%
% OUTPUT is a structure with the number of iterations taken in
% OUTPUT.iterations, the number of function evaluations in
% OUTPUT.funcCount, the algorithm used in OUTPUT.algorithm, the
% number of CG iterations (if used) in OUTPUT.cgiterations, and
% the first-order optimality (if used) in OUTPUT.firstorderopt.
%
% LAMBDA returns the Lagrange multipliers at the solution X:
% LAMBDA.lower for LB, LAMBDA.upper for UB, LAMBDA.ineqlin is for
% the linear inequalities, LAMBDA.eqlin is for the linear
% equalities, LAMBDA.ineqnonlin is for the nonlinear inequalities,
% and LAMBDA.eqnonlin is for the nonlinear equalities.
%
% GRAD returns the value of the gradient of FUN at the solution X.
```

EP.m

```
function EPreactor = EP(variables)

global iter k

% If the reactor is not simulated with the another 'variables' than
% the one in the global struct iter, the reactor system is simulated.
% This enables independent use of the function, and avoids excess calculations
if max(abs(iter.variables-variables))>1e-16
iter = simulate(variables);
end;

% the calculated entropy production rate is returned
EPreactor = iter.EP/k.Scales.EP;

% The intermediate results are presented with graphs in order to
% see what is happening
k.count = k.count + 1;

if (mod(k.count, 5) == 0)

figure(1)
```

```
subplot(2,2,1)
if (mod(k.count, 25) == 0)
cla
end
plot(iter.z, iter.T);
ylabel('temperature /K')
xlabel('reactor length /m')
hold on
drawnow

subplot(2,2,2)
if (mod(k.count, 25) == 0)
cla
end
plot(iter.z,iter.xi);
ylabel('conversion /-')
xlabel('reactor length /m')
hold on
drawnow

subplot(2,2,3)
if (mod(k.count, 25) == 0)
cla
end
plot(iter.z,iter.FT);
ylabel('flow / mol/s')
xlabel('reactor length /m')
hold on
drawnow

subplot(2,2,4)
if (mod(k.count, 25) == 0)
cla
end
plot(iter.z,iter.P/1E5);
ylabel('Pressure / bar')
xlabel('reactor length /m')
hold on
drawnow
end

% The results are saved in case of a crash
if (mod(k.count, 200) == 0)
save(k.RDfile)
end
```

constraints.m

```
function [C, Ceq] = constraints(variables)
global iter k

% If the reactor is not simulated with the another 'variables' than
% the one in the global struct iter, the reactor system is simulated.
% This enables independent use of the function, and avoids excess calculations
if max(abs(iter.variables-variables))>1e-16
iter = simulate(variables);
end;

% Equality constraints
Ceq = [(iter.ySO2-k.Settings.ySO2)/k.Scales.ySO2 (iter.Tout-k.Settings.T)/k.Scales.T];

% Inquality constraints
C = [(iter.sumheights - k.Settings.sumheights)/k.Scales.height
(iter.sumareas - k.Settings.sumareas)/k.Scales.area
max(max(1E-7 - iter.y))];
```

simulate.m

```
function result = simulate(variables)

global k

% initializing the matrices for building up the result matrices
result.z = [];
result.T = [];
result.P = [];
result.xi = [];
result.y = [];
result.FT = [];

% Initializing parameters from the file ReactorParameters.m.
% This file contains all the values of the inlet parameters
ReactorParameters;

% Giving the variables their physical names
DeltaT = variables(1:5);
height = variables(6:9);
A = variables(10:14);

% Heat exchanger number 1
[EPHX(1), k.T0, k.P0, Q(1), force(1), DeltaPHX(1)] = MODELHX(k.T0, k.P0, k.xi0,
DeltaT(1),A(1));

for i = 1:k.numberofbeds

% Bed number i
```

```
if height(i) > 0

% Initial values
profiles0 = [k.T0 k.P0 k.xi0];

% Modelling bed number i
[z, profiles, EPBED(i), DeltaP] = MODELBED(profiles0, height(i));

% Calculating molar flow rates and mole fractions
x = CALCx(profiles(:,3));
F = CALCF(profiles(:,3));

% Updating inlet properties
k.T0 = profiles(end,1);
k.P0 = profiles(end,2);
k.xi0 = profiles(end,3);
k.v0 = k.nT0 * k.R * k.T0 / k.P0;

% Result struct build up
if i ==1
result.z = z;
else
result.z = [ result.z z + (i-1)*1E-12+sum(height(1:i-1))];
end

% Putting the results in the result struct
result.T = [result.T; profiles(:,1)];
result.P = [result.P; profiles(:,2)];
result.xi = [result.xi; profiles(:,3)];
result.y = [result.y; x];
result.FT = [result.FT; sum(F, 2)];

end

% Modelling of heat exchanger number i+1
[EPHX(i+1), k.T0, k.P0, Q(i+1), force(i+1), DeltaPHX(i+1)] = MODELHX(k.T0, k.P0,
k.xi0, DeltaT(i+1), A(i+1));

% Updating the inlet flow rate [m/s]
k.v0 = k.nT0 * k.R * k.T0 / k.P0;

end

% Output
result.EPHX = sum(EPHX);
result.EPBED = sum(EPBED);
result.EP = sum(EPHX) + sum(EPBED);
result.variables = variables;
result.ySO2 = result.y(end,1);
```

```
result.Tout = k.T0;
result.Pout = k.P0;
result.sumheights = sum(height);
result.sumareas = sum(A);
result.sumQ = Q(1) + Q(2) + Q(4) + Q(5);
result.Q = Q;
result.DeltaPHX = DeltaPHX;
result.force = force;
```